This dissertation has been
microfilmed exactly as received 67-15,905

STOCKHAM, Leo Warren, 1934-
RADIATIVE HEAT TRANSFER FROM A FINITE CYLINDRICAL PARTICLE CLOUD.

The University of Oklahoma, Ph.D., 1967
Engineering, aeronautical

University Microfilms, Inc., Ann Arbor, Michigan

THE UNIVERSITY OF OKLAHOMA

GRADUATE COLLEGE

RADIATIVE HEAT TRANSFER FROM A FINITE CYLINDRICAL PARTICLE CLOUD

A DISSERTATION

SUBMITTED TO THE GRADUATE FACULTY

in partial fulfillment of the requirements for the

degree of

DOCTOR OF PHILOSOPHY

BY

LEO WARREN STOCKHAM

Norman, Oklahoma

1967

RADIATIVE HEAT TRANSFER FROM A FINITE

CYLINDRICAL PARTICLE CLOUD

APPROVED BY

[illegible]

James A. Payne

John E. Francis

Edward F. Blick

William N. Huff

DISSERTATION COMMITTEE

ACKNOWLEDGMENTS

This course of study and research was sponsored by the United States Air Force under the supervision of the Air Force Institute of Technology.

It is a distinct pleasure for the author to express his sincere thanks and appreciation to Dr. Tom J. Love for his guidance and support throughout the complete academic program and in particular the present work.

He would also like to thank the many other persons who contributed substantially to this endeavor. Some of them were:

Other members of the Dissertation Committee, Dr. W. N. Huff, Dr. E. F. Blick, Dr. J. E. Francis, and Dr. J. A. Payne, all of whom provided encouragement and help.

Mr. Eugene Haberman, who made available the computer facilities of the Air Force Rocket Propulsion Laboratory, Edwards, California, where the major portion of the computer computation was carried out.

Mr. Phil Morosky, member of the staff of the AFRPL Computer Facility, who helped get the programs running at AFRPL and who remained the author's point of contact throughout the research period.

And, finally, my wife, Ruth and our children for their patience and understanding.

ABSTRACT

The problem of radiative heat transfer from a metalized propellant rocket exhaust is of current concern to the aerospace industry. The problem involves the transfer of thermal radiation from an axisymmetric dispersion of metallic oxide particles and includes the effects of absorption, emission, and anisotropic scattering.

The present work differs from previous works in that all of the above mentioned effects are included in the analysis. Specifically this work considers thermal radiation to the base region of a finite cylindrical cloud of absorbing, emitting and anisotropically scattering particles.

A Monte Carlo model of the problem is developed which permits the radiation to orginate either within the cloud or from a black circular surface at the base of the cloud. The emitted photon (bundle of energy) is then followed through a series of probable paths until it leaves the cloud and hits or misses the base plane. Anisotropic scattering is introduced through the scattering distribution function which is characteristic of aluminum oxide dispersions.

The model is run through some twenty-six different cases and comparisons are made with regard to variations in such parameters as optical diameter, height to diameter ratio, and anisotropic versus isotropic scattering.

TABLE OF CONTENTS

LIST OF TABLES

LIST OF FIGURES

CHAPTER I

INTRODUCTION

For many years physical scientists have concerned themselves with the analysis of radiant energy transport through absorbing and scattering media. Until recently, however, engineers considering thermal effects have not been greatly involved with it. Now, largely through the impetus of aerospace requirements, engineers find themselves with a need to accurately predict radiative heating through a variety of such media in diverse configurations.

One such engineering problem is the prediction of the radiant heating of a spacecraft structure which views a rocket exhaust plume. The problem is particularly significant in connection with the use of metalized solid propellant rocket motors. A detailed review of the theory of thermal radiation as it relates to rocket exhaust plumes has recently been given by Rochelle (1). A less comprehensive but very clear discussion of the state of knowledge of the solid rocket problem is given by Carlson (2).

The current work is motivated by the rocket exhaust heating problem. However, in view of the existance of (1) and (2) no useful purpose would be served by a detailed review of the problem here. Hence, the discussion will be confined to those areas necessary to set the stage for this work.

The general formulation of the problem of radiative heat transfer in absorbing, emitting, and scattering media is thoroughly covered in the literature. The works of Love (3) and Sparrow and Cess (4) are specific examples. An excellent treatment of electromagnetic scattering is available in the work by Van de Hulst (5) and treatments of a variety of the aspects of scattering are contained in the work edited by Kerker (6).

The specific problem to be treated in this work is the radiative heat transfer from a finite cylindrical cloud of particles which absorb, emit and scatter radiation. The radiation can originate either within the cloud or from a black circular surface at the base of the cloud.

There are several methods which have been applied to related heat transfer problems involving scattering. Among these are the method of quadratures used by Love (7) and Love and Hsia (8), the numerical solution of Evans, Chu, and Churchill (9), and the two step procedure developed by Edwards and Bobco in (10) and applied by Bobco in (11).

In (7) Love studied the effect of anisotropic scattering on the heat transfer between plane diffuse walls and a medium which was either isothermal or in radiative equilibrium. The medium was infinite in extent in two dimensions and either finite or semi-infinite in the third. The work of Love and Hsia (8) essentially extended the previous work to cases in which a specified temperature distribution existed in the medium. The quadrature method involves replacing the scattering integral, appearing in the integrodifferential equation as written along a line of sight, by a Gaussian quadrature. This reduces the problem to the solution of a set of first order non homogeneous differential equations.

In (9) Evans, Chu and Churchill consider anisotropic scattering in parallel plane dispersions of finite thickness. The dispersions have free boundaries. The technique used involves a reduction of the integrodifferential equation to a set of integral equations. The integral equations are solved by numerical iteration using a Gaussian quadrature for the integrals. Scattering is limited to scattering functions which can be approximated by a very few terms of a series of Legendre polynomials.

The method of Edwards and Bobco (10) obtains a first order solution from the ordinary diffusion approximation and boundary conditions which are satisfied in the mean. This solution is then used in the "source term" (emission plus scattering) of the formal equation of transfer along with the exact boundary conditions to obtain a second order solution. In (11) Bobco applies this method to obtain solutions for a two dimensional, semi-infinite slab. Scattering is isotropic. In (12) the method is applied to a semi-infinite cone but the isotropic scattering restriction remains.

All of the above mentioned techniques incorporate either plane parallel geometry or isotropic scattering as a simplification. Means by which these restrictions can be removed and still permit a solution are not obvious.

A fourth method of solution is the Monte Carlo technique, which has recently been applied to radiative heat transfer by Perlmutter and Howell (13, 14, 15) and Corlett (16). An excellent description is given by Howell in (17). Although this method previously had not been applied to heat transfer problems involving scattering, the extension seemed tractable. The flexibility of the method seemed particularly attractive.

The particles in the cloud considered in this work are of aluminum oxide and were chosen to be in distributions believed typical of aluminized propellant rocket exhausts. Experimental data on the optical properties of alumina at rocket exhaust temperatures have been obtained by Gryvnak and Burch (18), Carlson (19) and Adams (20). Mie theory calculations for absorption and scattering coefficients have been reported by Bauer and Carlson (21) and Plass (22, 23). Bauer and Carlson present their calculations averaged over particle distributions believed typical of those occuring in rocket exhausts. Plass gives values as a function of particle radius. The values obtained by Plass (23) using the data of (18) are believed to be the most accurate available for alumina (1). Bartky and Bauer (24) present calculations based on (18) and averaged over suitable particle distributions. In addition, they present curves showing the angular scattering for these particle distributions. For this work an angular scattering distribution is required and the one chosen is based on the shape of those in (22). It should be noted that Love and Wheasler (25) and Love and Beattie (26) have experimentally obtained similarly shaped angular scattering distributions for particle clouds of aluminum, carbon, glass, silica and iron.

Among currently published practical methods of calculating radiative heat transfer from metalized rocket plumes are the methods of Fontenot (27), Morizumi and Carpenter (28), Bartky and Bauer (24) and Edwards and Bobco (12). The first three are thoroughly discussed in both (1) and (2). Fontenot assumes a single particle size and neglects all effects of scattering.

Morizumi and Carpenter use a neutron scattering analogy in an infinite cylindrical cloud to relate particle absorption to extinction ratio and cloud emittance. Heat transfer is calculated using an effective temperature and a configuration factor from surface elements of the cloud to the point of interest. Scattering is isotropic.

Bartky and Bauer discuss the application of solutions of the isothermal slab to the rocket exhaust problem. They indicate that a one dimensional beam approximation along a line of sight offers promise for handling inhomogeneous plumes if the plume is divided into increments in which the density, pressure and temperature do not change appreciably.

The isotropic scattering restriction to the work of Edwards and Bobco has been previously mentioned.

In addition to radiation originating from emission within the exhaust plume Carlson (2) points out another complication which should be considered. In (29) Carlson et al., show that "searchlight" emission, "transport of chamber emitted radiation into the plume with subsequent scattering by the particle cloud to the surroundings," may be important. The inclusion of this effect in the above mentioned methods of solution would appear to be extremely difficult.

In his closing remarks Howell (17) makes the following conclusion. "Monte Carlo appears to have a definite advantage over other radiative-transfer calculation techniques when the difficulty of the problem being treated lies above some undefined level. Just where this level is cannot be established, probably being a function of the experience, competence, and prejudice of the individual working the problem. However, problems above this nebulous benchmark in complexity can be treated with greater flexibility, simplicity, and speed."

It is the opinion of this investigator that cylindrical geometry, anisotropic scattering and searchlight effect combine to elevate this problem above that "nebulous benchmark".

CHAPTER II

MODEL DESCRIPTION

General Description

The Monte Carlo method is applied to calculate the radiative transfer from a finite cylindrical cloud of particles to the cylinder base region. The radiation originates either from uniformly distributed isotropic emission within the particle cloud or from a black circular surface at the base of the cloud. The radiative flux to a series of rings, concentric with the cylinder and lying in the base plane, is calculated. Directional properties of the cloud emittance are not determined.

The particles are assumed to be uniformly distributed throughout the cloud. Scattering is either isotropic or anisotropic and multiple scattering is included. The optical depth (diameter), scattering to extinction ratio, particle mass and size distribution, cylinder height to diameter, and scattering function are chosen consistant with each other and remain constant for a given calculation.

Continuum thermal radiation from the surface or the particles is the only mode of energy transport. The boundaries of the cylindrical cloud are considered free.

Monte Carlo Application

The Monte Carlo method used in this work consists of following, one at a time, a large number of photons, or bundles of energy, through a cylindrical particle cloud from suitably chosen emission points along probable paths until they leave the cloud and either hit or miss the base plane. At each decision point along the path the subsequent direction and length of travel are selected in accordance with the appropriate probability distribution functions (see Chapter III). In this model a photon is considered to be emitted from an appropriately chosen point in a direction randomly chosen from a distribution representing either isotropic emission if from a volume element or diffuse emission if from a surface element. The maximum distance which a photon could travel along this direction and remain in the cloud is then calculated. This maximum path length is compared with a probable path length chosen randomly according to the appropriate distribution function. If the probable path length is greater than the maximum path length, the photon is considered to exit the particle cloud. If the exit direction of travel intersects the base plane, the impact radius is calculated and recorded. If its direction of travel takes it away from the base plane it is recorded as a miss.

If the probable path length is less than the maximum path length the photon is scattered or absorbed. This is considered to take place at a point which is a distance equal to the probable path length along the maximum path direction. The decision as to whether the photon is absorbed or scattered is based on the scattering to extinction ratio. If the photon is absorbed and the cloud is considered in radiative equilibrium a new photon is immediately emitted from the same point in an appropriately determined direction since there can be no heat accumulation in the cloud. If the photon is scattered, a direction of scattering is chosen according to the scattering function. In either case, once the new direction is determined, the calculations proceed as before and continue cycling until the photon leaves the cloud and either hits or misses the base plane. A new photon history is begun after each hit or miss.

If the photon is absorbed and the cloud not considered in radiative equilibrium, the photon history is terminated immediately and a new history begun.

Model Geometry

The geometry of the model used in this investigation is depicted in Figure 2-1. The model consists of a finite right circular cylinder and the infinite plane through its base. A cylindrical coordinate system has its origin at the midpoint of the base of the cylinder with the z axis coinciding with the axis of the cylinder. The reference direction from which the azimuthal coordinate angle is measured is taken as the x direction of a right handed orthogonal cartesian system whose origin and z axis coincide with those of the cylindrical system. The x direction is arbitrarily located and fixed. The direction of departure from any given point (z_1, Φ_1, r_1) is given in a spherical coordinate system centered at the point and having as its reference for azimuthal angle (θ) a direction parallel to the above mentioned x direction and as its reference for polar angle (η) a direction parallel to the axis of the cylinder. The distance in the direction (θ, η) from the point (z_1, Φ_1, r_1) to the surface of the cylinder is called the maximum path length ℓ_m. The probable distance a photon would travel

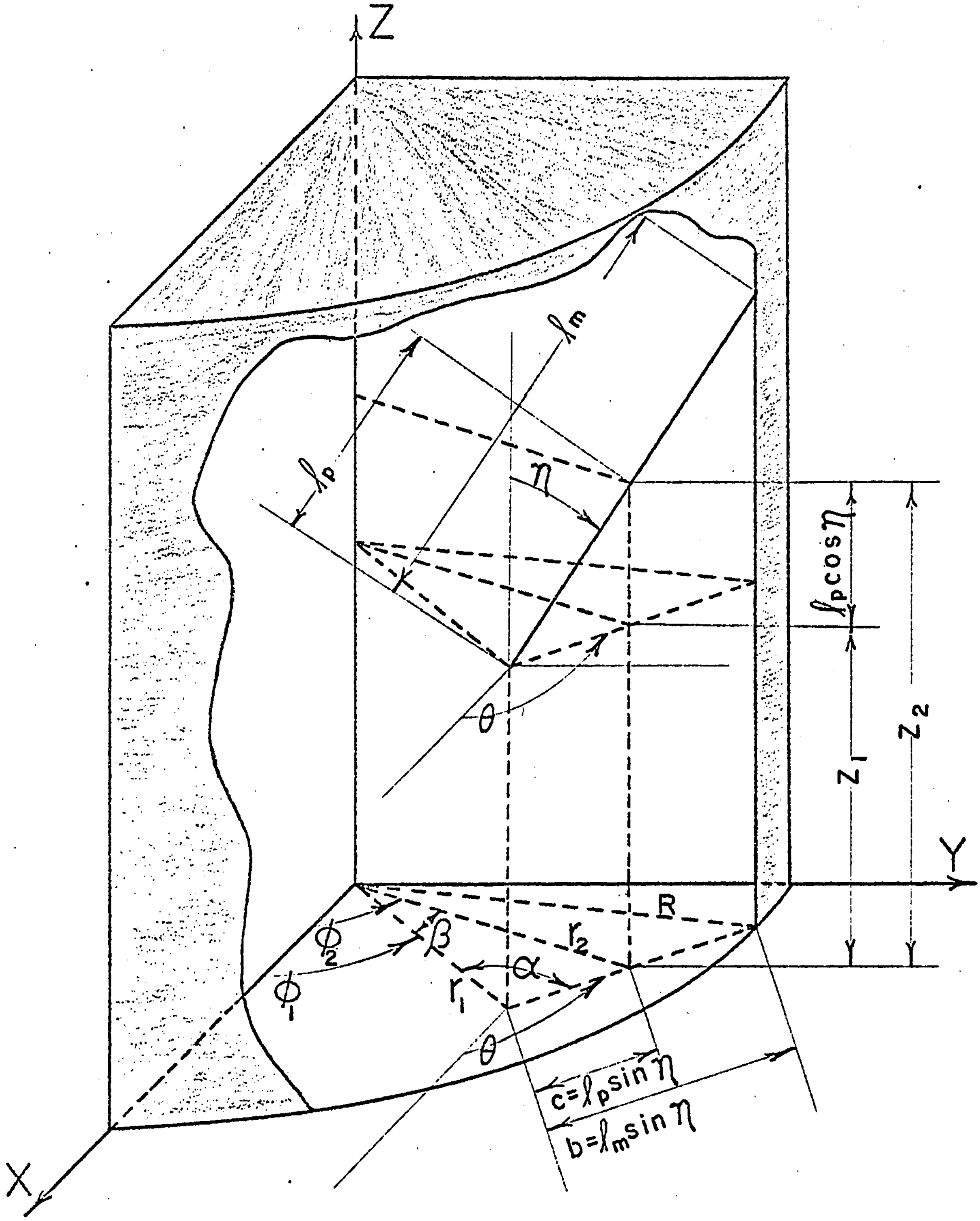

Figure 2-1. General Geometry

on any given trial is called the probable path length ℓ_p. If the probable path length is less than the maximum path length , the photon is assumed to travel a distance ℓ_p in the direction (θ, η) to a new point (z_2, Φ_2, r_2) at which a new direction of departure must be determined.

If the probable path length were greater than the maximum path length the photon would leave the cloud and would be considered to travel in a straight line until it hit the base plane $(\eta > 90^\circ)$ or be counted as a miss $(\eta \leq 90^\circ)$.

To follow photons from point to point through the cloud one must have expressions for r_2, z_2, Φ_2 in terms of r_1, z_1, Φ_1, ℓ_p, ℓ_m. These are obtained next.

The projection of the internal geometry on the base plane is shown for several values of r_1, Φ_1 and θ in Figure 2-2. Note that for given values of r_1, Φ_1 and θ the triangle with sides R, b, r_1 is completely determined. Note also that the angle θ can be considered to be the sum of the angle Φ_1 and an angle ζ where it is understood that θ is the principle value of the angle represented by this sum. Therefore

$$\zeta = \theta - \Phi_1, \ \theta > \Phi_1$$

$$\zeta = \theta - \Phi_1 + 2\pi, \ \theta < \Phi_1$$

The angle α is

$$\alpha = |\pi - \zeta|$$

Since $\cos x = \cos(-x)$

$$\cos\alpha = \cos(\pi - \zeta)$$

or

$$\cos\alpha = -\cos(\zeta)$$

Finally, substituting for ζ gives

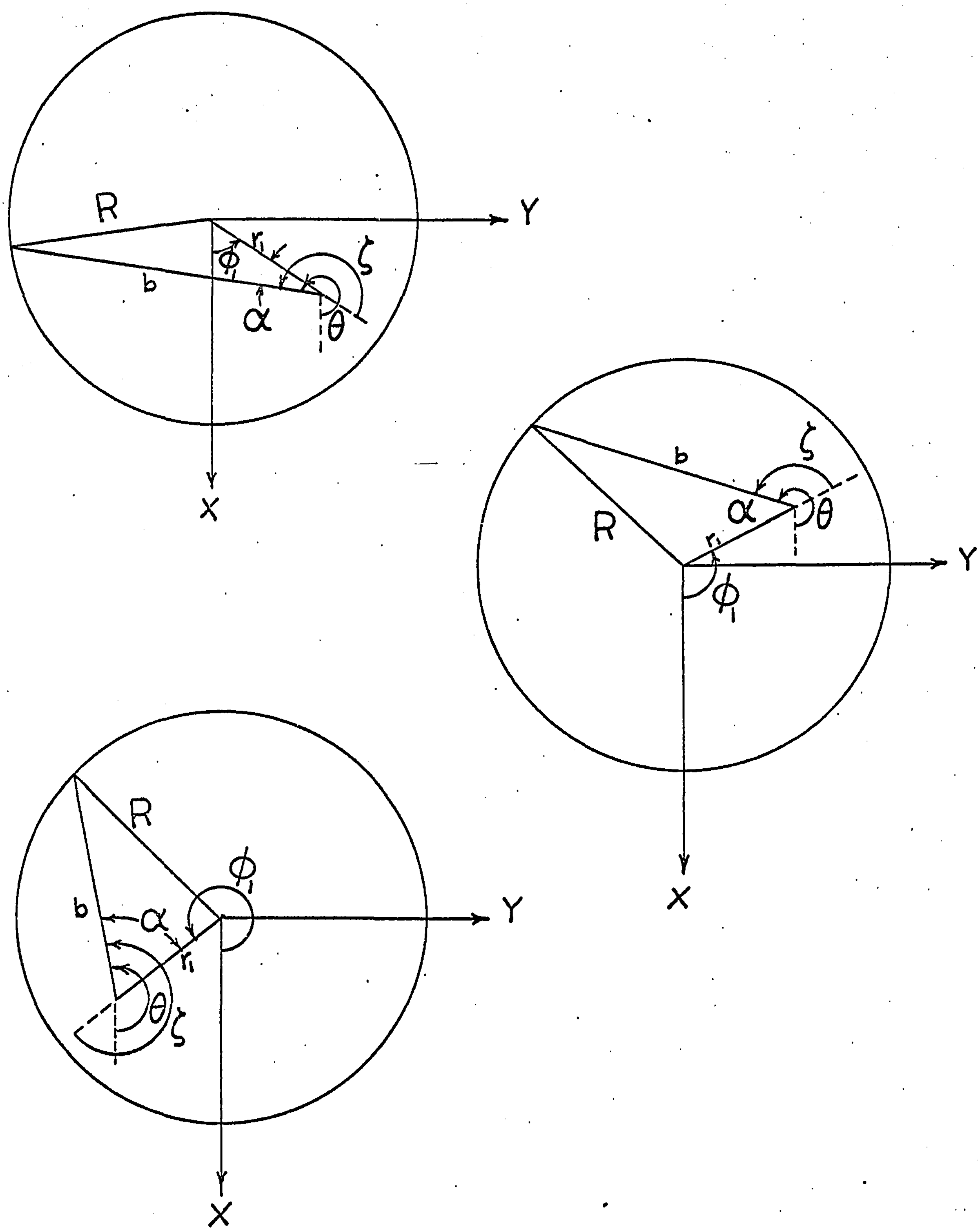

Figure 2-2. Projections of Internal Geometry

$$\cos \alpha = -\cos (\theta - \Phi_1) \tag{2-1}$$

Assuming for the moment that the maximum path length intersects the vertical surface of the cylinder, the length b represents the projection of ℓ_m on the base plane.

$$b = \ell_m \quad \sin \eta$$

Since R, r_1, and $\cos \alpha$ are known the value of b can be calculated using the law of cosines.

$$R^2 = b^2 + r_1^{\ 2} - 2br_1 \cos \alpha$$

or

$$b^2 - (2r_1 \cos \alpha)b + (r_1^{\ 2} - R^2) = 0$$

Applying the quadratic formula gives

$$b = r_1 \cos \alpha \pm (r_1^{\ 2} \cos^2\alpha + (R^2 - r_1^{\ 2}))^{\frac{1}{2}}$$

and since

$$R \geqq r_1$$

this is of the form

$$b = a \pm (a^2 + m^2)$$

Therefore since b is a scalar length and must be positive it is necessary to choose the positive root.

$$b = r_1 \cos \alpha + (r_1^{\ 2} \cos^2\alpha + (R^2 - r_1^{\ 2}))^{\frac{1}{2}} \tag{2-2}$$

The maximum path length is therefore

$$\ell_m = b/\sin \eta \tag{2-3}$$

If the direction of the path takes the photon out the top or bottom of the cylinder the value for ℓ_m as calculated above will be too large. The easiest way to determine whether this situation exists in the case of exit through the top is to compare the value of $z_1 + \ell_m$ x $\cos \eta$ and the height (H) of the cylinder. If $z_1 + \ell_m \cos \eta$ is greater than the height of the cylinder then the path leads through the top of the cylinder. The correct value for ℓ_m would then be

$$\ell_m = (H - z_1) / \cos \eta \tag{2-4}$$

If $z + \ell_m \cos \eta$ is negative, the path leads through the bottom of the cylinder. In this case

$$\ell_m = -z_1 / \cos \eta \tag{2-5}$$

It is important to notice that for given Φ_1, θ and r_1, the direction of the projection of ℓ_m on the base plane is fixed. Hence neither the distance traveled along ℓ_m nor the fact that ℓ_m intersects the top or bottom of the cylinder will have any effect on the angle α.

If a photon is scattered or absorbed at some point (r_2, Φ_2, z_2) on its path from (r_1, Φ_1, z_1), it will be as a result of the value ℓ_p, which is obtained from probability considerations, being less than ℓ_m. The path will be in the given direction, however, and its projection on the base plane will be shorter but coincide with b. This projection is shown as c in Figure 2-3. It will have the value

$$c = \ell_p \sin \eta \tag{2-6}$$

The values c, $\cos \alpha$, and r_1 completely determine the triangle with sides r_1, r_2, c. Hence the value of r_2 can be calculated using the law of cosines.

$$r_2 = + (c^2 + r_1^2 - 2cr_1 \cos \alpha)^{\frac{1}{2}} \tag{2-7}$$

The value of z_2 is simply the sum of the z_1 value of the starting point and the vertical component of ℓ_p. (Figure 2-1)

$$z_2 = z_1 + \ell_p \cos \eta \tag{2-8}$$

The azimuthal angles Φ_1 and Φ_2 are related through the angle β between r_1 and r_2. Figure 2-3 shows β. From the law of cosines

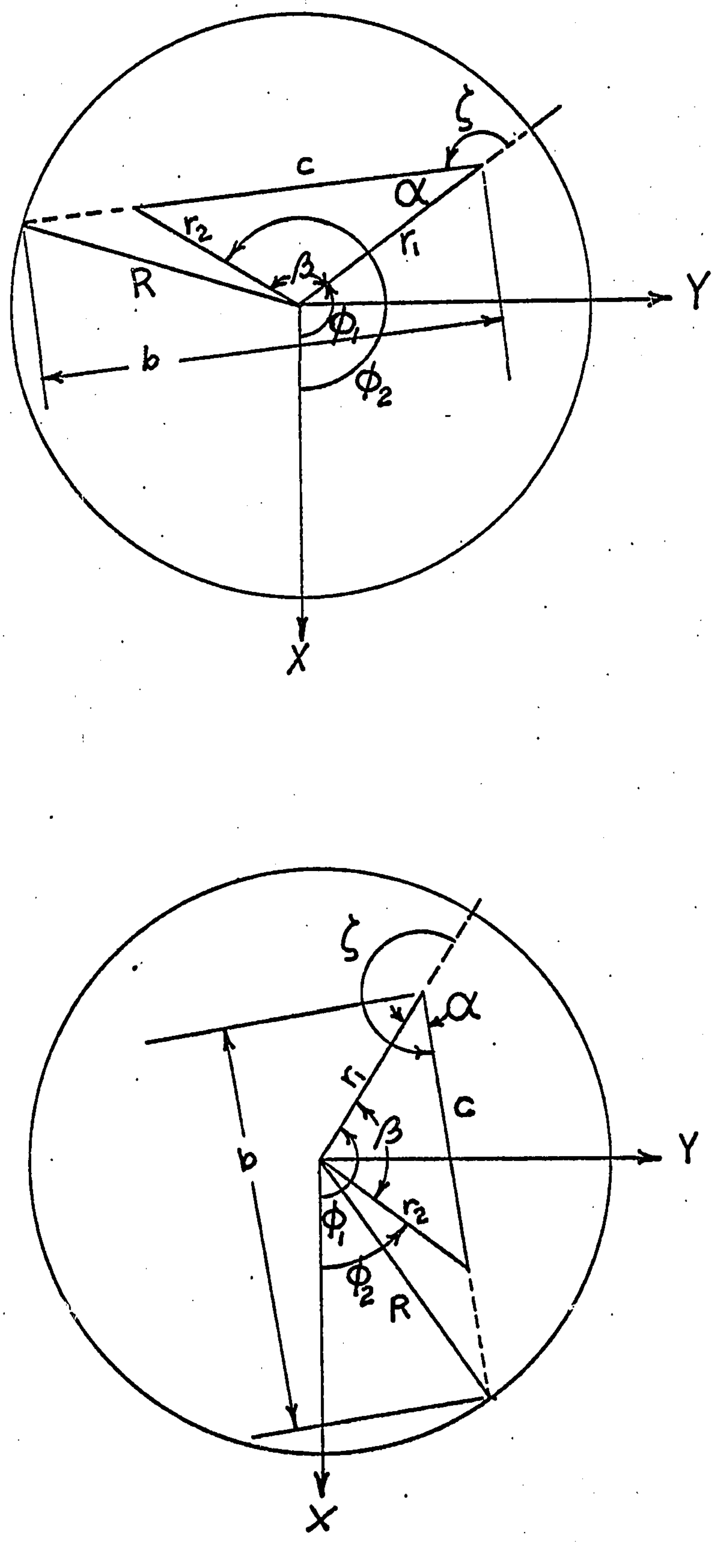

Figure 2-3. Projections of Internal Geometry

$$\cos \beta = \frac{-1}{2r_1r_2} (c^2 - r_1^{\,2} - r_2^{\,2})$$

and from the law of sines

$$\sin \beta = (c/r_2) \sin \alpha$$

In principle β could be calculated from either of the above equations. However, since some computer programming languages do not incorporate the inverse sine and inverse cosine functions but do recognize the inverse tangent it is convenient to calculate β from

$$\beta = \tan^{-1} (\sin \beta \ / \ \cos \beta)$$

$$\beta = \tan^{-1}\left[(-2cr_1 \sin \alpha) \ / \ (c^2 - r_1^{\,2} - r_2^{\,2})\right] \qquad (2\text{-}9)$$

The principle values of the angle generated by the arctangent function in a computer lie between $-\pi/2$ and $+\pi/2$. Since β has the range $0 \leqq \beta \leqq \pi$ it is necessary to add π to the angle generated by the computer if it is negative.

The value of Φ_2 can be calculated from

$$\Phi_2 = \Phi_1 + \beta \qquad 0 \leqq \zeta \leqq \pi \qquad (2\text{-}10)$$

or

$$\Phi_2 = \Phi_1 - \beta \qquad \pi \leqq \zeta \leqq 2\pi \qquad (2\text{-}11)$$

where it understood that Φ_2 is the principle value of the angle. $(0 \leqq \Phi_2 \leqq 2\pi)$

The radius to impact is derived from Figures 2-4 and 2-5 as

$$R_h = (c^2 + r_1^{\,2} - 2cr_1 \cos \alpha)^{\frac{1}{2}} \qquad (2\text{-}12)$$

where

$$c = z_1 \tan (\pi - \eta) = -z_1 \tan \eta \qquad (2\text{-}13)$$

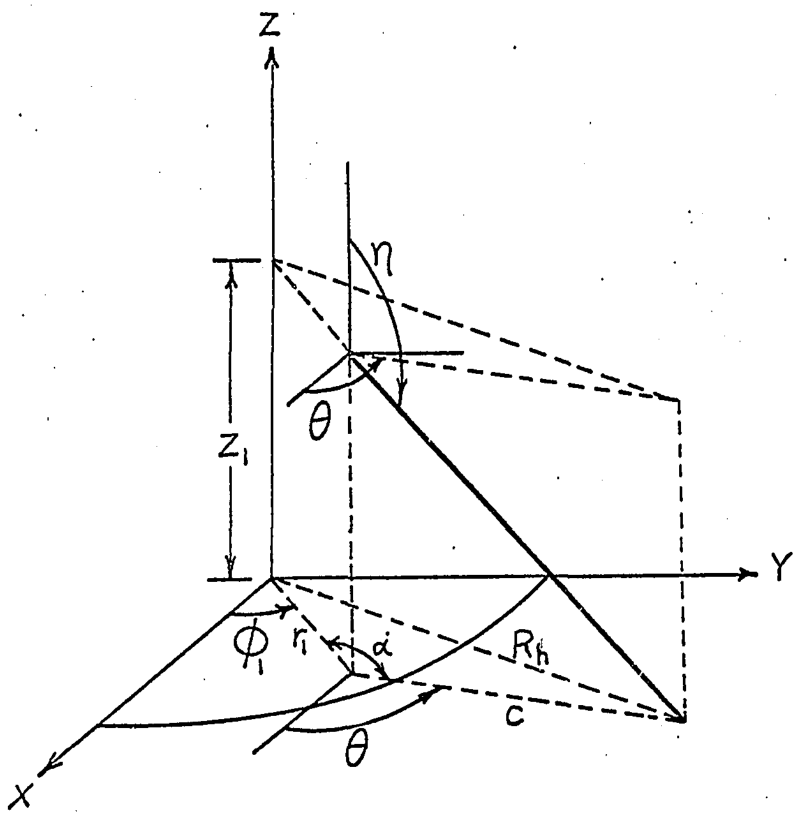

Figure 2-4. Geometry of Impact Radius

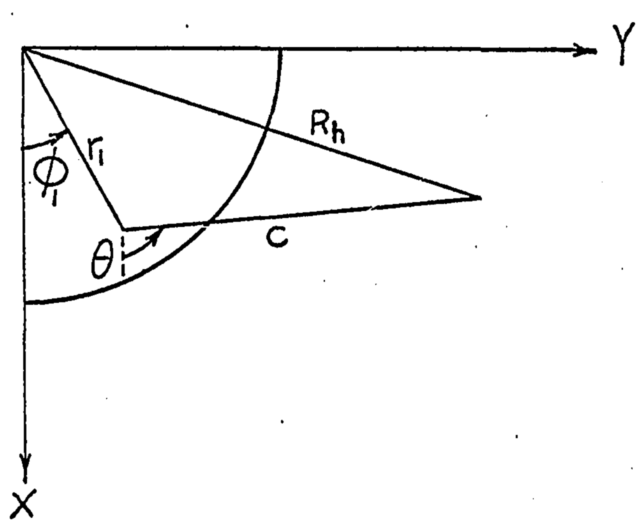

Figure 2-5. Projection of Impact Radius Geometry

CHAPTER III

THE DISTRIBUTION FUNCTIONS

Emission Point Selection

A differential volume element of a right circular cylinder can be expressed as

$$dV = r\ dr\ d\Phi\ dz$$

To select emission points in such a fashion that they will be uniformly distributed throughout the cylindrical cloud requires that the ratio of the number of points in dV to the total number of points selected be the same as the ratio of dV to the cylinder volume.

Hence

$$\frac{N_{dV}}{N_T} = \frac{r\ dr\ d\Phi\ dz}{\pi R^2 H}$$

The fact that

$$\int_0^H \int_0^{2\pi} \int_0^R \frac{r\ dr\ d\Phi\ dz}{\pi R^2 H} = 1$$

and that

$$f(r,\ \Phi,\ z) = \frac{r}{\pi R^2 H} \geq 0$$

makes $f(r, \Phi, z)$ the joint probability density function. Since $f(r, \Phi, z)\ dr\ d\Phi\ dz$ can be written as

$$\left(\frac{2r dr}{R^2}\right)\left(\frac{d\Phi}{2\pi}\right)\left(\frac{dz}{H}\right)$$

r, Φ, z are independent variables in the probability sense. Hence their individual distribution functions are

$$F(r) = \int_0^r \frac{2r}{R^2}\, dr = \frac{r^2}{R^2}$$

$$F(\Phi) = \int_0^{\Phi} \frac{d\Phi}{2\pi} = \frac{\Phi}{2\pi}$$

$$F(z) = \int_0^{z} \frac{dz}{H} = \frac{z}{H}$$

It is shown in Appendix B that the required probability distribution can be satisfied by taking the distribution function equal to a large number of random numbers. Therefore

$$r = R\sqrt{R_r} \tag{3-1}$$

$$\Phi = 2\pi\, R_{\Phi} \tag{3-2}$$

$$z = H\, R_z \tag{3-3}$$

where R_x denotes a random number for x.

The selection of emission points uniformly distributed over the base of the cylinder is accomplished by setting z = 0.

Direction of Emission from a Volume Element

For isotropic emission from a volume element the number of photons reaching an element of the surface area of a unit sphere surrounding the volume element must be proportional to the area of the surface element. Hence the ratio of the number hitting a differential surface element to the total number of photons hitting the sphere must equal the ratio of the area of the differential element to the area of the sphere. From Figure 3-1

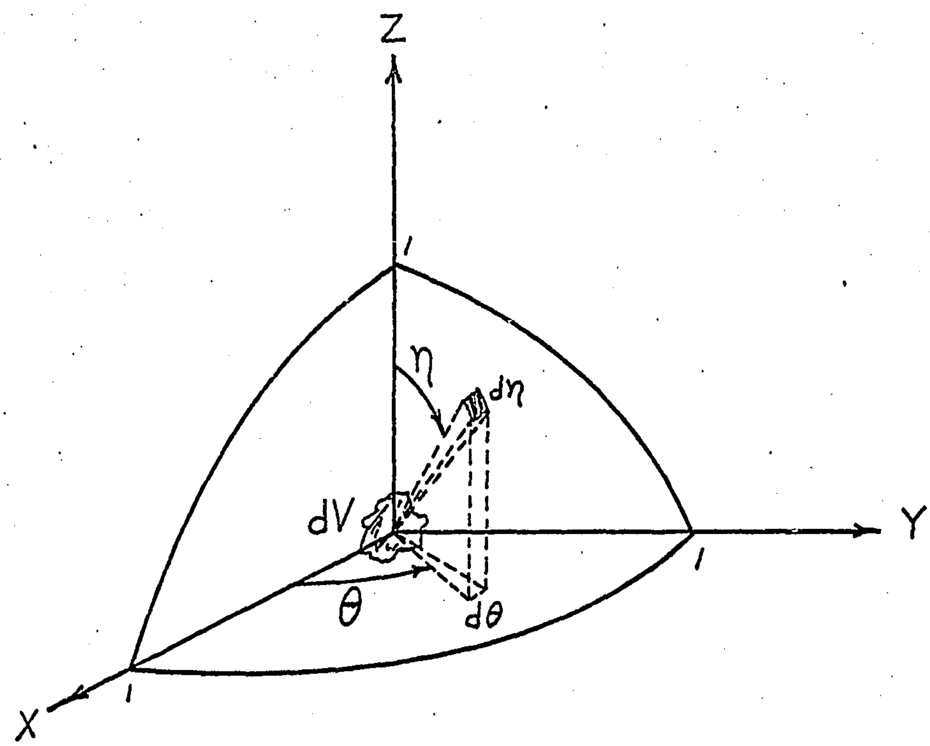

Figure 3-1. Isotropic Scattering or Emission from Volume Element

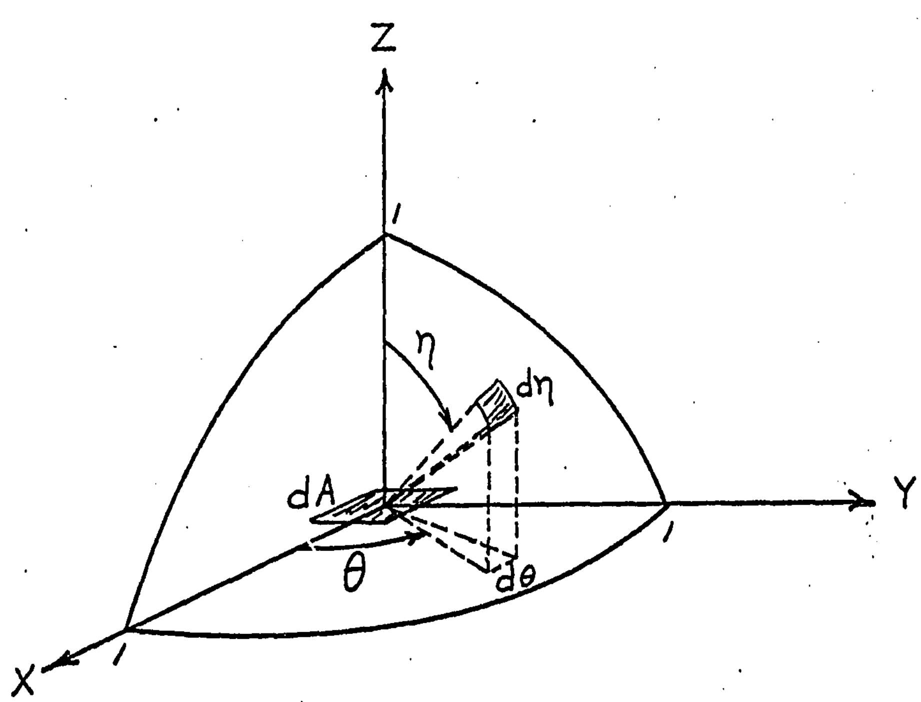

Figure 3-2. Diffuse Emission from a Surface Element

$$\frac{N_s}{N_T} = \frac{\sin \eta \, d\eta \, d\theta}{4\pi}$$

The fact that

$$\int_0^{2\pi}\int_0^{\pi} \frac{\sin \eta \, d\eta \, d\theta}{4\pi} = 1$$

and

$$\frac{\sin \eta \, d\eta \, d\theta}{4\pi} \geqq 0$$

and

$$\frac{\sin \eta \, d\eta \, d\theta}{4\pi} = \left(\frac{\sin \eta \, d\eta}{2}\right)\left(\frac{d\theta}{2\pi}\right)$$

shows that the probability density functions for η and θ are

$$f(\eta) = \frac{\sin \eta}{2} \quad , \quad f(\theta) = \frac{1}{2\pi}$$

These can be satisfied by setting the corresponding distribution functions equal to random numbers. Hence

$$\cos \eta = 1 - 2R_\eta \tag{3-4}$$

$$\theta = 2\pi R_\theta \tag{3-5}$$

Direction of Emission of a Photon from a Diffuse Surface

In the case of a diffuse emission from a surface the intensity (I) of the radiation is independent of direction. The geometry under consideration is shown in Figure 3-2. Since the intensity is not a function of direction the energy per unit time incident on a differential surface element of a unit hemisphere above dA can be expressed as

$$dE = I \cos \eta \, d\omega dA = I \sin \eta \cos \eta \, d\eta \, d\theta \, dA$$

The total energy per unit time incident on the surface of the hemisphere is then

$$E = \int_{2\pi} dE = dA \, I \int_0^{2\pi}\int_0^{\pi/2} \sin \eta \cos \eta \, d\eta \, d\theta$$

$$E = 2\pi \, dA \left[\frac{\sin^2}{2}\right]_0^{\pi/2} = \pi dAI$$

The fraction of the total number of photons or bundles of equal energy emitted by dA which strike ds, a differential surface element is

$$\frac{N_{ds}}{N_T} = \frac{dE}{E} = \frac{I \sin \eta \cos \eta \, d\eta \, d\theta \, dA}{\pi \, I \, dA}$$

$$\frac{N_{ds}}{N_T} = \frac{\sin \eta \cos \eta \, d\eta \, d\theta}{\pi}$$

Noting that

$$\int_0^{2\pi} \int_0^{\pi/2} \frac{\sin \eta \cos \eta \, d\eta \, d\theta}{\pi} = 1$$

and that

$$\frac{\sin \eta \cos \eta}{\pi} \geqq 0$$

gives the probability density functions for η and θ as

$$f(\eta) = 2 \sin \eta \cos \eta$$

$$f(\theta) = \frac{1}{2\pi}$$

Hence

$$F(\theta) = \frac{\theta}{2\pi}$$

and

$$F(\eta) = \sin^2\eta$$

These can be satisfied by taking

$$\theta = 2\pi R_\theta \tag{3-6}$$

and

$$\sin^2\eta = R_\eta$$

Since $\sin^2\eta = 1 - \cos^2\eta$ one could also take

$$\cos \eta = \sqrt{1 - R_\eta}$$

or since $1 - R_\eta$ is just another set of random numbers

$$\cos \eta = \sqrt{R_\eta} \tag{3-7}$$

Probable Path Length

In traversing a path through an absorbing and scattering medium a beam of photons is attenuated in proportion to its intensity and the optical depth of the path.

Let N be the number of photons at length ℓ

N_o be the number of photons at $\ell = o$

β be the mass extinction coefficient

ρ be the mass density of the particle cloud

Then

$$dN = -\rho\beta N d\ell$$

Integrating between o and ℓ, assuming $\rho\beta$ constant gives

$$\int_{N_o}^{N} \frac{dN}{N} = -\rho\beta \int_{o}^{\ell} d\ell$$

and

$$\ln (N/N_o) = -\rho\beta\ell$$

The fraction of the number of photons originally incident which remain at ℓ is then

$$N/N_o = e^{-\rho\beta\ell}$$

The fraction removed at or prior to ℓ is thus

$$1 - N/N_o = 1 - e^{-\rho\beta\ell}$$

This can be thought of as the probability that the path length will be less than or equal to ℓ, and as such is the distribution function for ℓ.

$$F(\ell) = 1 - e^{-\rho\beta\ell}$$

Hence one may choose values of probable path length ℓ_p from

$$R_{\ell_p} = 1 - e^{-\rho\beta\ell_p}$$

giving

$$\ell_p = -\frac{1}{\rho\beta} \ln (1 - R_{\ell_p})$$

or since $1 - R_{\ell_p}$ is simply another set of uniformly distributed random numbers

$$\ell_p = -\frac{1}{\rho\beta} \ln R_{\ell_p} \tag{3-8}$$

In this work a principle parameter is the optical diameter of the cylinder. The cylinder is given a physical diameter of two. Thus

$$\rho\beta D = TAU = 2\rho\beta$$

Substituting in (3-8) for $\rho\beta$ gives

$$\ell_p = -\frac{2}{TAU} \ln R_{\ell_p} \tag{3-9}$$

It should be noted that this represents the path length in a uniform medium. Since the cylinder has definite but free boundaries, if ℓ_p is greater than the distance to the cylinder boundaries, the photon is considered to exit the cloud.

Scattering Direction

The scattering function $s(\eta,\theta)$ is defined such that the probability of a photon, which is scattered by a particle, leaving in a direction contained in the solid angle $d\omega'$ about a direction (η,θ) with respect to the direction of incidence is given by

$$s(\eta,\theta) \frac{d\omega'}{4\pi} \tag{3-10}$$

The geometry is illustrated in Figure 3-3. Expression (3-10) can be written as

$$\frac{1}{4\pi}\, s(\eta,\theta)\ \sin\eta\ d\eta\ d\theta$$

which can be written

$$\left(\frac{1}{2}\, s(\eta)\ \sin\eta\ d\eta\right)\left(\frac{1}{2\pi}\, d\theta\right) \tag{3-11}$$

for the axisymmetric scattering functions used in this work. In view of (3-11) and since (3-10) integrated over 4π is equal to one,

$$f(\eta) = \frac{1}{2}\, s(\eta)\ \sin\eta$$

$$f(\theta) = \frac{1}{2\pi}$$

are probability density functions for η and θ respectively.

Thus

$$R_\theta = \frac{1}{2\pi}\int_0^\theta d\theta = \frac{\theta}{2\pi} \tag{3-12}$$

and

$$R_\eta = \frac{1}{2}\int_0^\eta s(\eta)\ \sin\eta\ d\eta \tag{3-13}$$

For isotropic scattering $s(\eta) = 1$ so that

$$R_\eta = \frac{1}{2}\int_0^\eta \sin\eta\ d\eta$$

or

$$\cos\eta = 1 - 2\,R_\eta \tag{3-14}$$

which is the same as (3-4) for volumetric emission.

As an approximation to the anisotropic case, one can plot the graph of $s(\eta)\sin\eta$ for $0 \le \eta \le \pi$ as in Figure 3-4 and approximate the graph by triangles and rectangles as in Figure 3-5. The sum of the areas of the triangles and rectangles is the total area (A_T) under the curve. Hence one can let

$$A(\eta) = R_\eta\, A_T$$

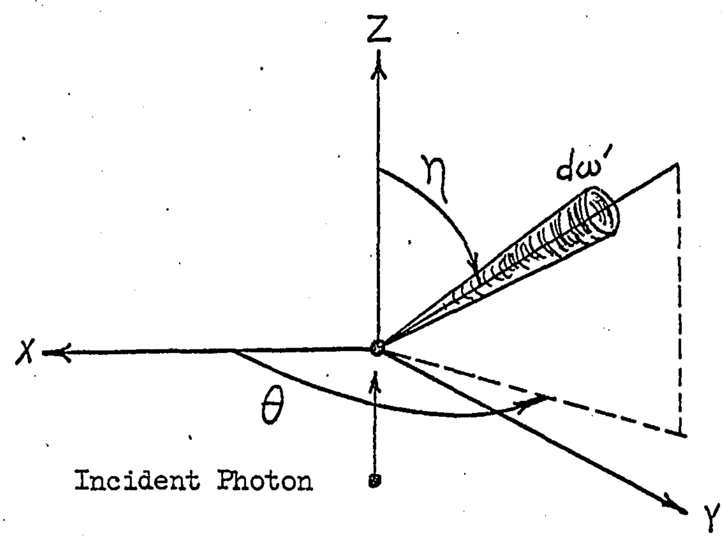

Figure 3-3. Geometry of Scattering

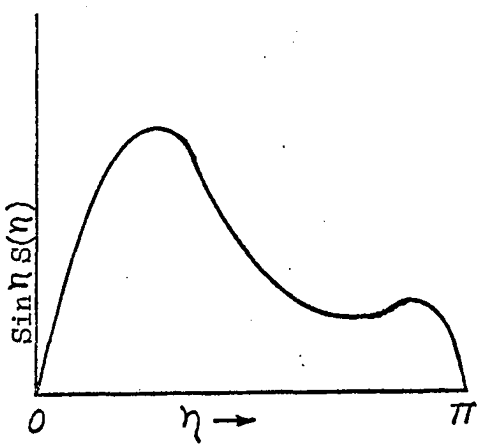

Figure3-4. Graph of Sin η S(η)

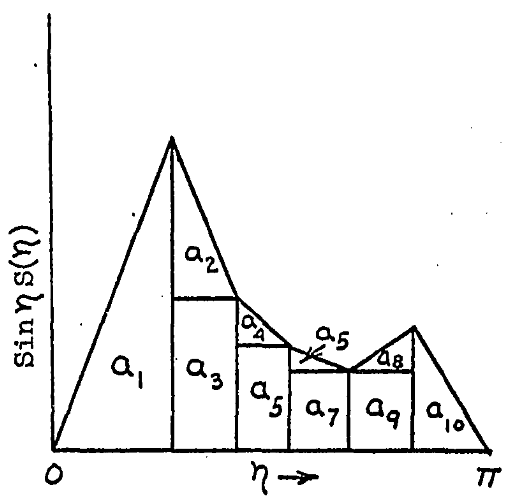

Figure 3-5. Approximation of Graph of Sin η S(η)

and solve for the η which gives the correct value for A. This is the approach used in this work.

CHAPTER IV

ANISOTROPIC SCATTERING

Coordinate Transformation for Anisotropic Scattering

For anisotropic scattering the scattering function is symmetric with respect to the incident direction of the photon and can be described in terms of a polar angle (η) measured with respect to the incident direction. Since the incident direction will not normally coincide with the vertical it is necessary to obtain relations for the polar and azimuthal angles (η_1, θ_1) of the direction of scatter as measured in the usual reference coordinate system in terms of the direction of scatter (η, θ) measured in the anisotropic scattering system and the direction of incidence (η_o, θ_o) measured in the reference system. The angles involved are illustrated in Figure 4-1.

Consider a unit vector in the direction of scatter (P). Let R_x, R_y, R_z be its components in the scattering coordinates and R_X, R_Y, R_Z be its components in the reference coordinates.

Then

$$\begin{aligned} R_x &= \sin \eta \cos \theta \\ R_y &= \sin \eta \sin \theta \\ R_z &= \cos \eta \end{aligned} \qquad (4\text{-}1)$$

and

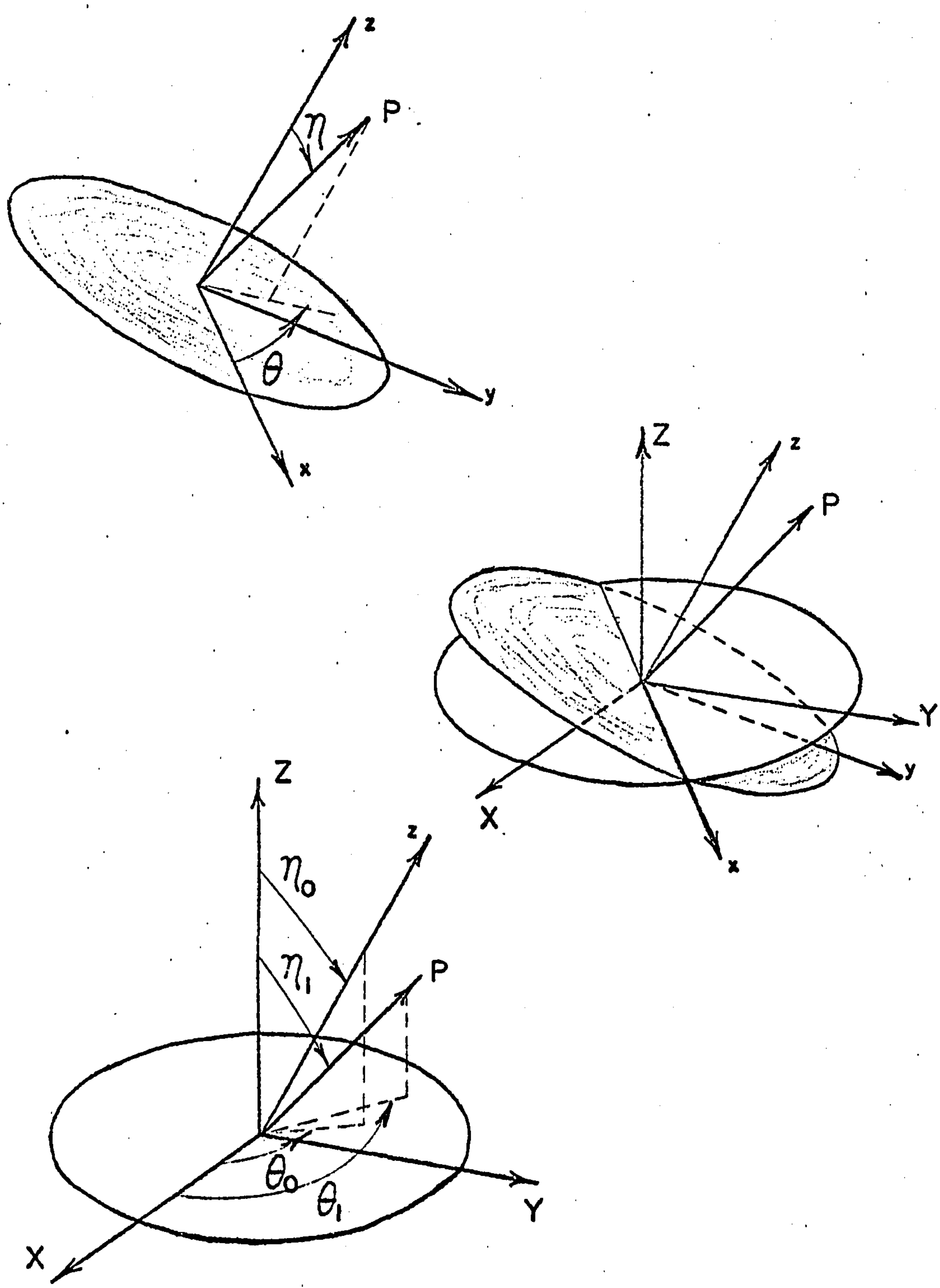

Figure 4-1. Anisotropic Scattering Coordinate Systems

$$R_X = R_x \sin\theta_o + R_y \cos\eta_o \cos\theta_o + R_z \sin\eta_o \cos\theta_o \quad (4\text{-}2)$$

$$R_Y = -R_x \cos\theta_o + R_y \cos\eta_o \sin\theta_o + R_z \sin\eta_o \sin\theta_o$$

$$R_Z = \qquad - R_y \sin\eta_o \qquad + R_z \cos\eta_o$$

In equations (4-2) use has been made of the Eulerian angles for locating one set of Cartesian coordinates with reference to another set having the same origin.

The components in the reference system can also be expressed as

$$\begin{aligned} R_X &= \sin\eta_1 \cos\theta_1 \\ R_Y &= \sin\eta_1 \sin\theta_1 \\ R_Z &= \cos\eta_1 \end{aligned} \quad (4\text{-}3)$$

Hence from (4-3), using the relation

$$\tan x = \sin x / \cos x$$

one obtains

$$\theta_1 = \tan^{-1}(R_Y/R_X) \quad (4\text{-}4)$$

$$\eta_1 = \tan^{-1}\left[R_X/(R_Z \cos\theta_1)\right] \quad (4\text{-}5)$$

The solution is obtained by solving equations (4-1) and (4-2) for R_X, R_Y, and R_Z and using these values in (4-4) and (4-5).

Approximation Technique

The method of approximating the distribution function for anisotropic scattering is outlined in the last section of Chapter III. This section is devoted to the derivation of specific expressions for the polar angle η.

The expressions used for calculating η in the approximation for anisotropic scattering are derived with the aid of Figure 4-2. By comparing the value of the product of the total area (A_T) and the ran-

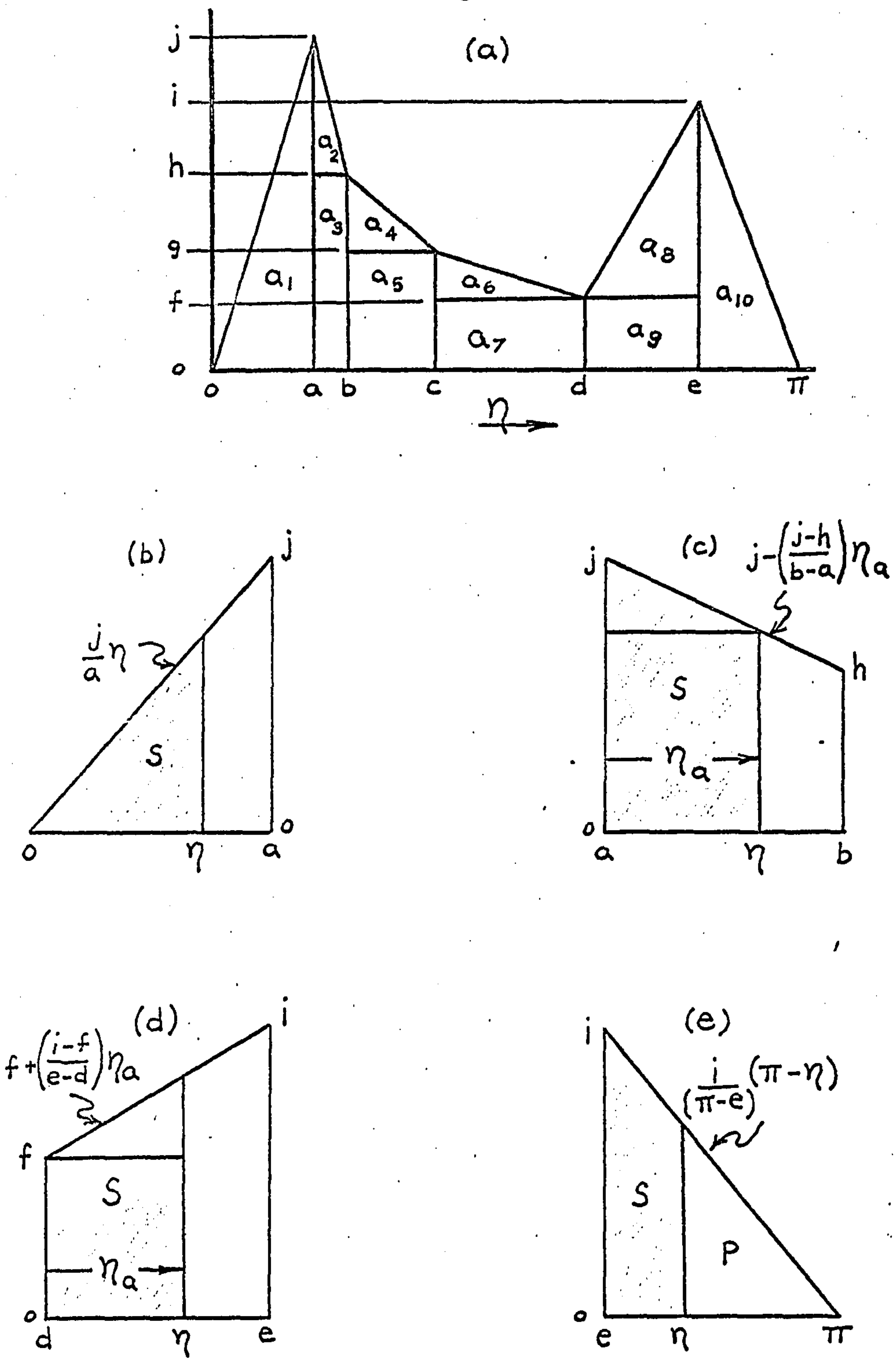

Figure 4-2. Anisotropic Scattering Approximation

dom number (R_η) with the partial sums of the individual areas in Figure 4-2a one can determine the points between which η must lie. The problem thus is reduced to deriving an expression for η corresponding to each of the conditions in Figure 4-2b, c, d, e.

Consider Figure 4-2b. s is the area of a triangle.

$$s = R_\eta A_T = \frac{1}{2} \eta^2 \frac{j}{a}$$

and since $0 \le \eta$

$$\eta = + \left(2 R_\eta A_T \frac{a}{j}\right)^{\frac{1}{2}} \qquad (4\text{-}6)$$

Equation (4-6) gives the correct value for η less than a.

The expressions for η between a and b, b and c, and c and d will be similar. The expression valid for $a < \eta < b$ is derived below.

Consider Figure 4-2c. The area s is the sum of the areas of a triangle and a rectangle. Hence

$$s = R_\eta A_T - a_1 = \frac{1}{2}\left[j - \left(j - \left(\frac{j - h}{b - a}\right)\eta_a\right)\right]\eta_a + \left(j - \left(\frac{j - h}{b - a}\right)\eta_a\right)\eta_a$$

$$= j\eta_a - \frac{1}{2}\left(\frac{j - h}{b - a}\right)\eta_a^{\,2}$$

Therefore

$$\eta_a^{\,2} - 2j\left(\frac{b - a}{j - h}\right)\eta_a + 2\left(\frac{b - a}{j - h}\right)(R_\eta A_T - a_1) = 0$$

Letting

$$s_2 = (b - a) \,/\, (j - h)$$

gives

$$\eta_a^{\,2} - 2j\, s_2 \eta_a + 2\, s_2\, (R_\eta A_T - a_1) = 0$$

Applying the quadratic formula gives

$$\eta_a = js_2 \pm \left[(js_2)^2 - 2s_2\,(R_\eta A_T - a_1)\right]^{\frac{1}{2}} \qquad (4\text{-}7)$$

Now

$$js_2 = j(\frac{b - a}{j - h}) > j(\frac{b - a}{j}) = b - a$$

And since

$$0 \le \eta_a \le (b - a)$$

One must choose the negative root in Equation (4-7).

Thus

$$\eta = a + js_2 - \left[(js_2)^2 - 2s_2 (R_\eta A_T - a_1)\right]^{\frac{1}{2}} \tag{4-8}$$

is the expression sought.

For $b < \eta < c$

$$\eta = b + hs_4 - \left[(hs_4)^2 - 2s_4(R_\eta A_T - c_1)\right]^{\frac{1}{2}} \tag{4-9}$$

$$s_4 = (c - b) / (h - g)$$

$$c_1 = a_1 + a_2 + a_3$$

For $c < \eta < d$

$$\eta = c + gs_6 - \left[(gs_6)^2 - 2s_6 (R_\eta A_T - c_2)\right]^{\frac{1}{2}} \tag{4-10}$$

$$s_6 = (d - c) / (g - f)$$

$$c_2 = a_1 + a_2 + a_3 + a_4 + a_5$$

The expression for $d < \eta < e$ is derived using Figure 4-2d. The area(s) is again considered as the sum of the areas of a rectangle and a triangle.

Defining $$c_3 = c_2 + a_6 + a_7$$

$$s = R_\eta A_T - c_3 = \eta_a f + \frac{1}{2} \eta_a (\frac{i - f}{e - d}) \eta_a$$

or

$$\eta_a^{\ 2} + 2f\ s_8\ \eta_a - 2s_8 (R_\eta A_T - c_3) = 0 \tag{4-11}$$

where

$$s_8 = (e - d) / (i - f)$$

Solving (4-11) for η_a gives

$$\eta_a = -fs_8 + \left[(fs_8)^2 + 2s_8\,(R_\eta\, A_T - c_3)\right]^{\frac{1}{2}} \tag{4-12}$$

where the positive root is required because of the negative first term and the necessity for positive η_a.

Thus

$$\eta = d - fs_8 + \left[(fs_8)^2 + 2s_8\,(R_\eta\, A_T - c_3)\right]^{\frac{1}{2}} \tag{4-13}$$

The final expression for $e < \eta < \pi$ comes from Figure 4-2e.

$$p = \frac{1}{2}\,(\pi - \eta)\,\frac{i}{(\pi - e)}\,(\pi - \eta) = (1 - R_\eta)A_T$$

$$(\pi - \eta)^2 = 2(\pi - e)(1 - R_\eta)A_T/i$$

$$\eta = \pi - \left[2(\pi - e)(1 - R_\eta)A_T/i\right]^{\frac{1}{2}}$$

Defining

$$s_{10} = \left[2(\pi - e)A_T/i\right]^{\frac{1}{2}}$$

$$\eta = \pi - s_{10}\,(1 - R_\eta)^{\frac{1}{2}} \tag{4-14}$$

The Anisotropic Scattering Function

The anisotropic scattering function used in this work is believed to be representative of the scattering function of a distribution of aluminum oxide particles in a rocket exhaust. Bartky and Bauer in reference (24) present scattering function curves for two representative particle distributions at a temperature of 1700° C and for several wavelengths of radiation. The curves all have the same general shape.

The scattering function chosen for this work has the same general shape as those of Bartky and Bauer and is shown in Figure 4-3. The shape is assumed not to vary with temperature or wavelength of radiation.

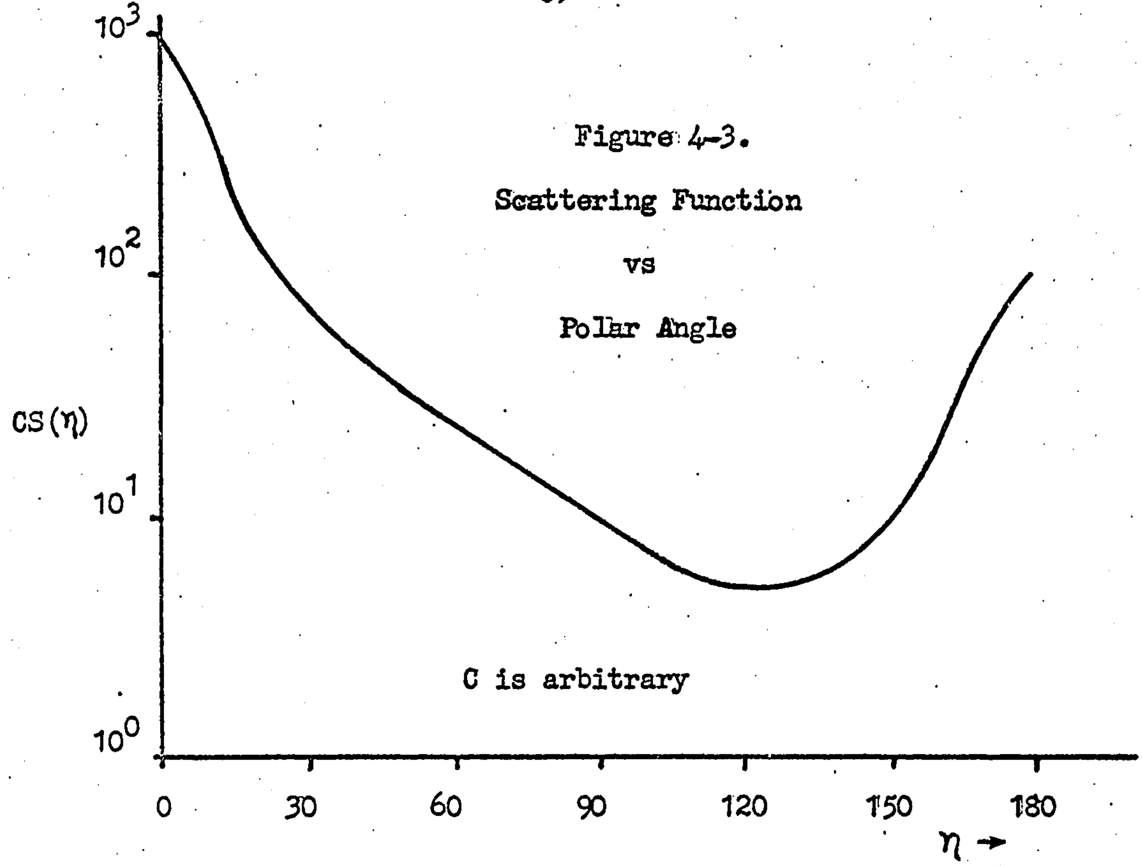

Figure 4-3.
Scattering Function
vs
Polar Angle
C is arbitrary
$CS(\eta)$
10^3
10^2
10^1
10^0
0
30
60
90
120
150
180
$\eta \rightarrow$

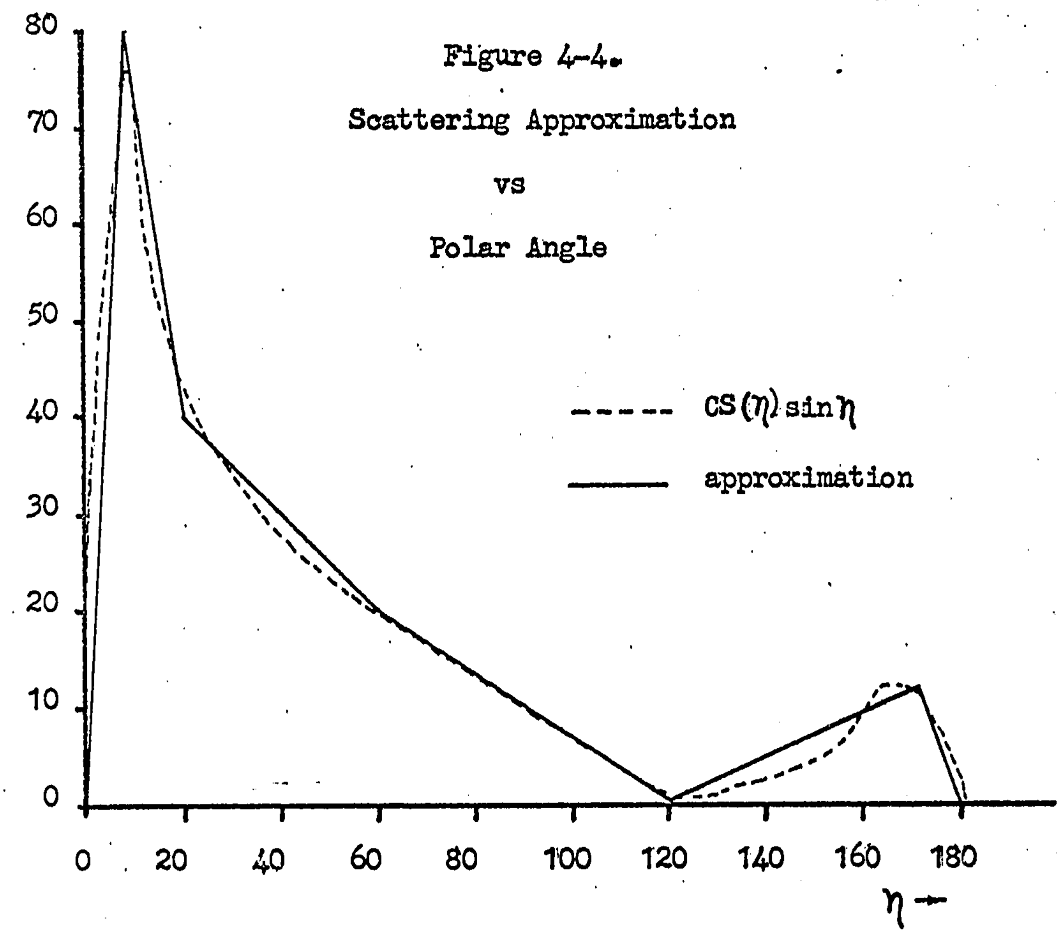

Figure 4-4.
Scattering Approximation
vs
Polar Angle
$CS(\eta)\sin\eta$
approximation
80
70
60
50
40
30
20
10
0
0
20
40
60
80
100
120
140
160
180
$\eta \rightarrow$

The scattering function approximation as described in the preceding section is applied (see Figure 4-4) giving the following values for the approximation parameters.

a =	8	f =	1
b =	20	g =	20
c =	60	h =	40
d =	120	i =	12
e =	170	j =	80

Rayleigh Scattering Approximation

The Rayleigh scattering function is commonly expressed as $\frac{3}{4}(1 + \cos^2\eta)$ where η is the polar angle between the direction of incidence and the direction of scatter. For this scattering function the probability density function for η is

$$f(\eta) = \frac{3}{8}(1 + \cos^2\eta)\,\sin\eta \tag{4-15}$$

Applying the scattering approximation to (4-15), see Figure 4-5, gives the following values for the approximation parameters.

a =	45	f =	.98
b =	45.01[1]	g =	1.1395[1]
c =	45.02[1]	h =	1.1397[1]
d =	90	i =	1.140
e =	135	j =	1.140

---

[1]These values are essentially 45 or 1.140. They are used to eliminate two sets of triangles and rectangles from the approximation without encountering internal difficulties which would occur in the computer program if b = c = a and g = h = j.

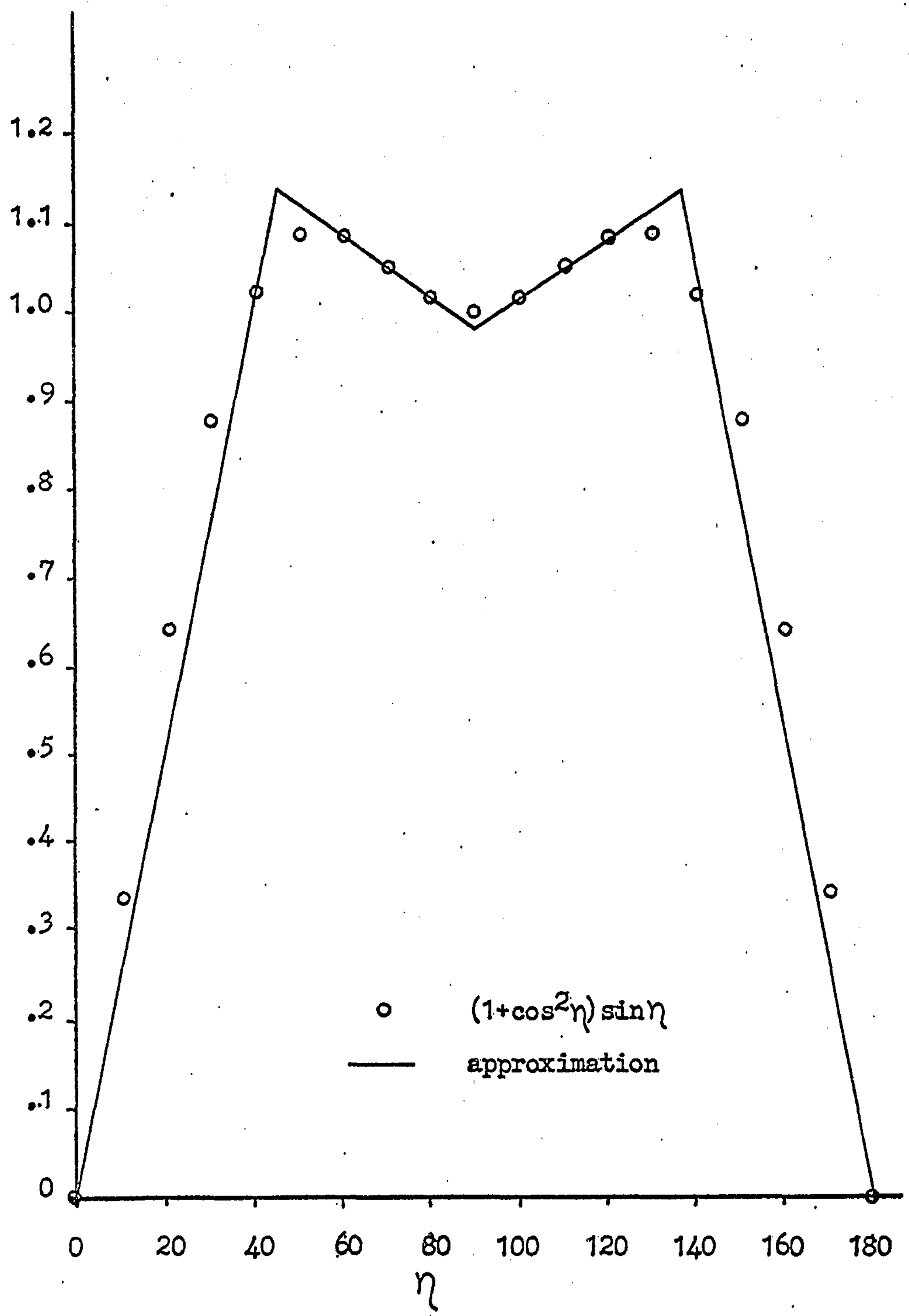

Figure 4-5. Rayleigh Scattering Approximation

CHAPTER V

NUMERICAL DATA

The numerical data presented in this section consists of the computer output for the various cases considered. The data is presented in tabular (computer printout) and graphical form.

The computer output listings are largely self explanatory. The values indicated for A through J are the parameters for the anisotropic scattering approximation described in Chapter IV. The number of emissions corresponds to the number of photons traced from original emission to exit from the cloud. The number "OUTSIDE" is the number of hits in the base plane outside the area covered by the rings.

In the case of emission from the surface the value given for each ring is the ratio of the number of hits per unit area in the nth ring divided by the number of emissions per unit area from the base surface. This corresponds to spectral flux incident on ring n divided by the spectral flux emitted by the surface. It will be called flux ratio.

For emission from the cloud the value given for the nth ring is the number of hits in ring n divided by the product of the number of original emissions and a factor (2n - 1). Flux calculations require the (2n - 1) factor. The ratio of hits in ring n to the number of original emissions corresponds to the spectral energy incident on ring n divided by the spectral energy leaving the cloud. It will be called energy ratio.

The graphical presentations are flux ratio vs radius ratio and energy ratio vs radius ratio. The radius ratio is the radius in the base plane, from the center of the cloud to the point considered, divided by the radius of the cloud. The point for each ring is plotted at a radius ratio corresponding to the radius of the areal bisector of the ring. The curve through the points is the author's estimate of best fit. The cases considered are listed in Tables V-1 and V-2.

TABLE V-1

CASES CONSIDERED FOR EMISSION
FROM CYLINDRICAL CLOUD

τ	H/D	σ/β	SCAT	Pages
.5	5	1	I	41,67
1	5	1	I	42,67
2	5	1	I	43,68
2	10	1	I	44,68
2	20	1	I	45,69
2	5	1	A	46,69
5	5	1	I	47,70
5	5	1	A	48,71
10	5	1	I	49,72

TABLE V-2

CASES CONSIDERED FOR EMISSION FROM BLACK SURFACE AT BASE OF CYLINDER

τ	H/D	σ/β	SCAT	RADEQ	Pages
.5	5	1	I	-	50,73
.5	5	1	A	-	51,74
1	5	1	I	-	52,75
1	5	1	A	-	53,76
1	5	1	R	-	54,77
2	5	1	I	-	55,78
2	5	1	A	-	56,79
2	5	1	R	-	57,80
2	10	1	I	-	58,81
2	10	1	A	-	59,82
2	20	1	I	-	60,83
2	5	.5	I	No	61,84
2	5	.5	A	Yes	62,85
5	5	1	I	-	63,86
5	5	1	A	-	64,87
10	5	1	I	-	65,88
10	5	1	A	-	66,89

EMISSION FROM CYLINDRICAL CLOUD

CYLINDER OPTICAL DEPTH	0.500
HEIGHT TO DIAMETER RATIO	5.000
BASE HEIGHT TO DIAMETER RATIO	-0.000
SCATTERING TO EXTINCTION RATIO	1.000
ISOTROPIC SCATTERING	

EMISSIONS	REEMISSIONS	ABSORPTIONS	SCATTERINGS	MISSES	OUTSIDE
200000	0	0	79228	100144	32173

HITS/EMISSIONS/(2N-1), RING WIDTH= 0.50R

1	0.01501000	2	0.01291500	3	0.00545300	4	0.00314714
5	0.00215389	6	0.00158182	7	0.00125923	8	0.00098800
9	0.00081765	10	0.00066000	11	0.00054690	12	0.00047804
13	0.00039420	14	0.00036537	15	0.00030897	16	0.00028161
17	0.00023894	18	0.00020643	19	0.00020149	20	0.00017551
21	0.00015500	22	0.00014558	23	0.00012444	24	0.00012074
25	0.00010949	26	0.00009324	27	0.00009019	28	0.00007891
29	0.00007842	30	0.00006864				

EMISSION FROM CYLINDRICAL CLOUD

CYLINDER OPTICAL DEPTH	1.000
HEIGHT TO DIAMETER RATIO	5.000
BASE HEIGHT TO DIAMETER RATIO	-0.000
SCATTERING TO EXTINCTION RATIO	1.000
ISOTROPIC SCATTERING	

EMISSIONS	REEMISSIONS	ABSORPTIONS	SCATTERINGS	MISSES	OUTSIDE
200000	0	0	160497	100330	34578

HITS/EMISSIONS/(2N-1), RING WIDTH= 0.50R

1	0.01430500	2	0.01209666	3	0.00460400	4	0.00278286
5	0.00197500	6	0.00144682	7	0.00117615	8	0.00094067
9	0.00077559	10	0.00065868	11	0.00055857	12	0.00047609
13	0.00039800	14	0.00036241	15	0.00030172	16	0.00027387
17	0.00024803	18	0.00021843	19	0.00020203	20	0.00017718
21	0.00015610	22	0.00015419	23	0.00013100	24	0.00012191
25	0.00012041	26	0.00010324	27	0.00008604	28	0.00008355
29	0.00007561	30	0.00007492				

43

EMISSION FROM CYLINDRICAL CLOUD

CYLINDER OPTICAL DEPTH	2.00C
HEIGHT TO DIAMETER RATIO	5.00C
BASE HEIGHT TO DIAMETER RATIO	-0.000
SCATTERING TO EXTINCTION RATIO	1.000
ISOTROPIC SCATTERING	

EMISSIONS	REEMISSIONS	ABSORPTIONS	SCATTERINGS	MISSES	CUTSIDE
100000	0	0	173681	50022	17948

HITS/EMISSIONS/(2N-1), RING WIDTH= 0.50R

1	0.01425000	2	0.01260000	3	0.00446400	4	0.00273143
5	0.00176333	6	0.00137182	7	0.00112769	8	0.00086133
9	0.00071412	10	0.00065316	11	0.00054095	12	C.00047217
13	0.00039800	14	0.00035889	15	C.0C031172	16	0.00027419
17	0.00023697	18	C.00022314	19	0.00020081	2C	C.00017231
21	0.00016000	22	0.00014977	23	0.00013556	24	0.00012489
25	0.00010980	26	0.000C9902	27	0.0C009849	28	C.00009200
29	0.00008088	30	0.000C7203				

EMISSION FROM CYLINDRICAL CLOUD

CYLINDER OPTICAL DEPTH	2.000
HEIGHT TO DIAMETER RATIO	10.000
BASE HEIGHT TO DIAMETER RATIO	-0.000
SCATTERING TO EXTINCTION RATIO	1.000
ISOTROPIC SCATTERING	

EMISSIONS	REEMISSIONS	ABSORPTIONS	SCATTERINGS	MISSES	OUTSIDE
200000	0	0	370953	100079	57700

HITS/EMISSIONS/(2N-1), RING WIDTH= 0.50R

1	0.00684500	2	0.00593166	3	0.00213900	4	0.00131500
5	0.00098611	6	0.00076455	7	0.00065192	8	0.00053667
9	0.00045765	10	0.00040816	11	0.00033952	12	0.00030696
13	0.00029100	14	0.00026389	15	0.00022793	16	0.00020952
17	0.00018439	18	0.00017714	19	0.00016162	20	0.00015090
21	0.00014829	22	0.00012442	23	0.00012211	24	0.00010585
25	0.00010918	26	0.00010451	27	0.00008934	28	0.00008191
29	0.00008421	30	0.00008059				

EMISSION FROM CYLINDRICAL CLOUD

CYLINDER OPTICAL DEPTH	2.000
HEIGHT TO DIAMETER RATIO	20.000
BASE HEIGHT TO DIAMETER RATIO	-0.000
SCATTERING TO EXTINCTION RATIO	1.000
ISOTROPIC SCATTERING	

EMISSIONS	REEMISSIONS	ABSORPTIONS	SCATTERINGS	MISSES	OUTSIDE
200000	0	0	381086	99948	71558

HITS/EMISSIONS/(2N-1),RING WIDTH= 0.50R

1	0.00471500	2	0.00392667	3	0.00142500	4	0.00089500
5	0.00061278	6	0.00048409	7	0.00039000	8	0.00034467
9	0.00029294	10	0.00025395	11	0.00022619	12	0.00020630
13	0.00018520	14	0.00017370	15	0.00014621	16	0.00013597
17	0.00013409	18	0.00011086	19	0.00011824	20	0.00011013
21	0.00009634	22	0.00008442	23	0.00008989	24	0.00008415
25	0.00007857	26	0.00007029	27	0.00007038	28	0.00006582
29	0.00006465	30	0.00005771				

EMISSION FROM CYLINDRICAL CLOUD

12

CYLINDER OPTICAL DEPTH 2.000
HEIGHT TO DIAMETER RATIO 5.000
BASE HEIGHT TO DIAMETER RATIO -0.000
SCATTERING TO EXTINCTION RATIO 1.000
ANISOTROPIC SCATTERING

A= 8.0000 B= 20.000 C= 60.000 D=120.000 E=170.000

F= 1.0000 G= 20.000 H= 40.000 I= 12.000 J= 80.000

EMISSIONS	REEMISSIONS	ABSORPTIONS	SCATTERINGS	MISSES	OUTSIDE
100000	0	0	149866	49773	16671

HITS/EMISSIONS/(2N-1), RING WIDTH= 0.50R

1	0.01324000	2	0.01388000	3	0.00501000	4	0.00286857
5	0.00203222	6	0.00154455	7	0.00118462	8	0.00105267
9	0.00079882	10	0.00064737	11	0.00058667	12	0.00045957
13	0.00042080	14	0.00035778	15	0.00033172	16	0.00028097
17	0.00023394	18	0.00022143	19	0.00020946	20	0.00017667
21	0.00015537	22	0.00014419	23	0.00012444	24	0.00012511
25	0.00010510	26	0.00009412	27	0.00009132	28	0.00008691
29	0.00007140	30	0.00006780				

EMISSION FROM CYLINDRICAL CLOUD

CYLINDER OPTICAL DEPTH	5.000
HEIGHT TO DIAMETER RATIO	5.000
BASE HEIGHT TO DIAMETER RATIO	-0.000
SCATTERING TO EXTINCTION RATIO	1.000
ISOTROPIC SCATTERING	

EMISSIONS	REEMISSIONS	ABSORPTIONS	SCATTERINGS	MISSES	OUTSIDE
100000	0	0	561346	49936	19082

HITS/EMISSIONS/(2N-1), RING WIDTH= 0.50R

1	0.01672000	2	0.01487333	3	0.00386000	4	0.00213714
5	0.00154889	6	0.00121091	7	0.00093308	8	0.00074800
9	0.00065059	10	0.00058632	11	0.00049714	12	0.00042000
13	0.00037560	14	0.00033444	15	0.00029586	16	0.00026548
17	0.00023939	18	0.00022914	19	0.00019784	20	0.00016897
21	0.00016537	22	0.00014535	23	0.00014000	24	0.00012851
25	0.00011878	26	0.00011333	27	0.00009849	28	0.00009455
29	0.00007895	30	0.00007390				

EMISSION FROM CYLINDRICAL CLOUD

CYLINDER OPTICAL DEPTH	5.000
HEIGHT TO DIAMETER RATIO	5.000
BASE HEIGHT TO DIAMETER RATIO	-0.000
SCATTERING TO EXTINCTION RATIO	1.000
ANISOTROPIC SCATTERING	

A= 8.0000   B= 20.000   C= 60.000   D=120.000   E=170.000

F= 1.0000   G= 20.000   H= 40.000   I= 12.000   J= 80.000

EMISSIONS	REEMISSIONS	ABSORPTIONS	SCATTERINGS	MISSES	OUTSIDE
100000	0	0	415554	49927	17941

HITS/EMISSIONS/(2N-1), RING WIDTH= 0.50R

1	0.01288000	2	0.01537666	3	0.00424200	4	0.00245714
5	0.00173778	6	0.00131818	7	0.00103923	8	0.00088733
9	0.00073647	10	0.00065053	11	0.00052333	12	0.00044522
13	0.00039320	14	0.00036519	15	0.00031621	16	0.00028065
17	0.00024515	18	0.00021457	19	0.00019108	20	0.00019436
21	0.00014805	22	0.00014209	23	0.00013533	24	0.00012255
25	0.00011510	26	0.00010078	27	0.00009340	28	0.00008309
29	0.00007368	30	0.00007610				

EMISSION FROM CYLINDRICAL CLOUD

CYLINDER OPTICAL DEPTH	10.000
HEIGHT TO DIAMETER RATIO	5.000
BASE HEIGHT TO DIAMETER RATIO	-0.000
SCATTERING TO EXTINCTION RATIO	1.000
ISOTROPIC SCATTERING	

EMISSIONS	REEMISSIONS	ABSORPTIONS	SCATTERINGS	MISSES	OUTSIDE
100000	0	0	1555672	49826	18637

HITS/EMISSIONS/(2N-1), RING WIDTH= 0.50R

1	0.02101000	2	0.02093000	3	0.00361200	4	0.00193429
5	0.00147778	6	0.00107727	7	0.00084692	8	0.00072467
9	0.00063765	10	0.00052632	11	0.00044381	12	0.00039913
13	0.00034480	14	0.00031778	15	0.00028552	16	0.00025355
17	0.00022212	18	0.00020143	19	0.00018730	20	0.00017179
21	0.00015585	22	0.00014256	23	0.00013178	24	0.00011915
25	0.00010204	26	0.00009745	27	0.00008906	28	0.00008655
29	0.00008000	30	0.00007102				

EMISSION FROM BLACK SURFACE AT BASE OF CYLINDER

CYLINDER OPTICAL DEPTH	0.500
HEIGHT TO DIAMETER RATIO	5.000
SCATTERING TO EXTINCTION RATIO	1.000
ISOTROPIC SCATTERING	

EMISSIONS	REEMISSIONS	ABSORPTIONS	SCATTERINGS	MISSES	OUTSIDE
200000	0	0	107194	157435	4488

FLUX RATIO,RING WIDTH= 0.50R

1	0.10465998	2	0.07785330	3	0.01905199	4	0.00806000
5	0.00424000	6	0.00280909	7	0.00195846	8	0.00137867
9	0.00096706	10	0.00082737	11	0.00069048	12	0.00054261
13	0.00040720	14	0.00036815	15	0.00029724	16	0.00023226
17	0.00020788	18	0.00018343	19	0.00014919	20	0.00014154
21	0.00011024	22	0.00010930	23	0.00009200	24	0.00008213
25	0.00007143	26	0.00006980	27	0.00006038	28	0.00005564
29	0.00005228	30	0.00005966				

EMISSION FROM BLACK SURFACE AT BASE OF CYLINDER

CYLINDER OPTICAL DEPTH	0.500
HEIGHT TO DIAMETER RATIO	5.000
SCATTERING TO EXTINCTION RATIO	1.000
ANISOTROPIC SCATTERING	

A= 8.0000 B= 20.000 C= 60.000 D=120.000 E=170.000

F= 1.0000 G= 20.000 H= 40.000 I= 12.000 J= 80.000

EMISSIONS	REEMISSIONS	ABSORPTIONS	SCATTERINGS	MISSES	OUTSIDE
200000	0	0	114252	179193	2255

FLUX RATIO,RING WIDTH= 0.50R

1	0.05189999	2	0.04146665	3	0.01031200	4	0.00402000
5	0.00209111	6	0.00121636	7	0.00078462	8	0.00056133
9	0.00045529	10	0.00033158	11	0.00029143	12	0.00019217
13	0.00016960	14	0.00013333	15	0.00012000	16	0.00009097
17	0.00008364	18	0.00006857	19	0.00006811	20	0.00006154
21	0.00005317	22	0.00004372	23	0.00003911	24	0.00003787
25	0.00003265	26	0.00002431	27	0.00002264	28	0.00002473
29	0.00002246	30	0.00001932				

EMISSION FROM BLACK SURFACE AT BASE OF CYLINDER

CYLINDER OPTICAL DEPTH	1.000
HEIGHT TO DIAMETER RATIO	5.000
SCATTERING TO EXTINCTION RATIO	1.000
ISOTROPIC SCATTERING	

EMISSIONS	REEMISSIONS	ABSORPTIONS	SCATTERINGS	MISSES	OUTSIDE
200000	0	0	188310	135867	4991

FLUX RATIO,RING WIDTH= 0.50R

1	0.17527996	2	0.13817994	3	0.02981199	4	0.01163428
5	0.00645778	6	0.00395273	7	0.00273077	8	0.00188000
9	0.00140588	10	0.00109684	11	0.00081143	12	0.00066348
13	0.00054560	14	0.00042667	15	0.00038138	16	0.00030839
17	0.00026545	18	0.00021657	19	0.00019784	20	0.00016718
21	0.00014732	22	0.00013256	23	0.00011556	24	0.00010340
25	0.00009388	26	0.00009020	27	0.00007019	28	0.00005527
29	0.00006561	30	0.00004610				

EMISSION FROM BLACK SURFACE AT BASE OF CYLINDER

CYLINDER OPTICAL DEPTH	1.000
HEIGHT TO DIAMETER RATIO	5.000
SCATTERING TO EXTINCTION RATIO	1.000
ANISOTROPIC SCATTERING	

A= 8.0000	B= 20.000	C= 60.000	D=120.000	E=170.000
F= 1.0000	G= 20.000	H= 40.000	I= 12.000	J= 80.000

EMISSIONS	REEMISSIONS	ABSORPTIONS	SCATTERINGS	MISSES	OUTSIDE
125000	0	0	127418	102950	2065

FLUX RATIO,RING WIDTH= 0.50R

1	0.08636799	2	0.07289598	3	0.01807359	4	0.00661486
5	0.00352355	6	0.00210909	7	0.00146215	8	0.00104960
9	0.00068518	10	0.00050189	11	0.00050590	12	0.00036313
13	0.00032000	14	0.00026667	15	0.00018759	16	0.00017858
17	0.00014352	18	0.00013349	19	0.00010724	20	0.00008862
21	0.00007180	22	0.00007144	23	0.00006258	24	0.00006672
25	0.00005224	26	0.00005145	27	0.00004106	28	0.00003258
29	0.00004042	30	0.00002603				

EMISSION FROM BLACK SURFACE AT BASE OF CYLINDER

CYLINDER OPTICAL DEPTH	1.000
HEIGHT TO DIAMETER RATIO	5.000
SCATTERING TO EXTINCTION RATIO	1.000

ANISOTROPIC SCATTERING

A=45.0000	B= 45.010	C= 45.020	D= 90.000	E=135.000
F= 0.9800	G= 1.140	H= 1.140	I= 1.140	J= 1.140

EMISSIONS	REEMISSIONS	ABSORPTIONS	SCATTERINGS	MISSES	OUTSIDE
100000	0	0	91812	68837	2163

FLUX RATIO,RING WIDTH= 0.50R

1	0.16735998	2	0.13099997	3	0.03224799	4	0.01235428
5	0.00667555	6	0.00410182	7	0.00264308	8	0.00188267
9	0.00138353	10	0.00097895	11	0.00080190	12	0.00064522
13	0.00051040	14	0.00037185	15	0.00033931	16	0.00027484
17	0.00027030	18	0.00021600	19	0.00017730	20	0.00015795
21	0.00016098	22	0.00010791	23	0.00009333	24	0.00009872
25	0.00009143	26	0.00007373	27	0.00005509	28	0.00005018
29	0.00005895	30	0.00004407				

EMISSION FROM BLACK SURFACE AT BASE OF CYLINDER

CYLINDER OPTICAL DEPTH	2.000
HEIGHT TO DIAMETER RATIO	5.000
SCATTERING TO EXTINCTION RATIO	1.000
ISOTROPIC SCATTERING	

EMISSIONS	REEMISSIONS	ABSORPTIONS	SCATTERINGS	MISSES	OUTSIDE
100000	0	0	167430	55650	2260

FLUX RATIO,RING WIDTH= 0.50R

1	0.27855997	2	0.22854662	3	0.04291199	4	0.01506285
5	0.00783111	6	0.00449818	7	0.00310461	8	0.00216800
9	0.00161412	10	0.00118947	11	0.00085714	12	0.00072348
13	0.00059840	14	0.00043111	15	0.00040414	16	0.00031871
17	0.00025212	18	0.00021600	19	0.00019135	20	0.00018462
21	0.00017073	22	0.00013209	23	0.00011733	24	0.00009191
25	0.00009959	26	0.00007843	27	0.00005887	28	0.00006545
29	0.00004421	30	0.00005288				

EMISSION FROM BLACK SURFACE AT BASE OF CYLINDER

CYLINDER OPTICAL DEPTH	2.000
HEIGHT TO DIAMETER RATIO	5.000
SCATTERING TO EXTINCTION RATIO	1.000

ANISOTROPIC SCATTERING

A= 8.0000	B= 20.000	C= 60.000	D=120.000	E=170.000
F= 1.0000	G= 20.000	H= 40.000	I= 12.000	J= 80.000

EMISSIONS	REEMISSIONS	ABSORPTIONS	SCATTERINGS	MISSES	OUTSIDE
100000	0	0	179094	72180	1990

FLUX RATIO,RING WIDTH= 0.50R

1	0.14275998	2	0.12681330	3	0.02935199	4	0.01032571
5	0.00520444	6	0.00341454	7	0.00226769	8	0.00165867
9	0.00113176	10	0.00080211	11	0.00060000	12	0.00053043
13	0.00039360	14	0.00032444	15	0.00029379	16	0.00020387
17	0.00022182	18	0.00017829	19	0.00012541	20	0.00012718
21	0.00010927	22	0.00009209	23	0.00011467	24	0.00007489
25	0.00007102	26	0.00006902	27	0.00006340	28	0.00005964
29	0.00004982	30	0.00004610				

EMISSION FROM BLACK SURFACE AT BASE OF CYLINDER

CYLINDER OPTICAL DEPTH	2.000
HEIGHT TO DIAMETER RATIO	5.000
SCATTERING TO EXTINCTION RATIO	1.000

ANISOTROPIC SCATTERING

A=45.0000 B= 45.010 C= 45.020 D= 90.000 E=135.000

F= 0.9800 G= 1.140 H= 1.140 I= 1.140 J= 1.140

EMISSIONS	REEMISSIONS	ABSORPTIONS	SCATTERINGS	MISSES	OUTSIDE
100000	0	0	162121	57077	2020

FLUX RATIO,RING WIDTH= 0.50R

1	0.26939997	2	0.21307995	3	0.04475199	4	0.01641142
5	0.00800444	6	0.00471636	7	0.00307385	8	0.00215467
9	0.00149176	10	0.00120421	11	0.00095048	12	0.00060174
13	0.00056320	14	0.00043111	15	0.00036276	16	0.00026968
17	0.00024485	18	0.00022629	19	0.00016541	20	0.00015282
21	0.00013268	22	0.00010512	23	0.00009067	24	0.00008170
25	0.00008735	26	0.00006980	27	0.00006717	28	0.00005309
29	0.00005474	30	0.00004407				

EMISSION FROM BLACK SURFACE AT BASE OF CYLINDER

CYLINDER OPTICAL DEPTH	2.000
HEIGHT TO DIAMETER RATIO	10.000
SCATTERING TO EXTINCTION RATIO	1.000
ISOTROPIC SCATTERING	

EMISSIONS	REEMISSIONS	ABSORPTIONS	SCATTERINGS	MISSES	OUTSIDE
100000	0	0	167086	55433	2286

FLUX RATIO,RING WIDTH= 0.50R

1	0.28471996	2	0.22905328	3	0.04224799	4	0.01552000
5	0.00797778	6	0.00496727	7	0.00301538	8	0.00216000
9	0.00149412	10	0.00113053	11	0.00086095	12	0.00073913
13	0.00056320	14	0.00049926	15	0.00036966	16	0.00033806
17	0.00028121	18	0.00018514	19	0.00017730	20	0.00016410
21	0.00015415	22	0.00012465	23	0.00010489	24	0.00008426
25	0.00009143	26	0.00008000	27	0.00007396	28	0.00007127
29	0.00004842	30	0.00004203				

EMISSION FROM BLACK SURFACE AT BASE OF CYLINDER

CYLINDER OPTICAL DEPTH	2.000
HEIGHT TO DIAMETER RATIO	10.000
SCATTERING TO EXTINCTION RATIO	1.000
ANISOTROPIC SCATTERING	

A= 8.0000 B= 20.000 C= 60.000 D=120.000 E=170.000

F= 1.0000 G= 20.000 H= 40.000 I= 12.000 J= 80.000

EMISSIONS	REEMISSIONS	ABSORPTIONS	SCATTERINGS	MISSES	OUTSIDE
100000	0	0	178357	72319	2014

FLUX RATIO,RING WIDTH= 0.50R

1	0.14027998	2	0.12733330	3	0.02862399	4	0.01030285
5	0.00530222	6	0.00337818	7	0.00220000	8	0.00144267
9	0.00112471	10	0.00087368	11	0.00067810	12	0.00052522
13	0.00042560	14	0.00032741	15	0.00029379	16	0.00025935
17	0.00019394	18	0.00017600	19	0.00013946	20	0.00011795
21	0.00010146	22	0.00008930	23	0.00008889	24	0.00008170
25	0.00005959	26	0.00006353	27	0.00006340	28	0.00004873
29	0.00005474	30	0.00004203				

EMISSION FROM BLACK SURFACE AT BASE OF CYLINDER

CYLINDER OPTICAL DEPTH	2.000
HEIGHT TO DIAMETER RATIO	20.000
SCATTERING TO EXTINCTION RATIO	1.000
ISOTROPIC SCATTERING	

EMISSIONS	REEMISSIONS	ABSORPTIONS	SCATTERINGS	MISSES	OUTSIDE
100000	0	0	167004	55517	2273

FLUX RATIO, RING WIDTH= 0.50R

1	0.27807996	2	0.22769328	3	0.04293599	4	0.01589143
5	0.00806666	6	0.00475273	7	0.00316615	8	0.00217333
9	0.00148941	10	0.00117895	11	0.00093714	12	0.00064522
13	0.00057120	14	0.00040889	15	0.00036000	16	0.00036258
17	0.00025818	18	0.00022743	19	0.00020757	20	0.00016513
21	0.00015415	22	0.00013860	23	0.00011467	24	0.00008681
25	0.00008653	26	0.00008235	27	0.00006264	28	0.00006691
29	0.00005193	30	0.00004949				

EMISSION FROM BLACK SURFACE AT BASE OF CYLINDER

CYLINDER OPTICAL DEPTH 2.000
HEIGHT TO DIAMETER RATIO 5.000
SCATTERING TO EXTINCTION RATIO 0.500
ISOTROPIC SCATTERING

EMISSIONS	REEMISSIONS	ABSORPTIONS	SCATTERINGS	MISSES	OUTSIDE
200000	0	99120	99166	71987	1078

FLUX RATIO,RING WIDTH= 0.50R

1	0.10563998	2	0.08237997	3	0.01364399	4	0.00454857
5	0.00227555	6	0.00122727	7	0.00084154	8	0.00062533
9	0.00038706	10	0.00031579	11	0.00021048	12	0.00018087
13	0.00015440	14	0.00010519	15	0.00009241	16	0.00006710
17	0.00006000	18	0.00005029	19	0.00004162	20	0.00003641
21	0.00003220	22	0.00003721	23	0.00002756	24	0.00002213
25	0.00002082	26	0.00001725	27	0.00001170	28	0.00000945
29	0.00001474	30	0.00001288				

EMISSION FROM BLACK SURFACE AT BASE OF CYLINDER

CYLINDER OPTICAL DEPTH	2.000
HEIGHT TO DIAMETER RATIO	5.000
SCATTERING TO EXTINCTION RATIO	0.500

ANISOTROPIC SCATTERING

A= 8.0000	B= 20.000	C= 60.000	D=120.000	E=170.000
F= 1.0000	G= 20.000	H= 40.000	I= 12.000	J= 80.000

EMISSIONS	REEMISSIONS	ABSORPTIONS	SCATTERINGS	MISSES	OUTSIDE
100000	86508	86508	86613	62447	2259

FLUX RATIO,RING WIDTH= 0.50R

1	0.21771997	2	0.18015995	3	0.03852799	4	0.01364000
5	0.00689333	6	0.00422545	7	0.00287077	8	0.00200800
9	0.00149882	10	0.00106526	11	0.00076762	12	0.00066957
13	0.00050560	14	0.00042222	15	0.00037241	16	0.00030065
17	0.00025576	18	0.00021600	19	0.00020216	20	0.00015897
21	0.00013366	22	0.00012000	23	0.00010311	24	0.00008766
25	0.00007347	26	0.00007373	27	0.00005887	28	0.00004873
29	0.00005754	30	0.00004339				

EMISSION FROM BLACK SURFACE AT BASE OF CYLINDER

(10)

CYLINDER OPTICAL DEPTH	5.000
HEIGHT TO DIAMETER RATIO	5.000
SCATTERING TO EXTINCTION RATIO	1.000
ISOTROPIC SCATTERING	

EMISSIONS	REEMISSIONS	ABSORPTIONS	SCATTERINGS	MISSES	OUTSIDE
100000	0	0	381580	38750	1548

FLUX RATIO, RING WIDTH= 0.50R

1	0.45983995	2	0.39354657	3	0.05428799	4	0.01691428
5	0.00801333	6	0.00480000	7	0.00278769	8	0.00190933
9	0.00139529	10	0.00099789	11	0.00081333	12	0.00050087
13	0.00048160	14	0.00035407	15	0.00031034	16	0.00024645
17	0.00023394	18	0.00019771	19	0.00014703	20	0.00011385
21	0.00010927	22	0.00009953	23	0.00009956	24	0.00008851
25	0.00006122	26	0.00006431	27	0.00006189	28	0.00004364
29	0.00003579	30	0.00004271				

EMISSICN FROM BLACK SURFACE AT BASE OF CYLINDER

CYLINDER OPTICAL DEPTH	5.000
HEIGHT TO CIAMETER RATIO	5.000
SCATTERING TO EXTINCTION RATIO	1.000
ANISCTROPIC SCATTERING	

A= 8.0000 B= 20.000 C= 60.0CO D=120.000 E=170.COO

F= 1.0000 G= 20.000 H= 40.000 I= 12.000 J= 80.COC

EMISSIONS	REEMISSIONS	ABSORPTIONS	SCATTERINGS	MISSES	OUTSIDE
100000	0	0	391879	54511	2C47

FLUX RATIO,RING WIDTH= 0.50R

1	0.24175997	2	C.25447994	3	0.04777599	4	0.01563428
5	0.00778666	6	0.00484727	7	0.C0316000	8	0.00206133
9	0.00147765	10	C.00108421	11	0.00077333	12	0.00063130
13	0.00052320	14	0.00042519	15	0.C0038897	16	0.00029032
17	0.00026182	18	0.00021371	19	0.C0017946	2C	0.00014769
21	0.00014341	22	0.C0010419	23	0.0C010311	24	0.00009106
25	0.00008327	26	0.C0006431	27	0.00006642	28	0.00005600
29	0.00005754	30	0.00004068				

EMISSION FROM BLACK SURFACE AT BASE OF CYLINDER

CYLINDER OPTICAL DEPTH	10.000
HEIGHT TO DIAMETER RATIO	5.000
SCATTERING TO EXTINCTION RATIO	1.000
ISOTROPIC SCATTERING	

EMISSIONS	REEMISSIONS	ABSORPTIONS	SCATTERINGS	MISSES	OUTSIDE
100000	0	0	734189	27548	1007

FLUX RATIO,RING WIDTH= 0.50R

1	0.57603991	2	0.54925320	3	0.05518399	4	0.01389143
5	0.00642667	6	0.00335273	7	0.00216923	8	0.00138933
9	0.00100235	10	0.00078947	11	0.00056762	12	0.00037391
13	0.00031840	14	0.00026074	15	0.00018759	16	0.00018581
17	0.00014303	18	0.00013829	19	0.00010054	20	0.00008205
21	0.00007415	22	0.00006140	23	0.00006222	24	0.00005617
25	0.00004245	26	0.00004863	27	0.00004000	28	0.00002545
29	0.00002526	30	0.00002034				

EMISSION FROM BLACK SURFACE AT BASE OF CYLINDER

CYLINDER OPTICAL DEPTH	10.000
HEIGHT TO DIAMETER RATIO	5.000
SCATTERING TO EXTINCTION RATIO	1.000

ANISOTROPIC SCATTERING

A= 8.0000 B= 20.000 C= 60.000 D=120.000 E=170.000

F= 1.0000 G= 20.000 H= 40.000 I= 12.000 J= 80.000

EMISSIONS	REEMISSIONS	ABSORPTIONS	SCATTERINGS	MISSES	OUTSIDE
100000	0	0	738399	41393	1534

FLUX RATIO,RING WIDTH= 0.50R

1	0.32595997	2	0.39343990	3	0.05994399	4	0.01710285
5	0.00843555	6	0.00468727	7	0.00296308	8	0.00191733
9	0.00126118	10	0.00096842	11	0.00074095	12	0.00056000
13	0.00046400	14	0.00036444	15	0.00031724	16	0.00024645
17	0.00019636	18	0.00016114	19	0.00014270	20	0.00013538
21	0.00011220	22	0.00012093	23	0.00007556	24	0.00009532
25	0.00007347	26	0.00004863	27	0.00005736	28	0.00003927
29	0.00003860	30	0.00003458				

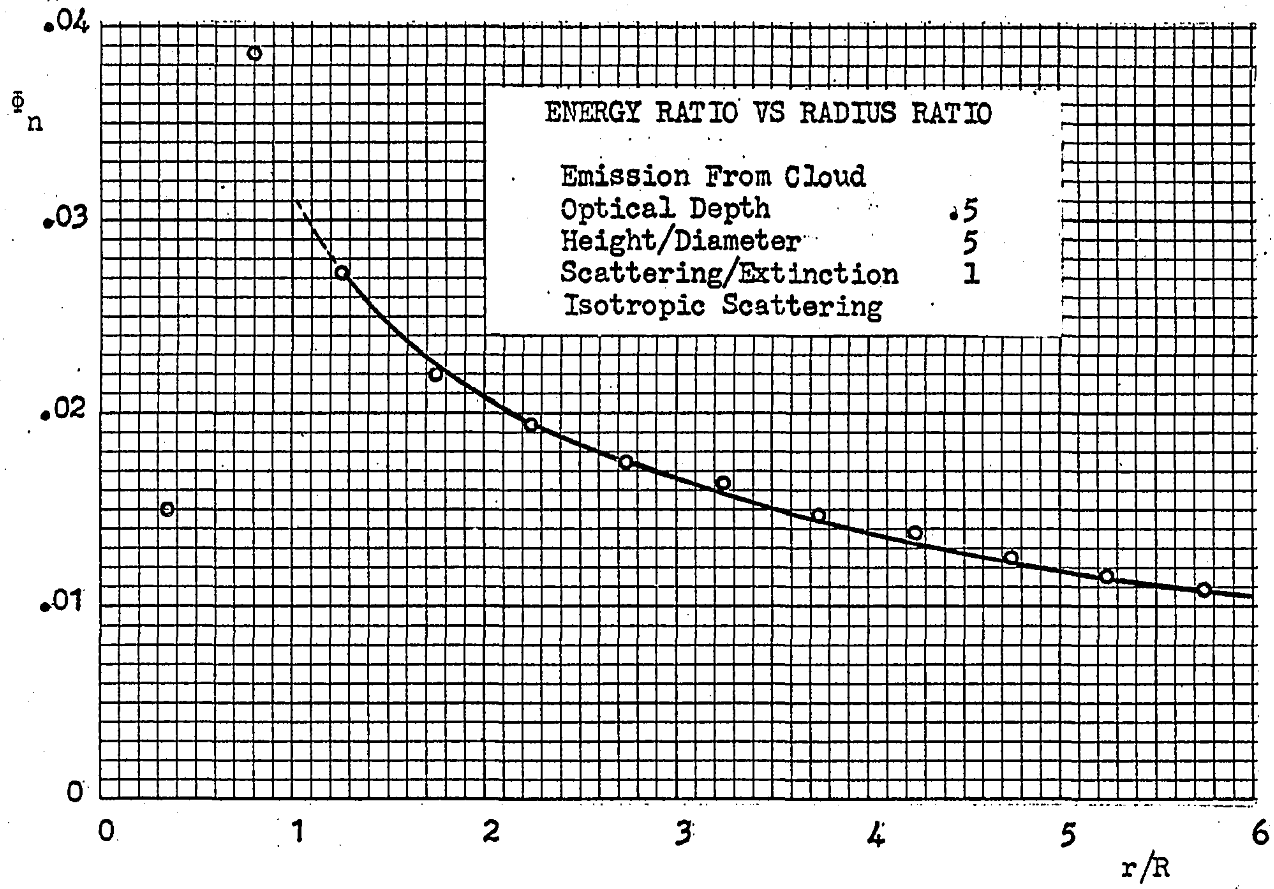

ENERGY RATIO VS RADIUS RATIO
Emission From Cloud
Optical Depth .5
Height/Diameter 5
Scattering/Extinction 1
Isotropic Scattering
Φ_n
.04
.03
.02
.01
0
0
1
2
3
4
5
6
r/R

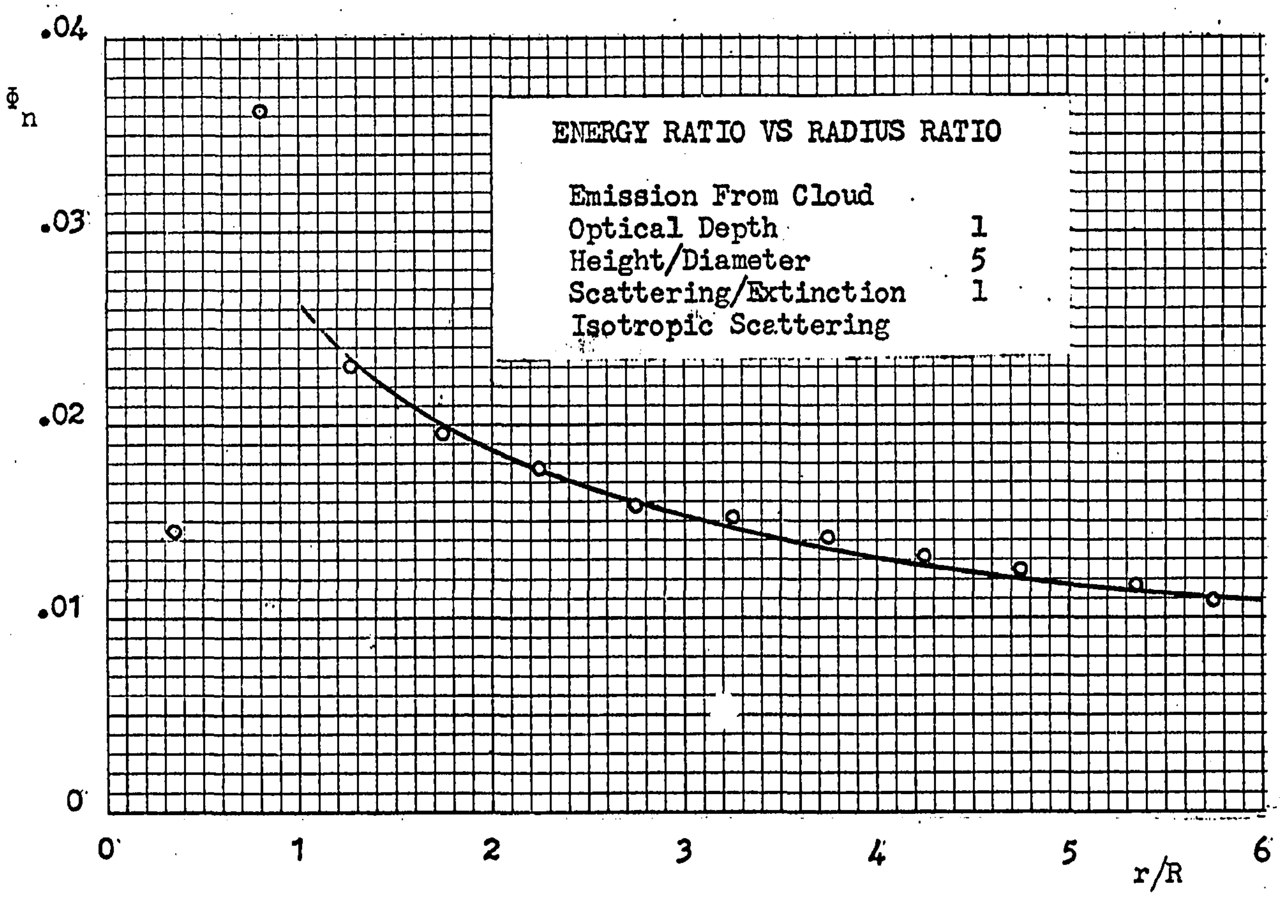

ENERGY RATIO VS RADIUS RATIO
Emission From Cloud
Optical Depth 1
Height/Diameter 5
Scattering/Extinction 1
Isotropic Scattering
Φ_n
.04
.03
.02
.01
0
0
1
2
3
4
5
6
r/R

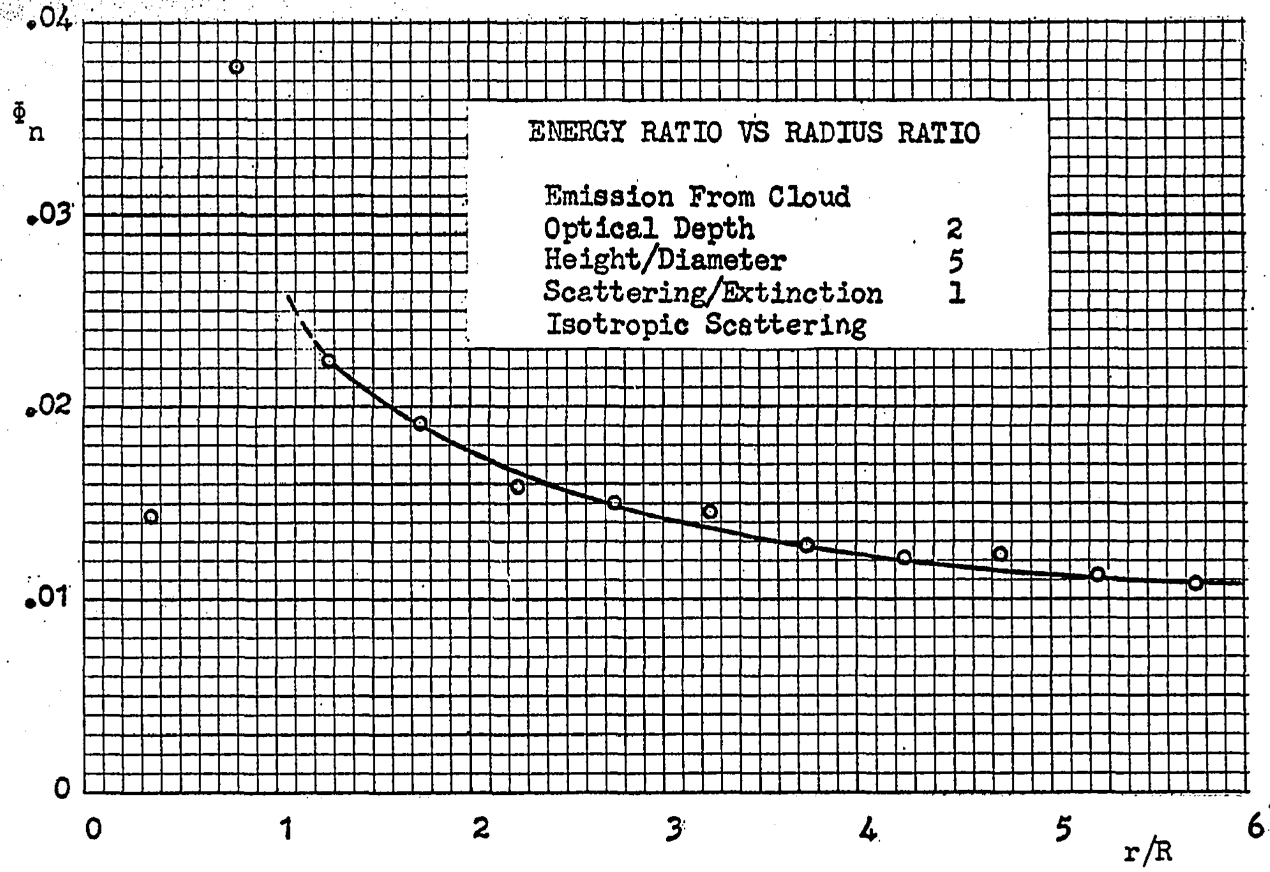
ENERGY RATIO VS RADIUS RATIO
Emission From Cloud
Optical Depth 2
Height/Diameter 5
Scattering/Extinction 1
Isotropic Scattering
Φ_n
.04
.03
.02
.01
0
0
1
2
3
4
5
6
r/R

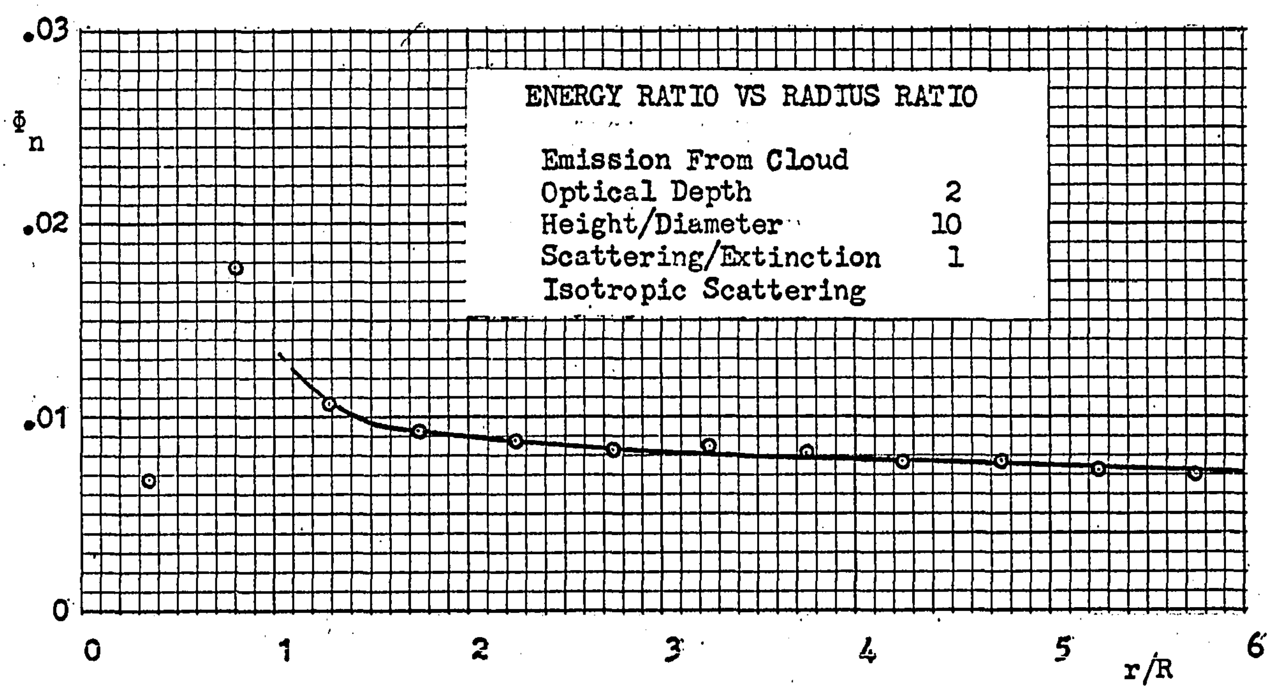
ENERGY RATIO VS RADIUS RATIO
Emission From Cloud
Optical Depth 2
Height/Diameter 10
Scattering/Extinction 1
Isotropic Scattering
Φ_n
.03
.02
.01
0
0
1
2
3
4
5
6
r/R

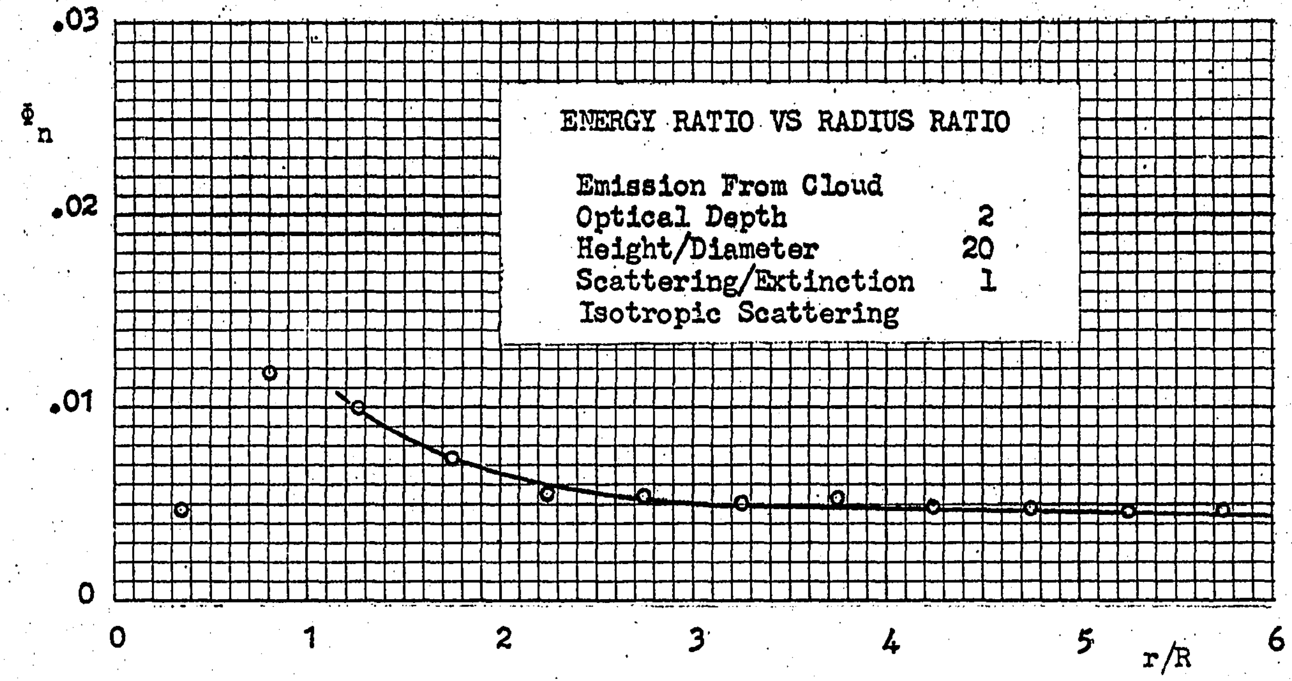
.03
Φ_n
.02
.01
0
0
1
2
3
4
5
6
r/R
ENERGY RATIO VS RADIUS RATIO
Emission From Cloud
Optical Depth 2
Height/Diameter 20
Scattering/Extinction 1
Isotropic Scattering

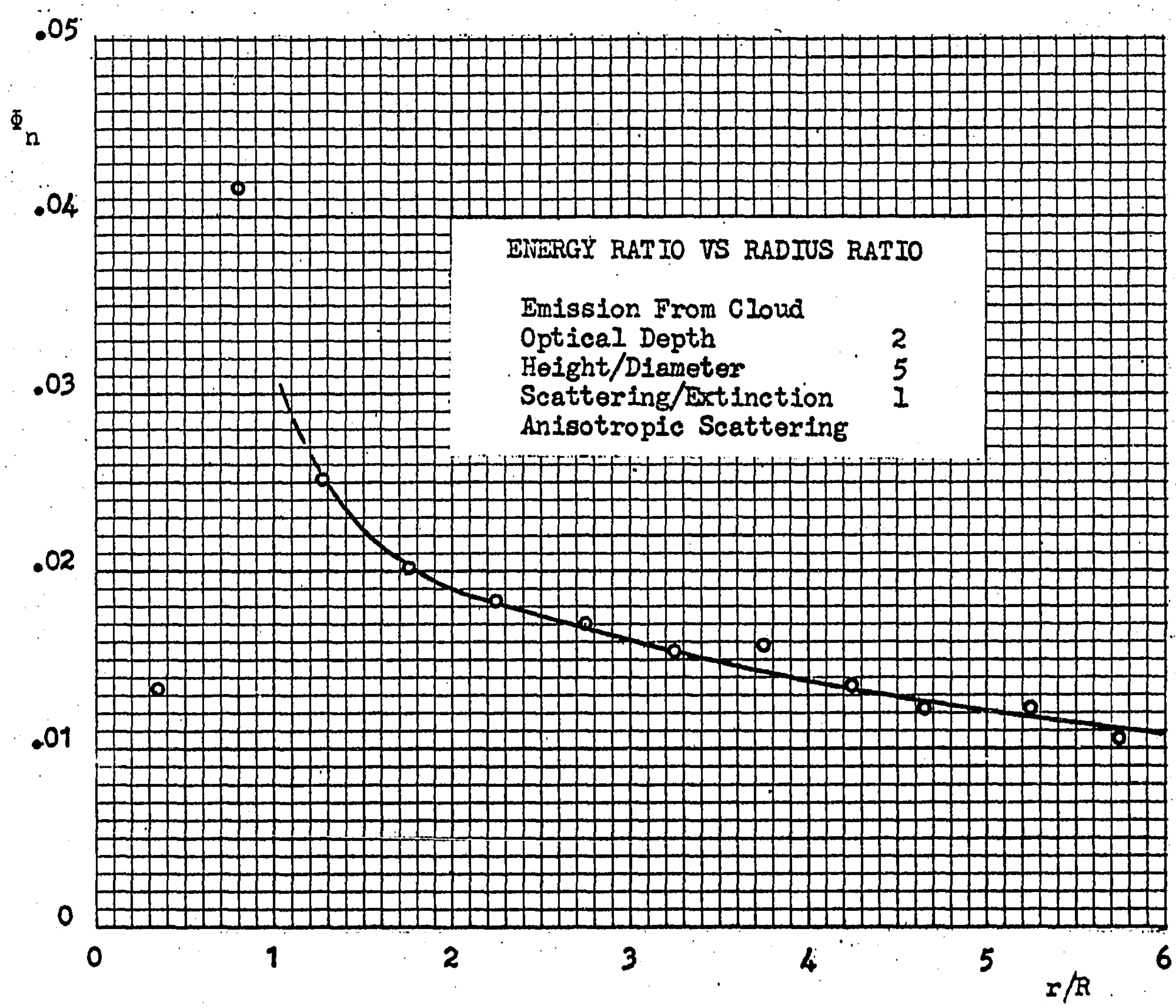
.05
Φ_n
.04
.03
.02
.01
0
0
1
2
3
4
5
6
r/R
ENERGY RATIO VS RADIUS RATIO
Emission From Cloud
Optical Depth 2
Height/Diameter 5
Scattering/Extinction 1
Anisotropic Scattering

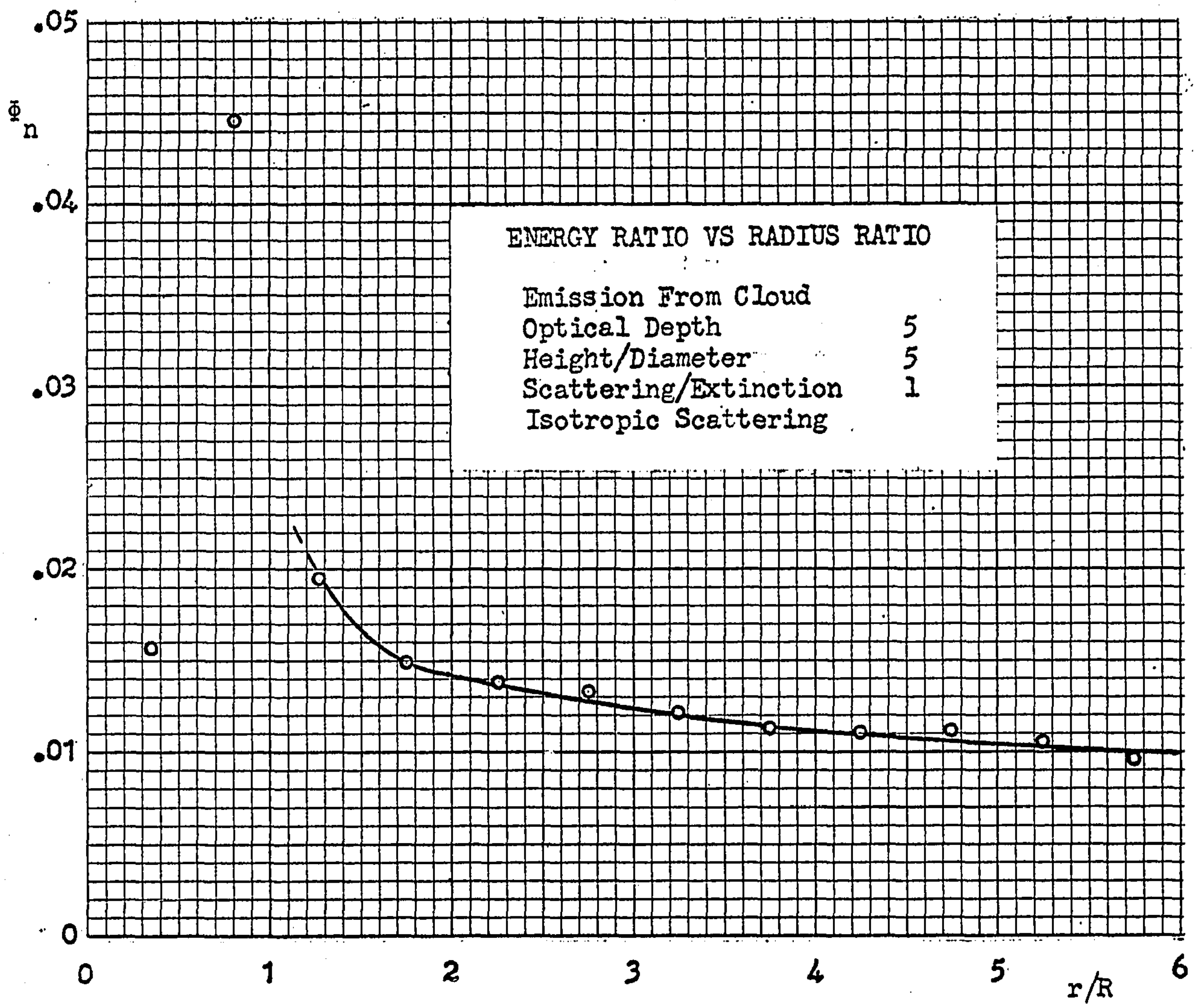
.05
Φ_n
.04
.03
.02
.01
0
0
1
2
3
4
5
6
r/R
ENERGY RATIO VS RADIUS RATIO
Emission From Cloud
Optical Depth 5
Height/Diameter 5
Scattering/Extinction 1
Isotropic Scattering

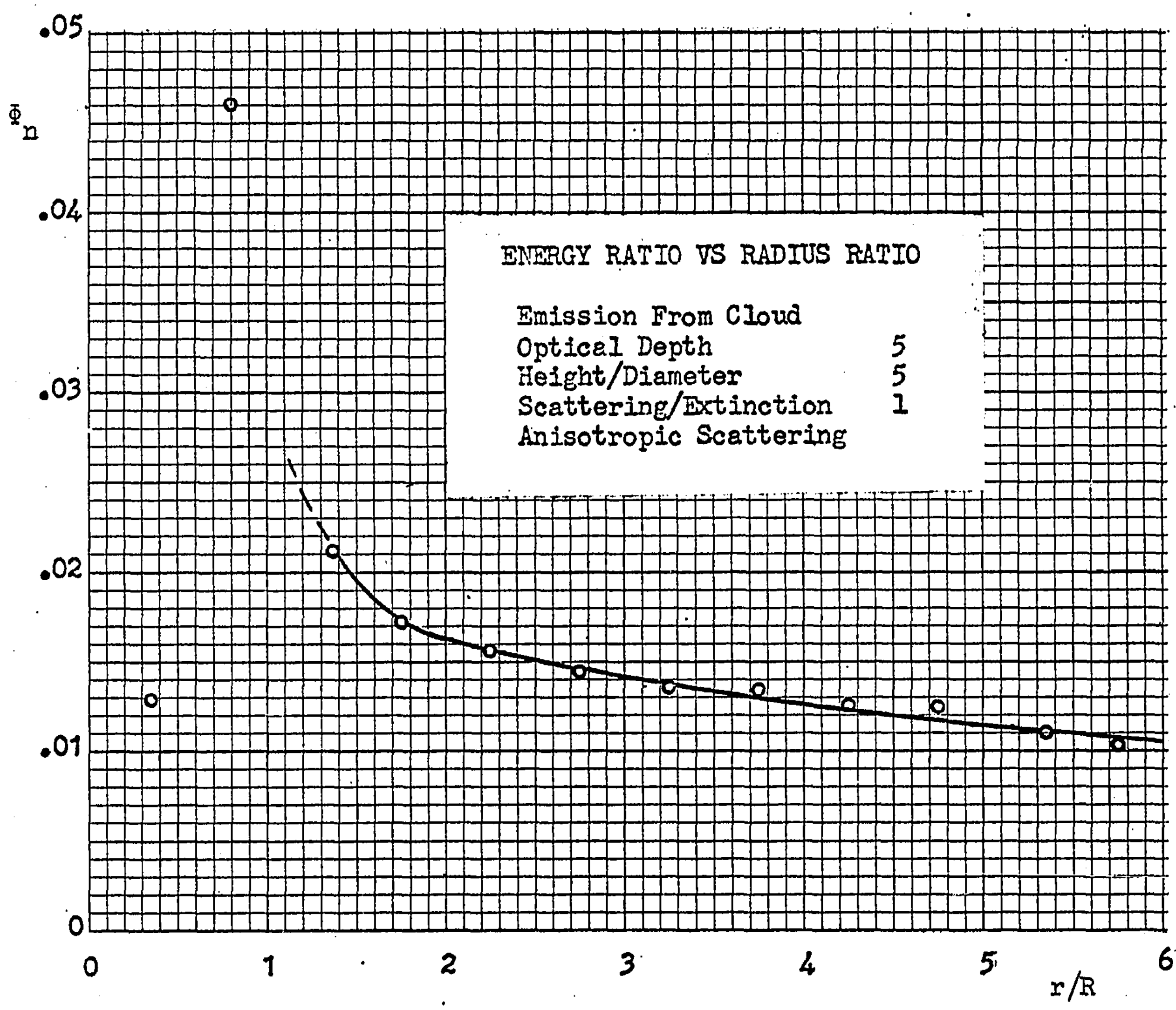
.05
.04
.03
.02
.01
0
Φ_n
0
1
2
3
4
5
6
r/R
ENERGY RATIO VS RADIUS RATIO
Emission From Cloud
Optical Depth 5
Height/Diameter 5
Scattering/Extinction 1
Anisotropic Scattering

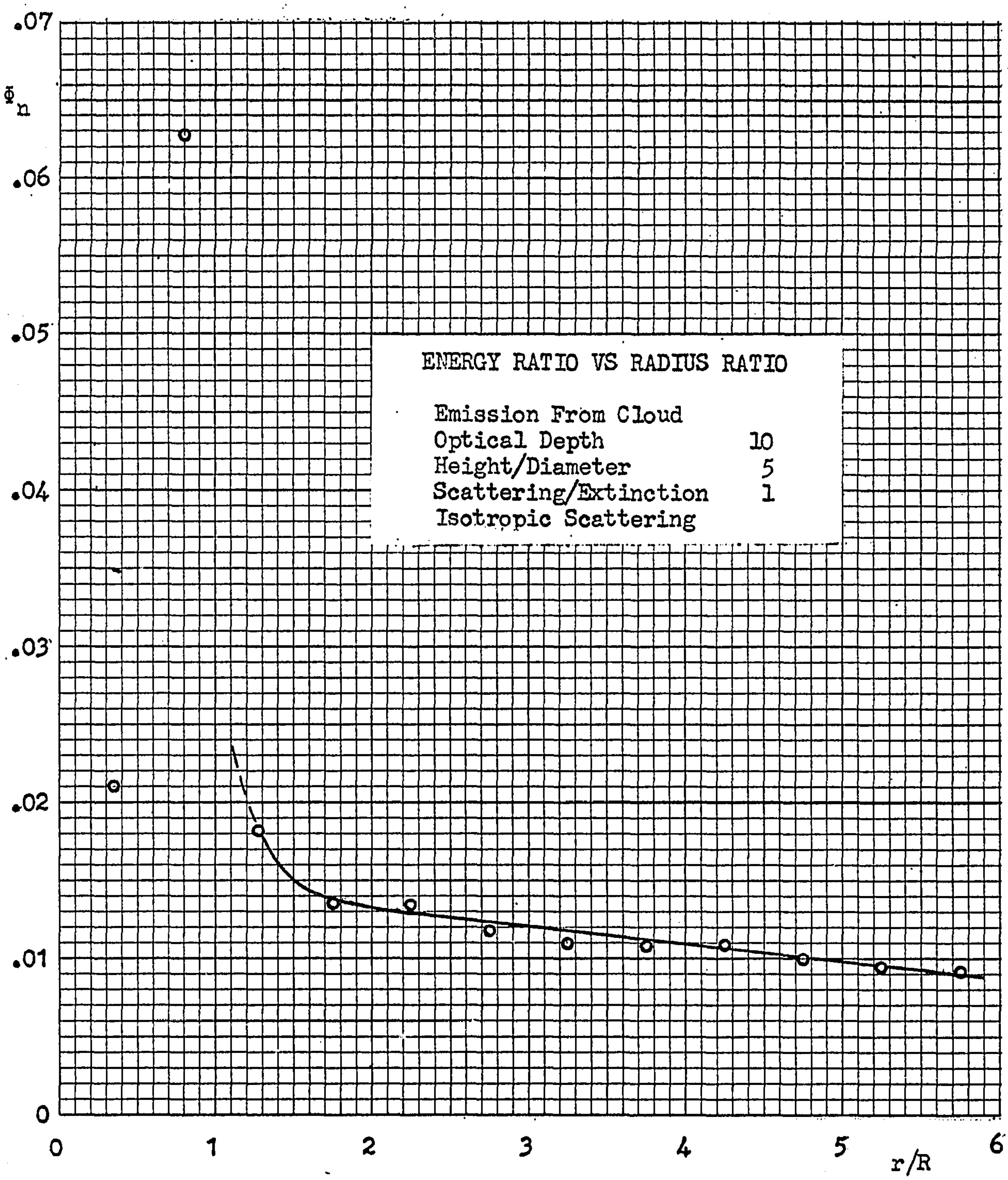

.07
Φ_n
.06
.05
.04
.03
.02
.01
0
0
1
2
3
4
5
6
r/R
ENERGY RATIO VS RADIUS RATIO
Emission From Cloud
Optical Depth 10
Height/Diameter 5
Scattering/Extinction 1
Isotropic Scattering

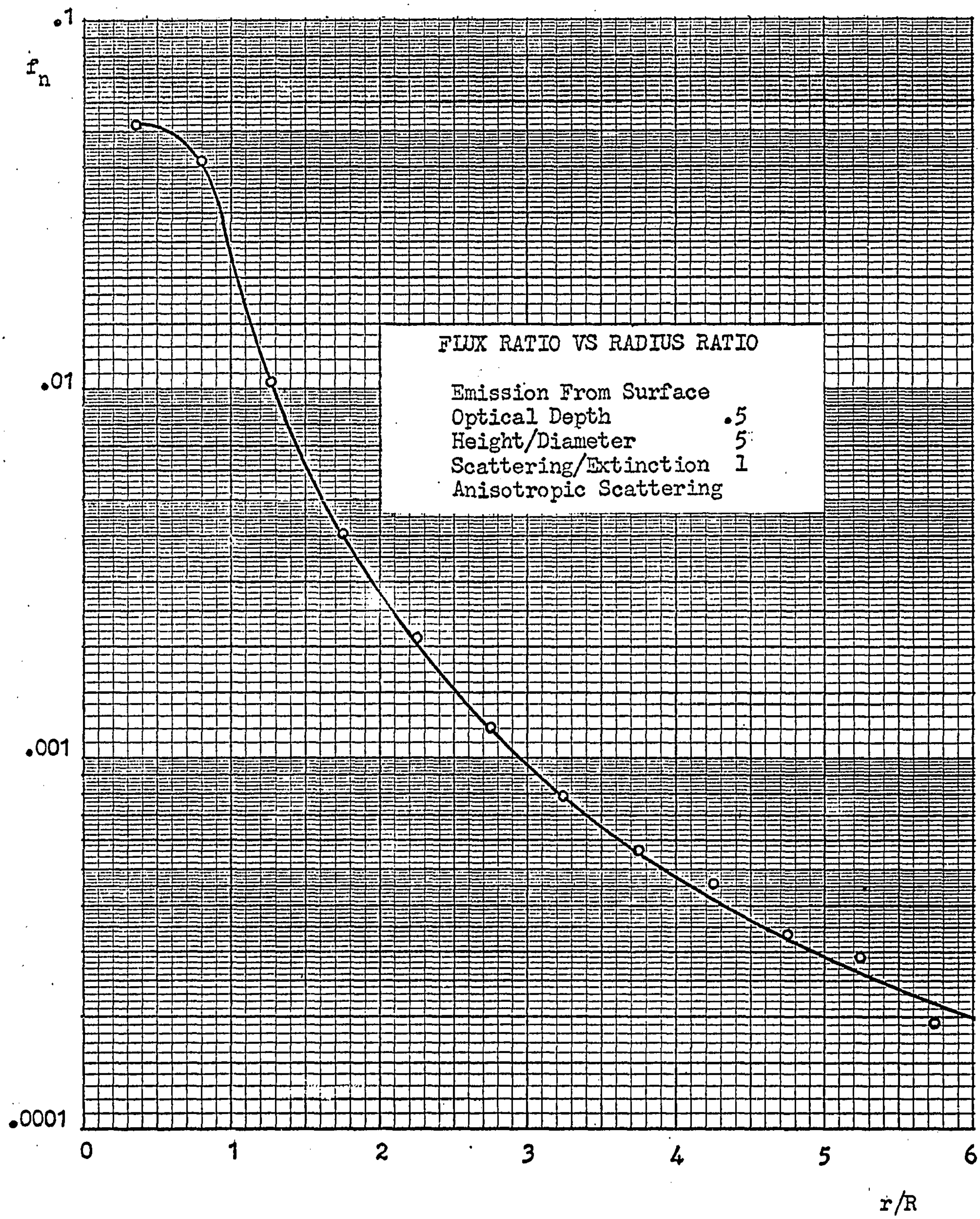

.1
f_n
.01
.001
.0001
0
1
2
3
4
5
6
r/R
FLUX RATIO VS RADIUS RATIO
Emission From Surface
Optical Depth .5
Height/Diameter 5
Scattering/Extinction 1
Anisotropic Scattering

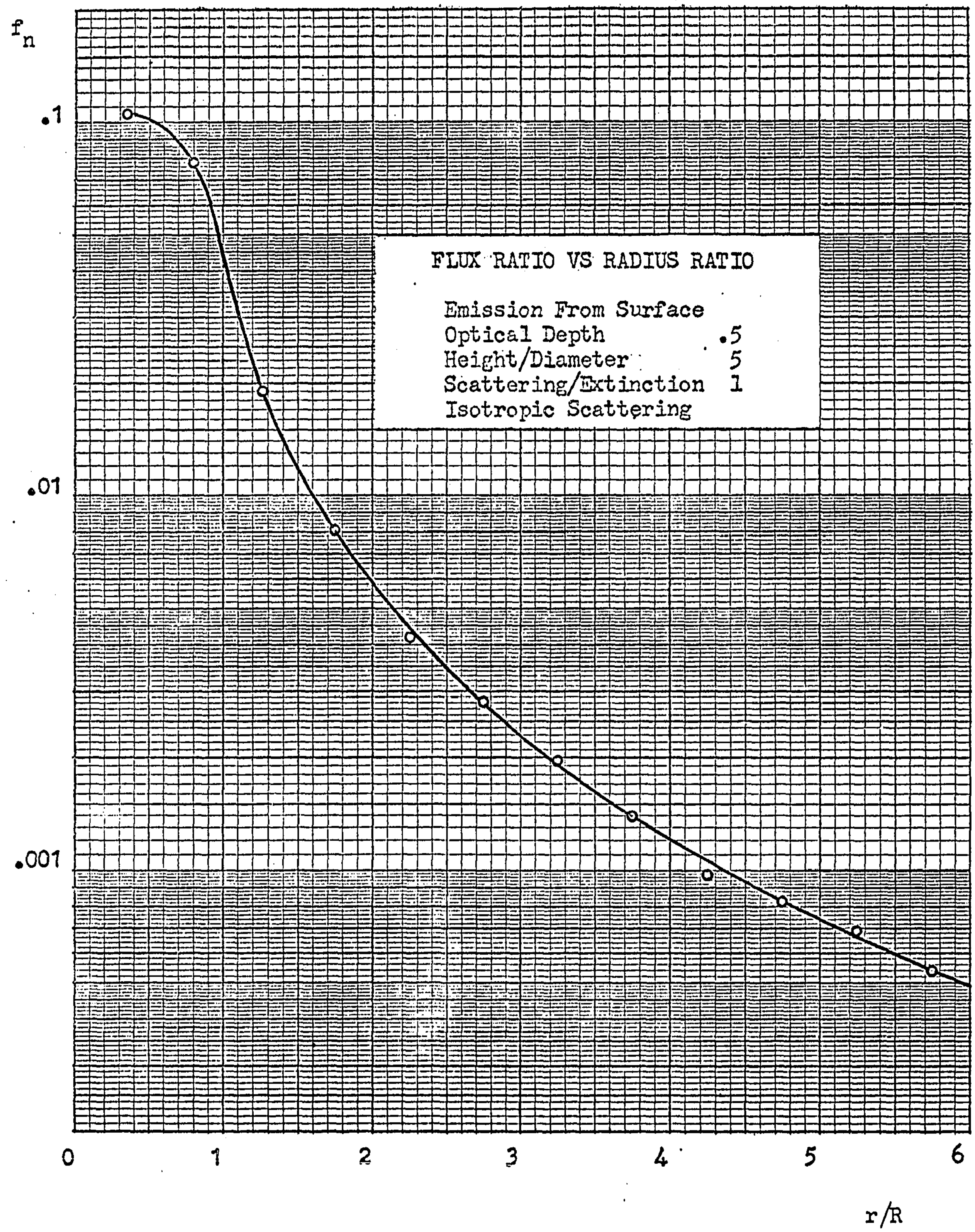

FLUX RATIO VS RADIUS RATIO
Emission From Surface
Optical Depth .5
Height/Diameter 5
Scattering/Extinction 1
Isotropic Scattering
f_n
.1
.01
.001
0
1
2
3
4
5
6
r/R

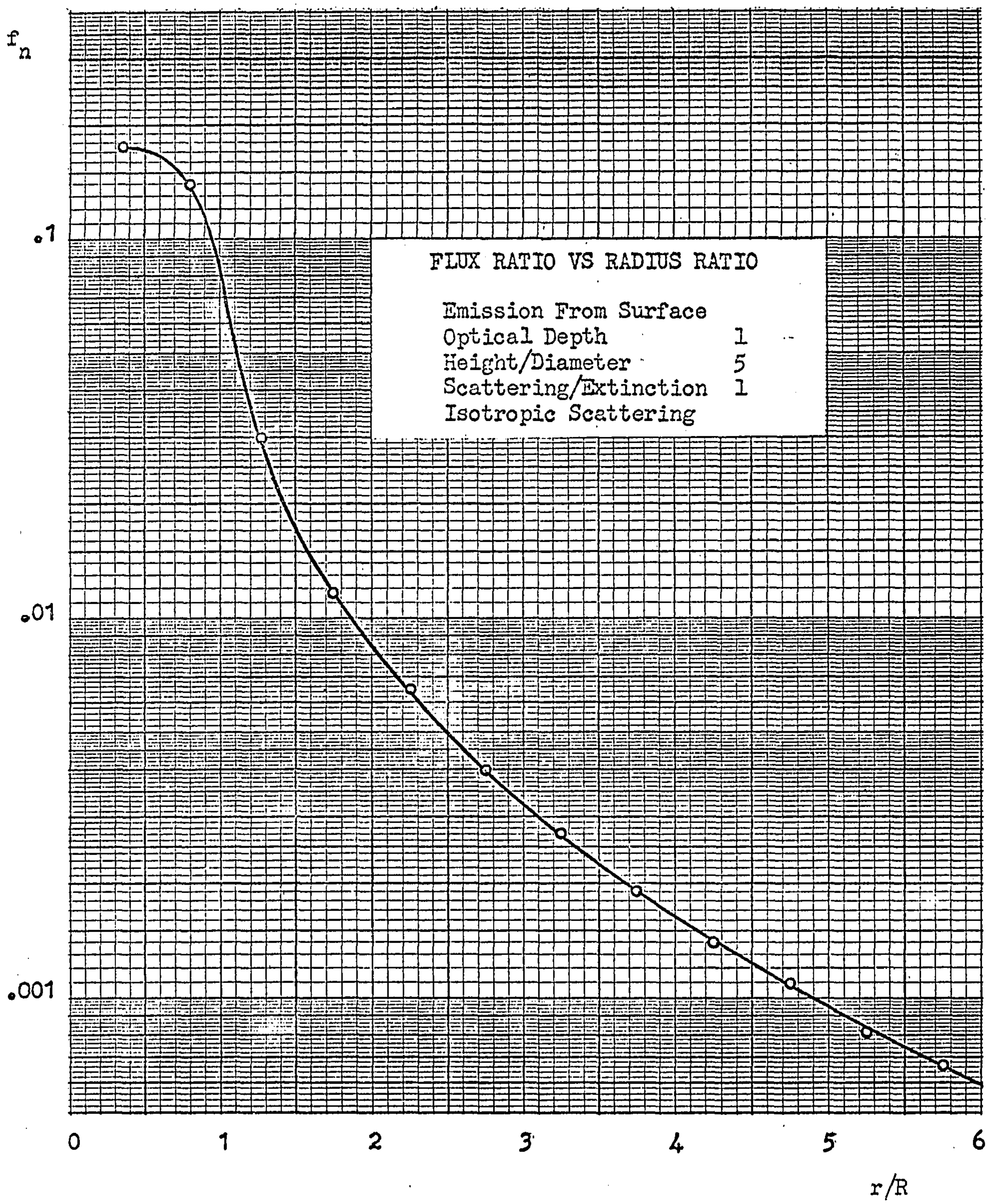

f_n
.1
.01
.001
FLUX RATIO VS RADIUS RATIO
Emission From Surface
Optical Depth 1
Height/Diameter 5
Scattering/Extinction 1
Isotropic Scattering
0
1
2
3
4
5
6
r/R

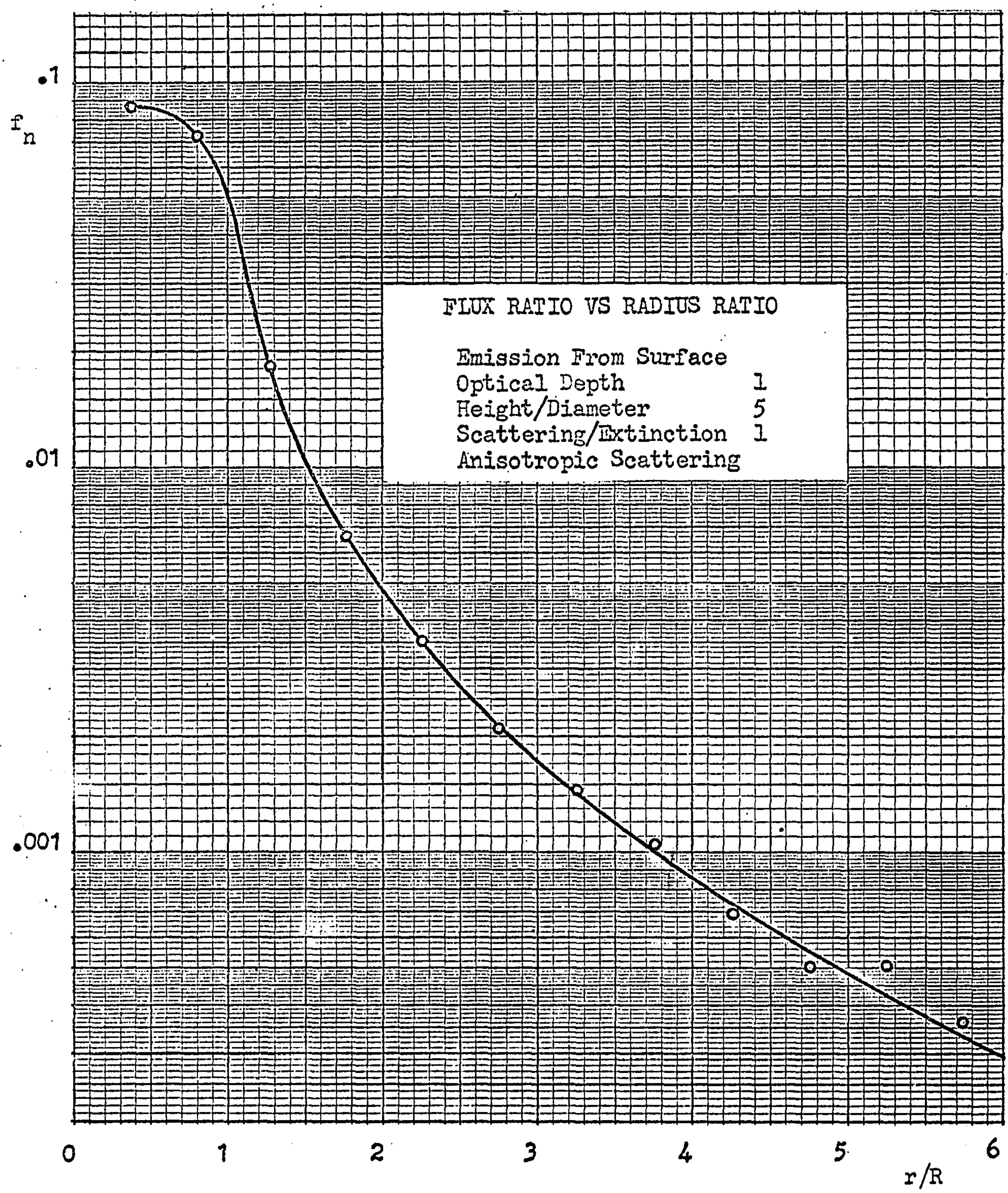

FLUX RATIO VS RADIUS RATIO
Emission From Surface
Optical Depth 1
Height/Diameter 5
Scattering/Extinction 1
Anisotropic Scattering
f_n
.1
.01
.001
0
1
2
3
4
5
6
r/R

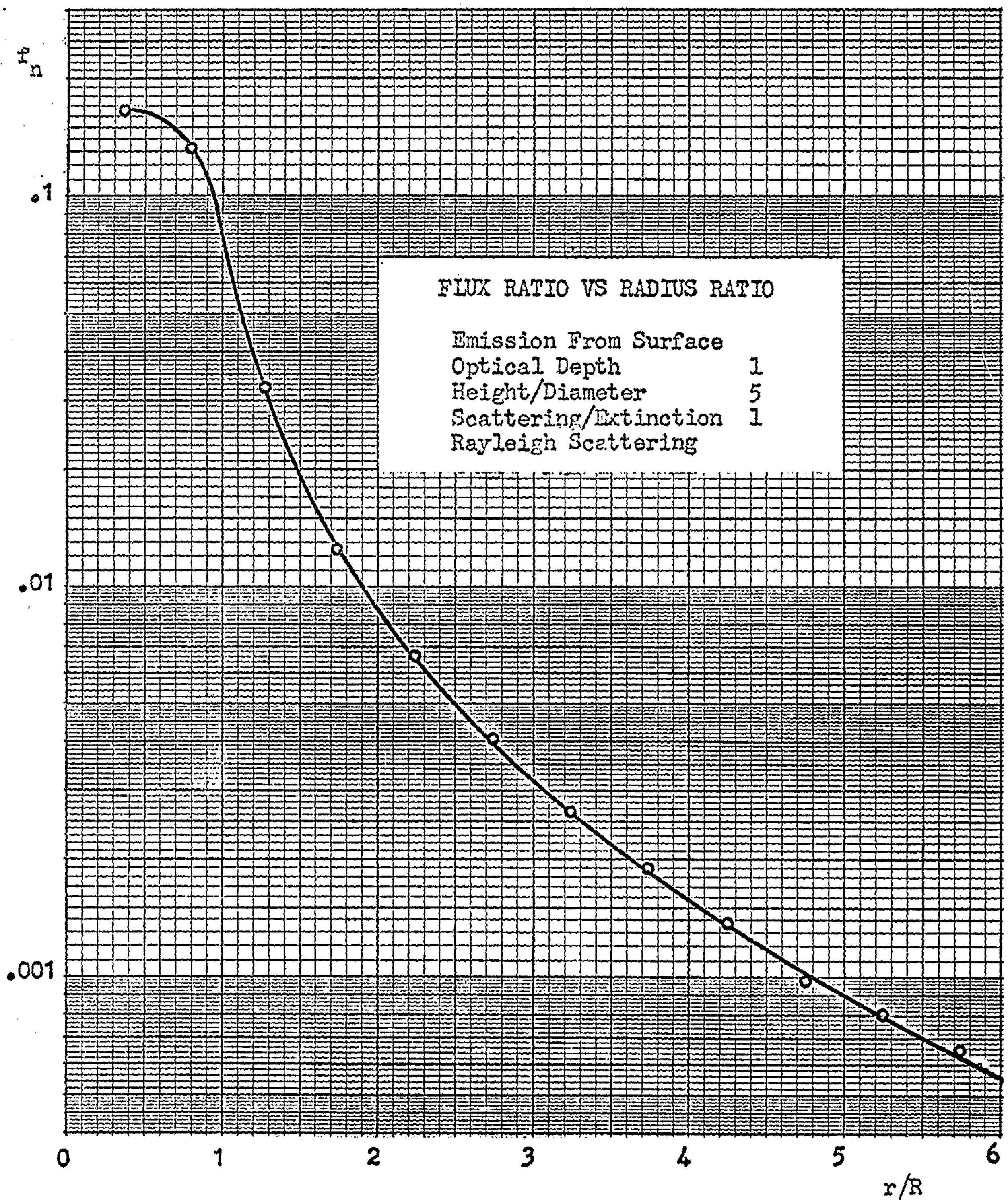

f_n
.1
.01
.001
FLUX RATIO VS RADIUS RATIO
Emission From Surface
Optical Depth 1
Height/Diameter 5
Scattering/Extinction 1
Rayleigh Scattering
0
1
2
3
4
5
6
r/R

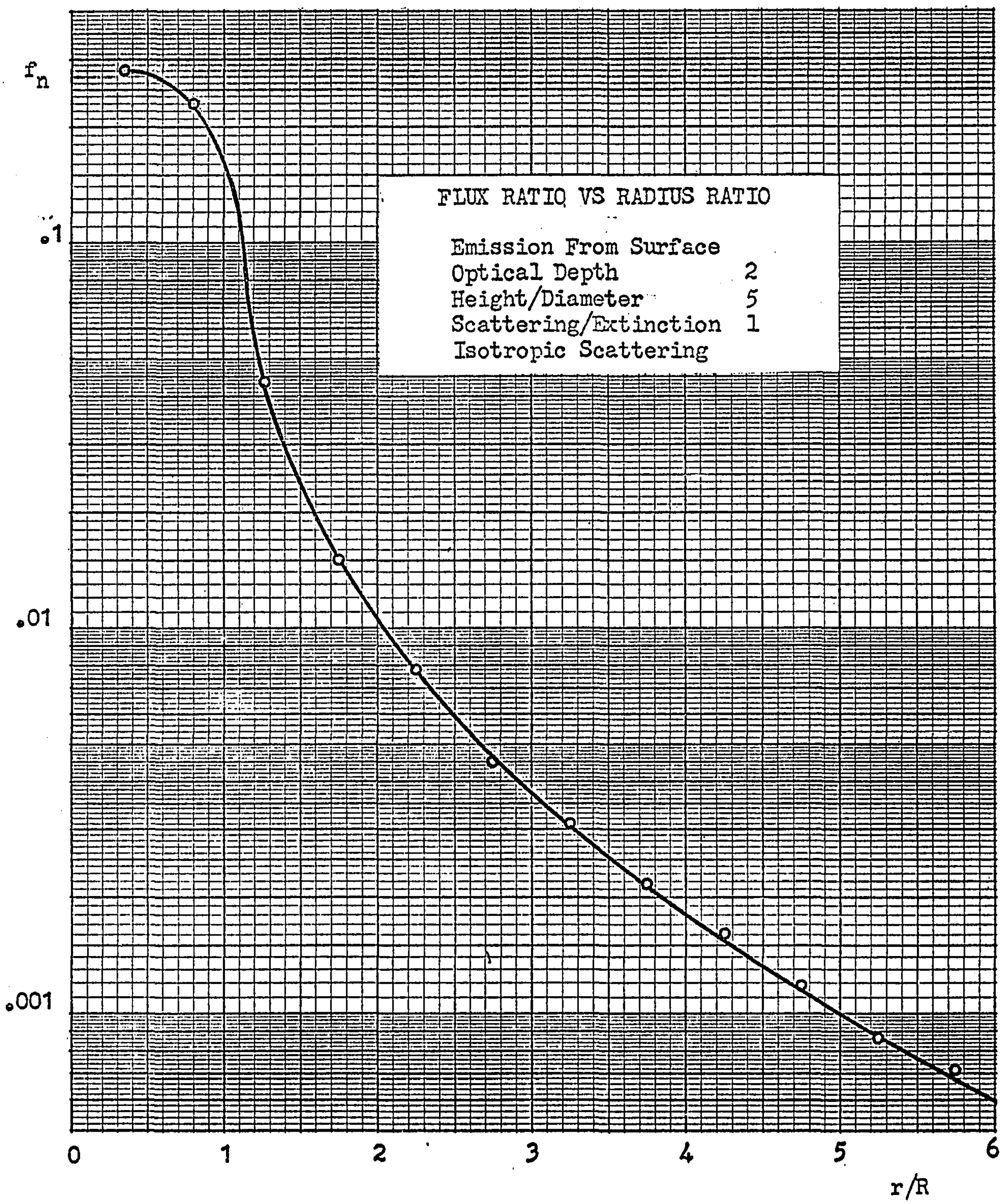
FLUX RATIO VS RADIUS RATIO
Emission From Surface
Optical Depth 2
Height/Diameter 5
Scattering/Extinction 1
Isotropic Scattering
f_n
.1
.01
.001
0
1
2
3
4
5
6
r/R

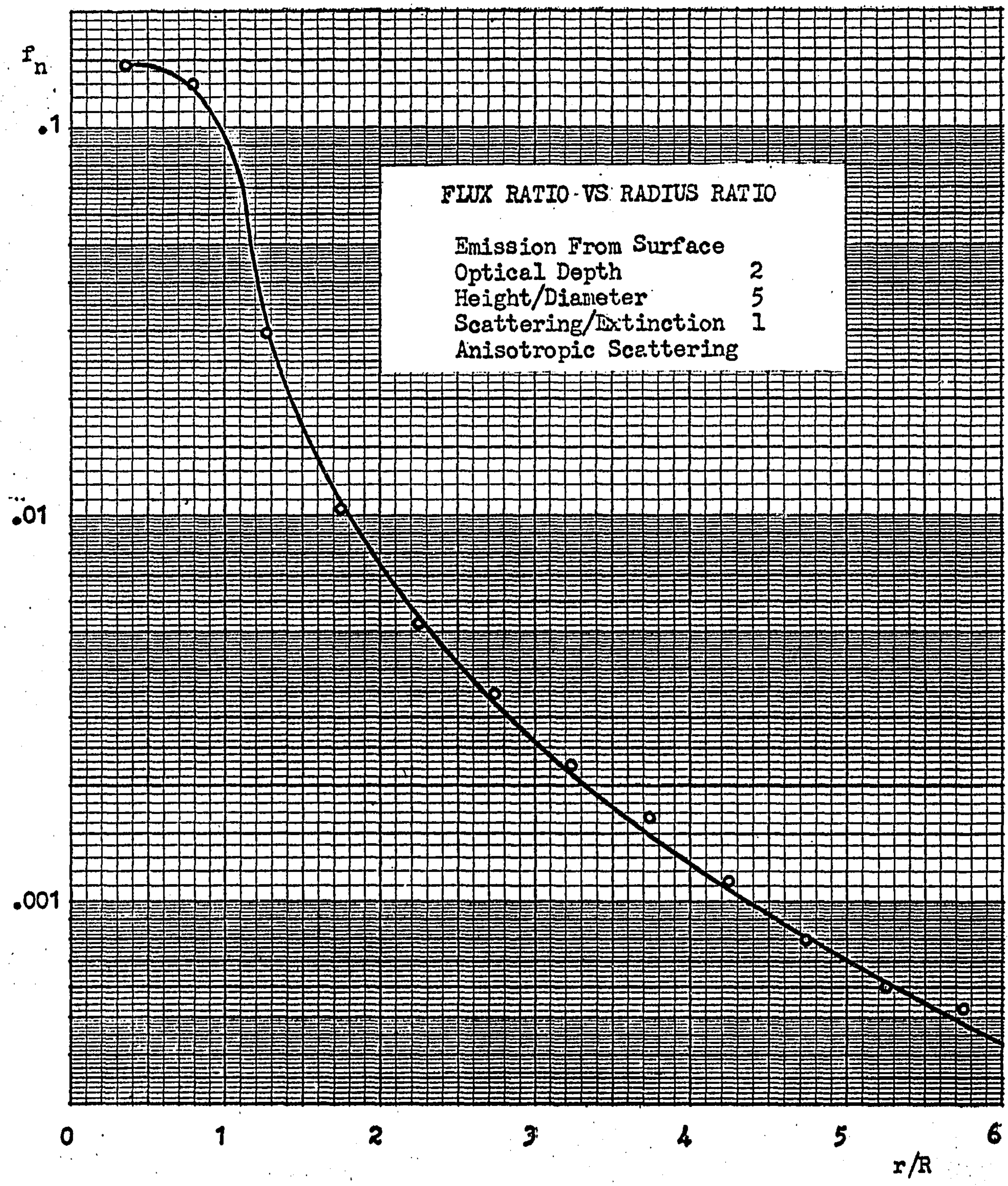

f_n
.1
.01
.001
FLUX RATIO VS RADIUS RATIO
Emission From Surface
Optical Depth 2
Height/Diameter 5
Scattering/Extinction 1
Anisotropic Scattering
0
1
2
3
4
5
6
r/R

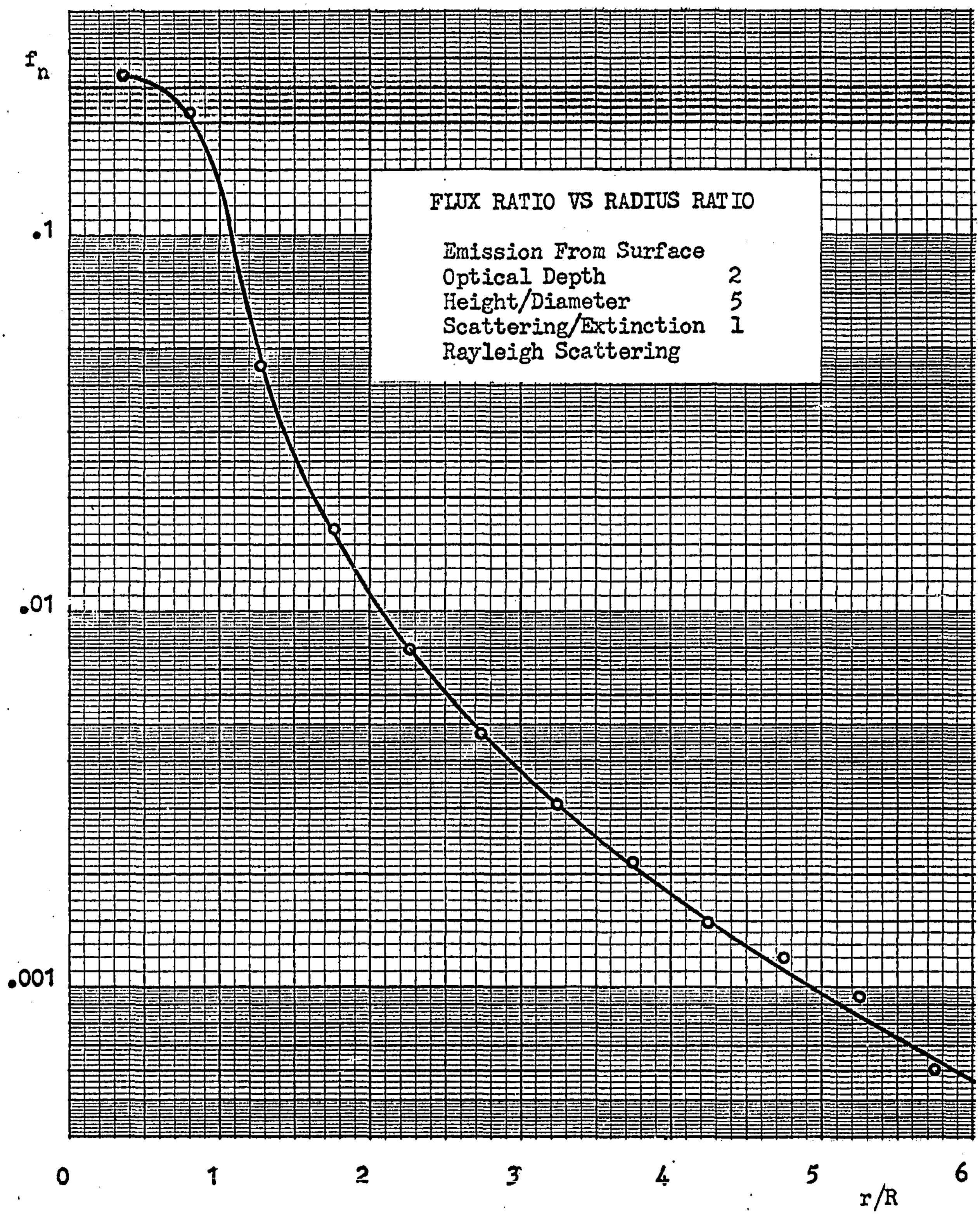

FLUX RATIO VS RADIUS RATIO
Emission From Surface
Optical Depth 2
Height/Diameter 5
Scattering/Extinction 1
Rayleigh Scattering
f_n
.1
.01
.001
0
1
2
3
4
5
6
r/R

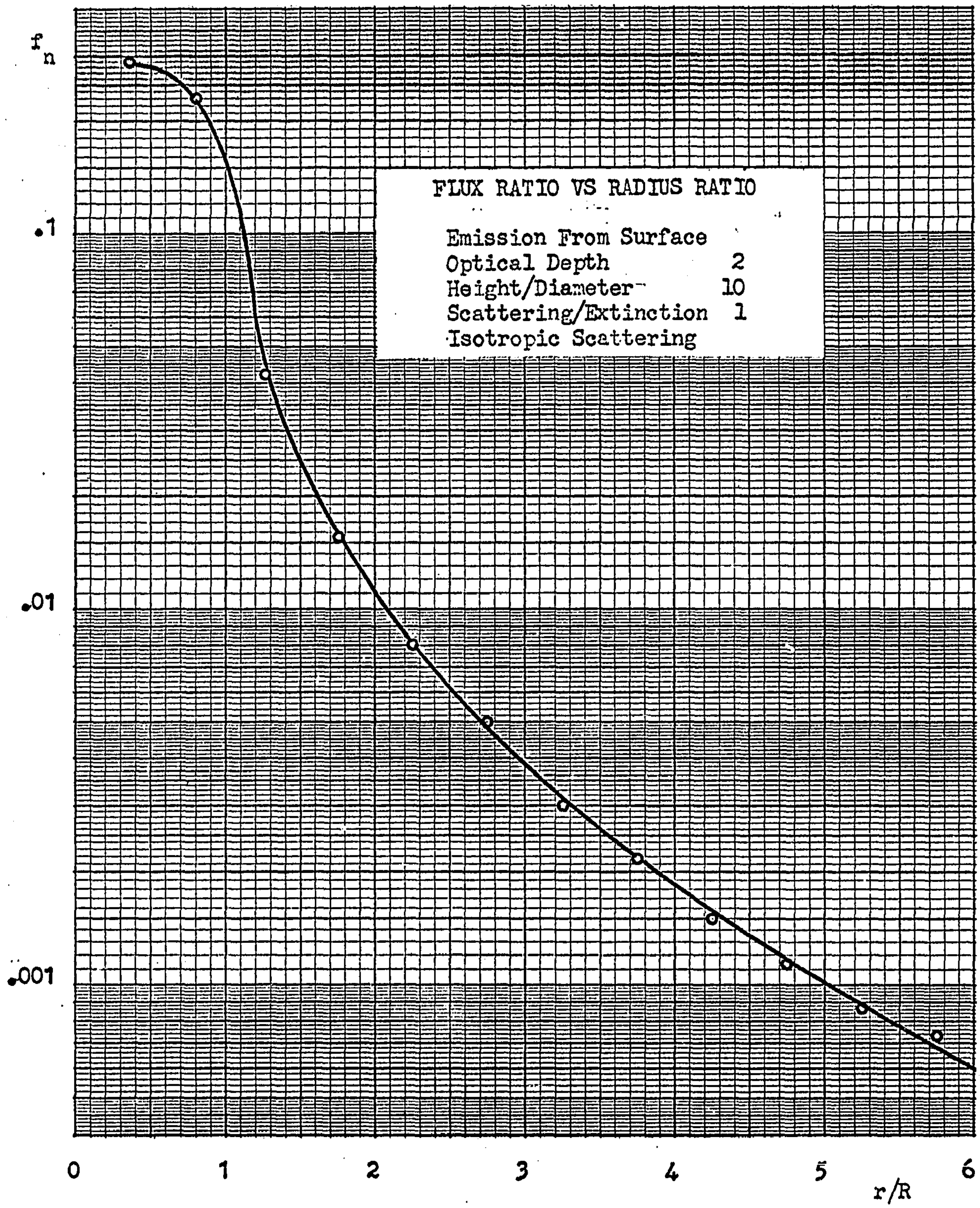

FLUX RATIO VS RADIUS RATIO
Emission From Surface
Optical Depth 2
Height/Diameter 10
Scattering/Extinction 1
Isotropic Scattering
f_n
.1
.01
.001
0
1
2
3
4
5
6
r/R

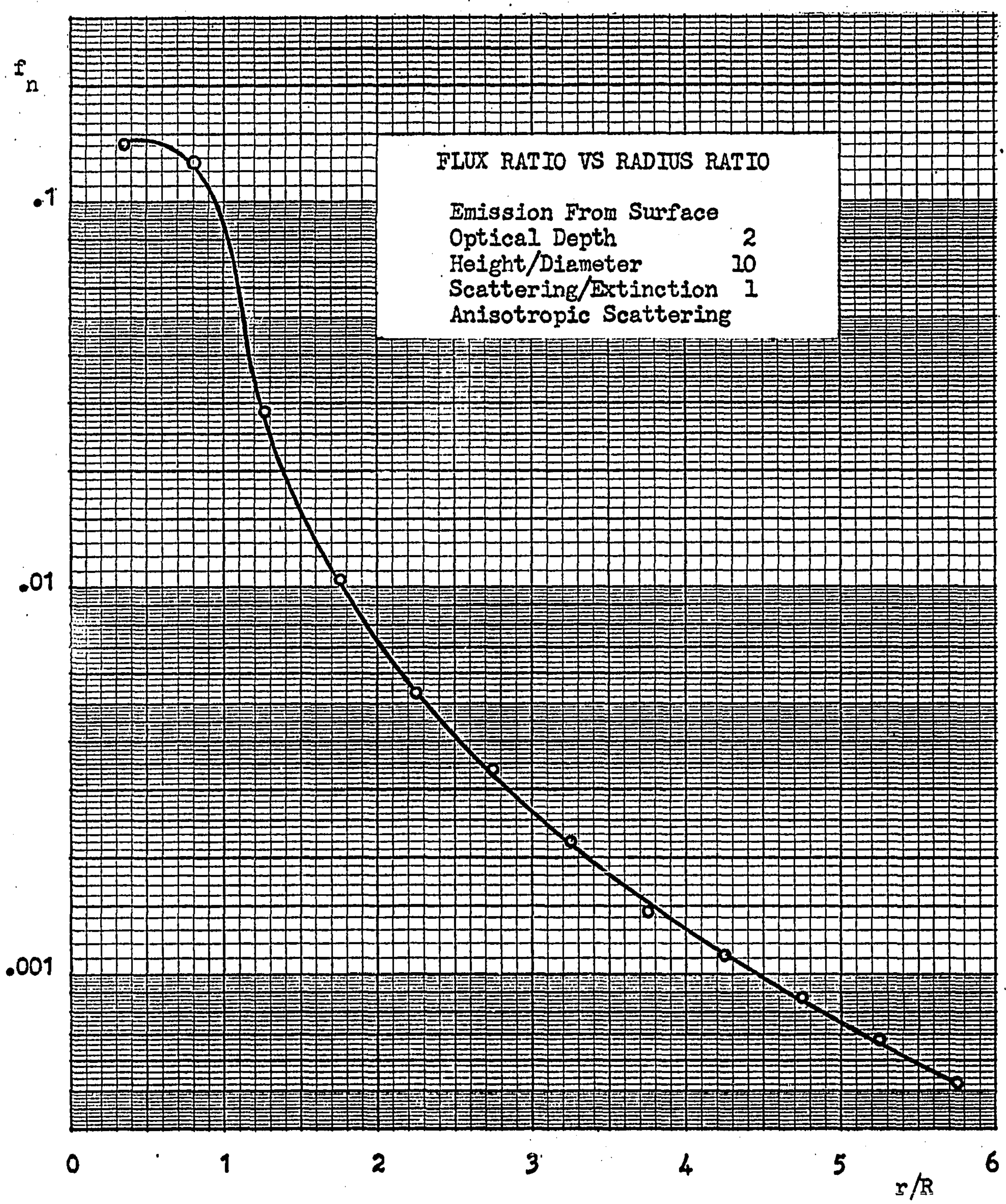
FLUX RATIO VS RADIUS RATIO
Emission From Surface
Optical Depth 2
Height/Diameter 10
Scattering/Extinction 1
Anisotropic Scattering
f n
.1
.01
.001
0
1
2
3
4
5
6
r/R

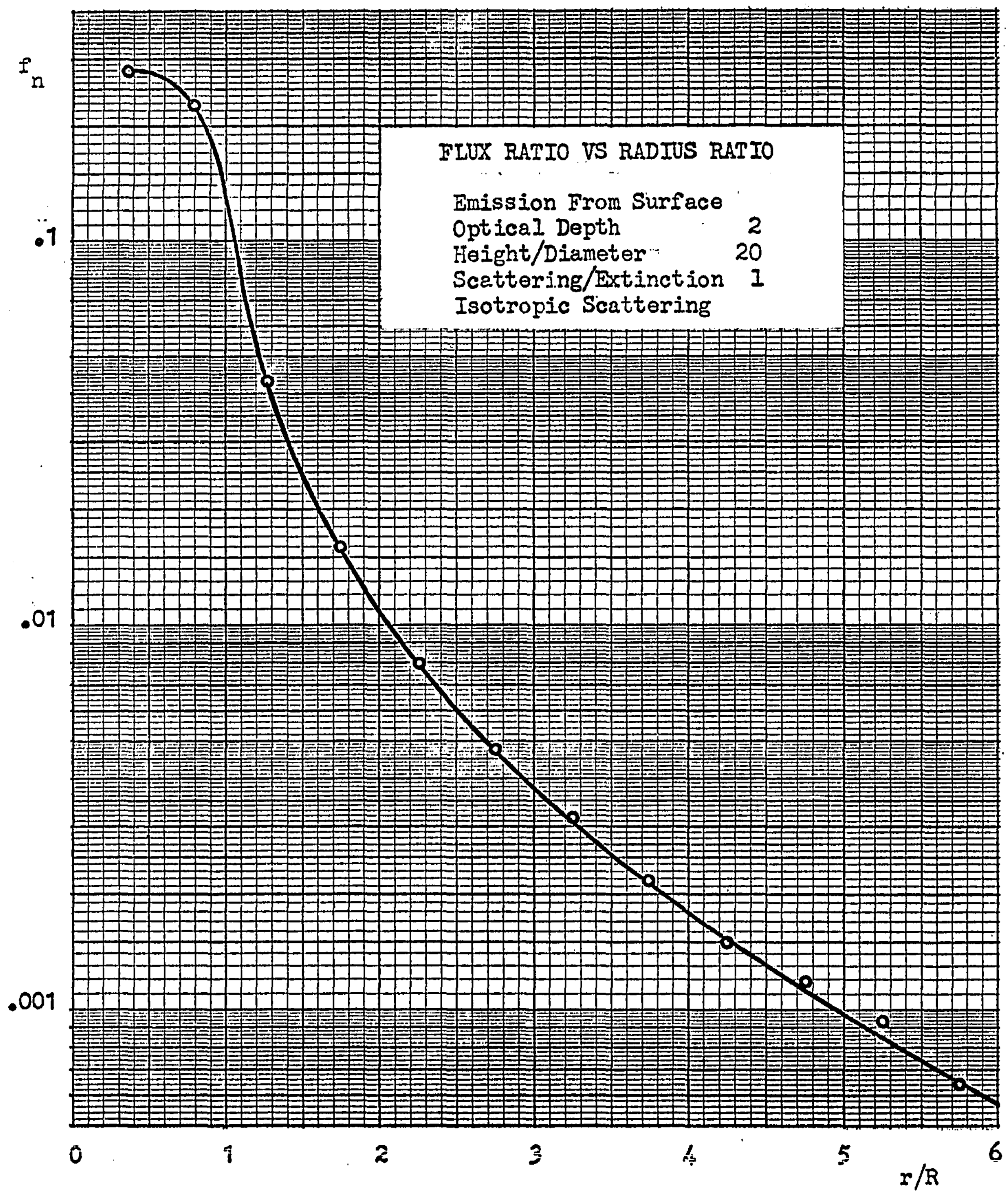

FLUX RATIO VS RADIUS RATIO
Emission From Surface
Optical Depth 2
Height/Diameter 20
Scattering/Extinction 1
Isotropic Scattering
f_n
.1
.01
.001
0
1
2
3
4
5
6
r/R

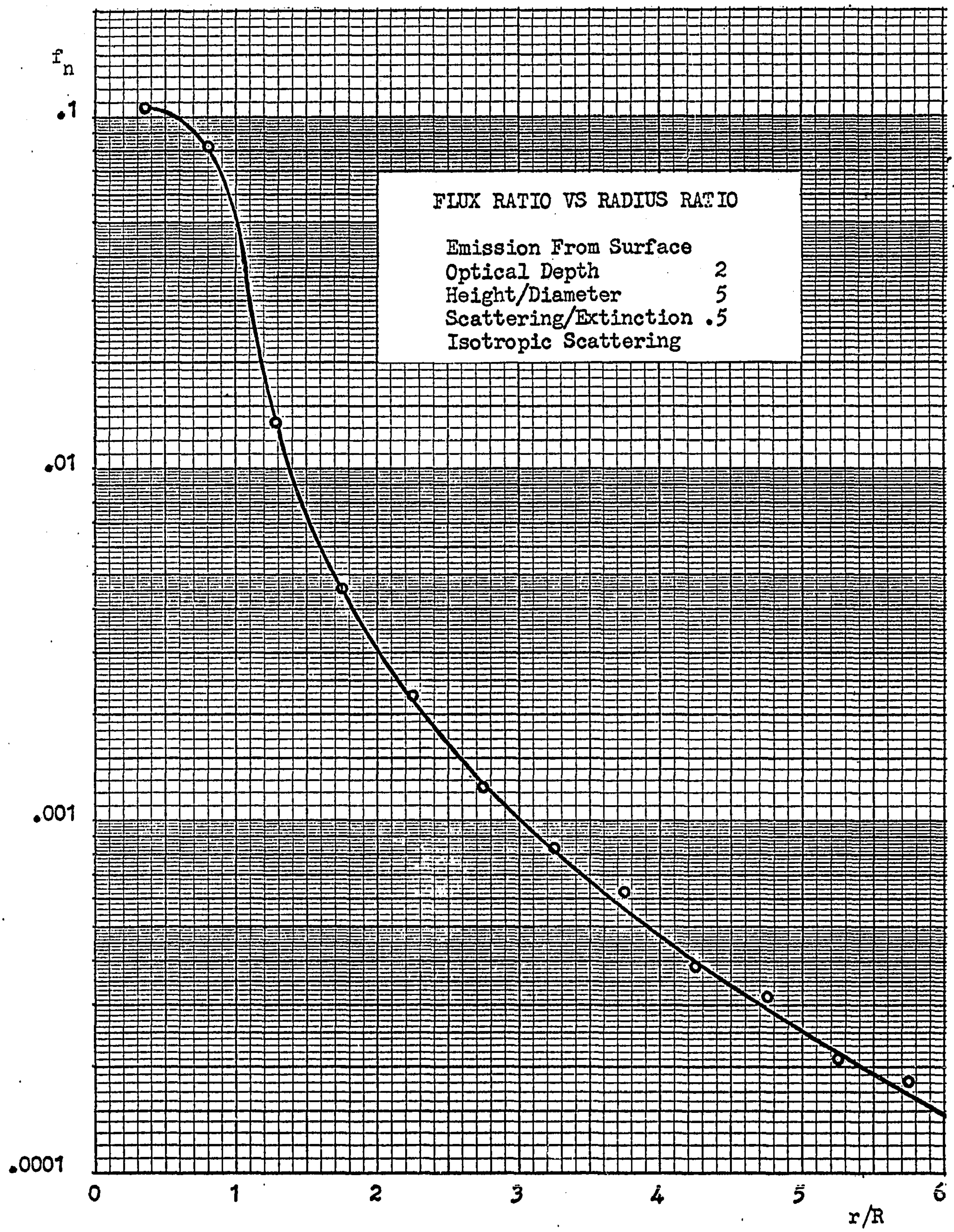
f_n
.1
.01
.001
.0001
0
1
2
3
4
5
6
r/R
FLUX RATIO VS RADIUS RATIO
Emission From Surface
Optical Depth 2
Height/Diameter 5
Scattering/Extinction .5
Isotropic Scattering

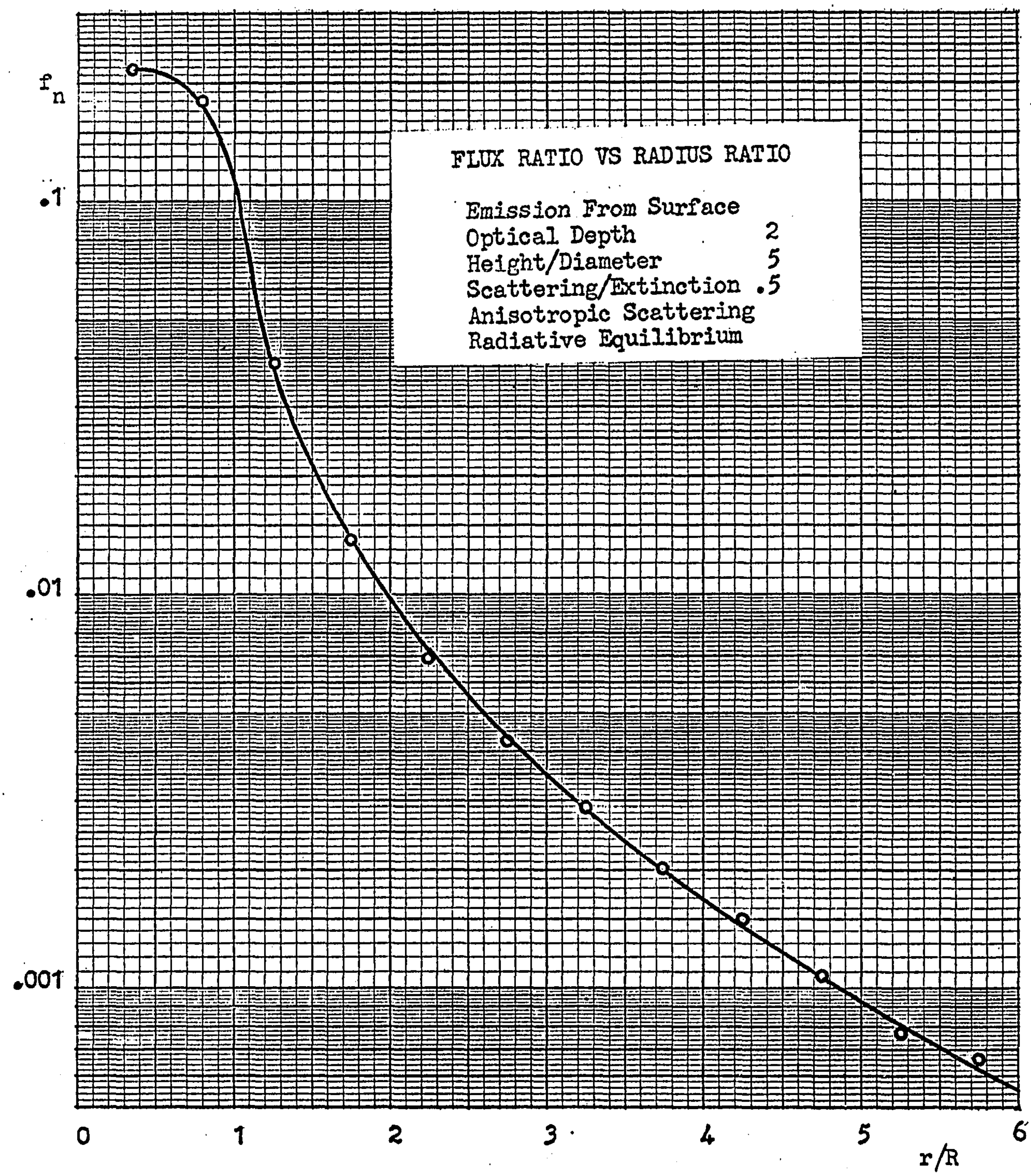
FLUX RATIO VS RADIUS RATIO
Emission From Surface
Optical Depth 2
Height/Diameter 5
Scattering/Extinction .5
Anisotropic Scattering
Radiative Equilibrium
f_n
.1
.01
.001
0
1
2
3
4
5
6
r/R

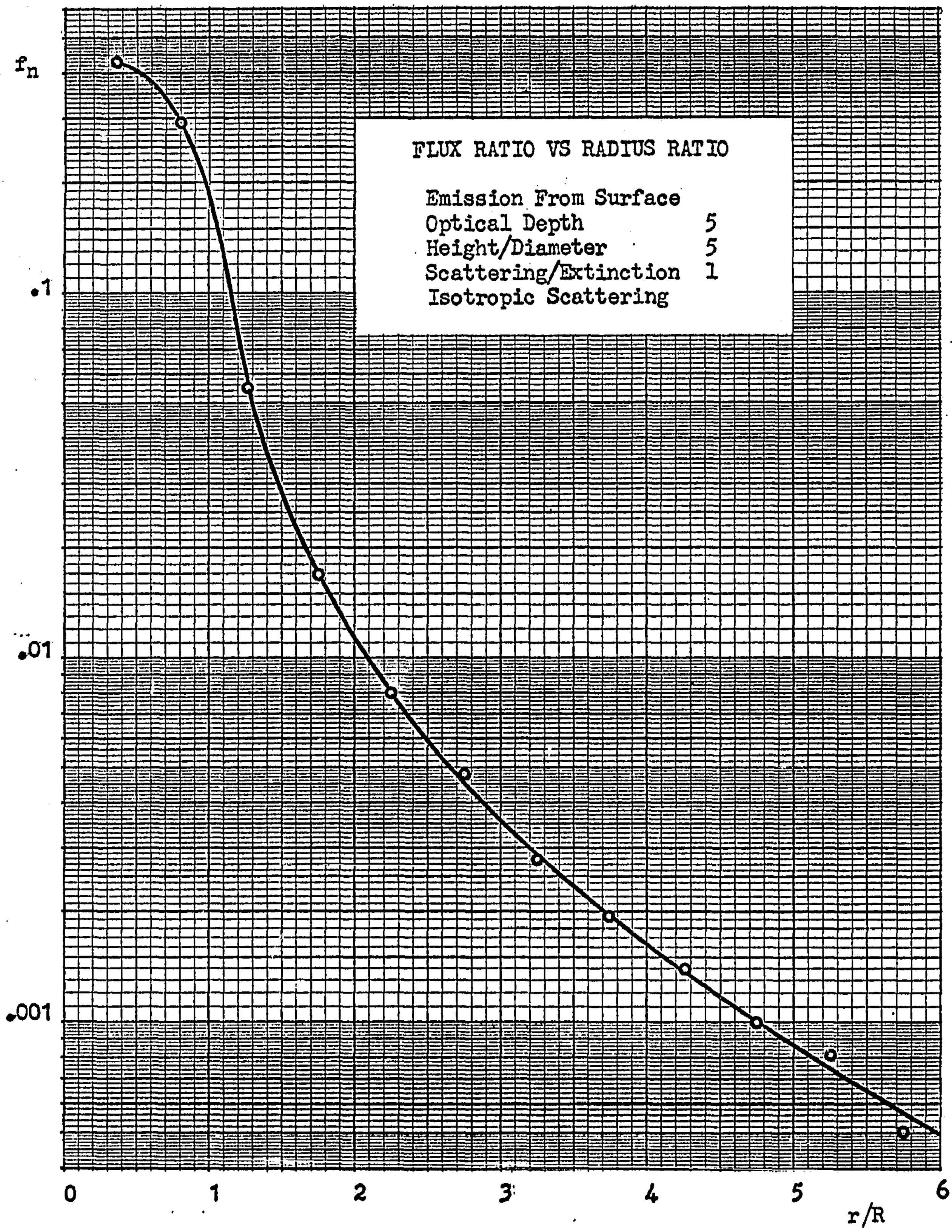

FLUX RATIO VS RADIUS RATIO
Emission From Surface
Optical Depth 5
Height/Diameter 5
Scattering/Extinction 1
Isotropic Scattering
f_n
.1
.01
.001
0
1
2
3
4
5
6
r/R

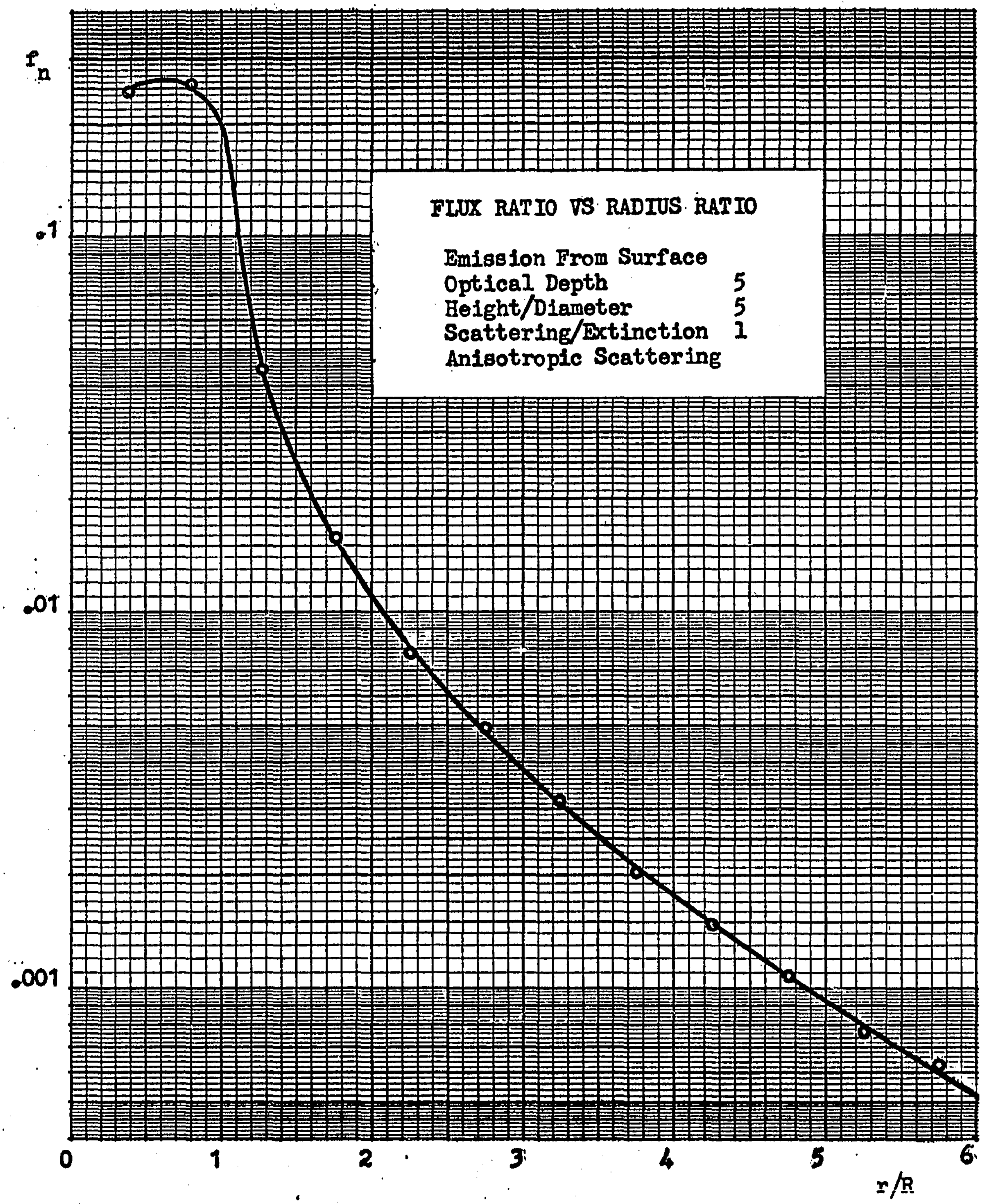

FLUX RATIO VS RADIUS RATIO
Emission From Surface
Optical Depth 5
Height/Diameter 5
Scattering/Extinction 1
Anisotropic Scattering
f_n
.1
.01
.001
0
1
2
3
4
5
6
r/R

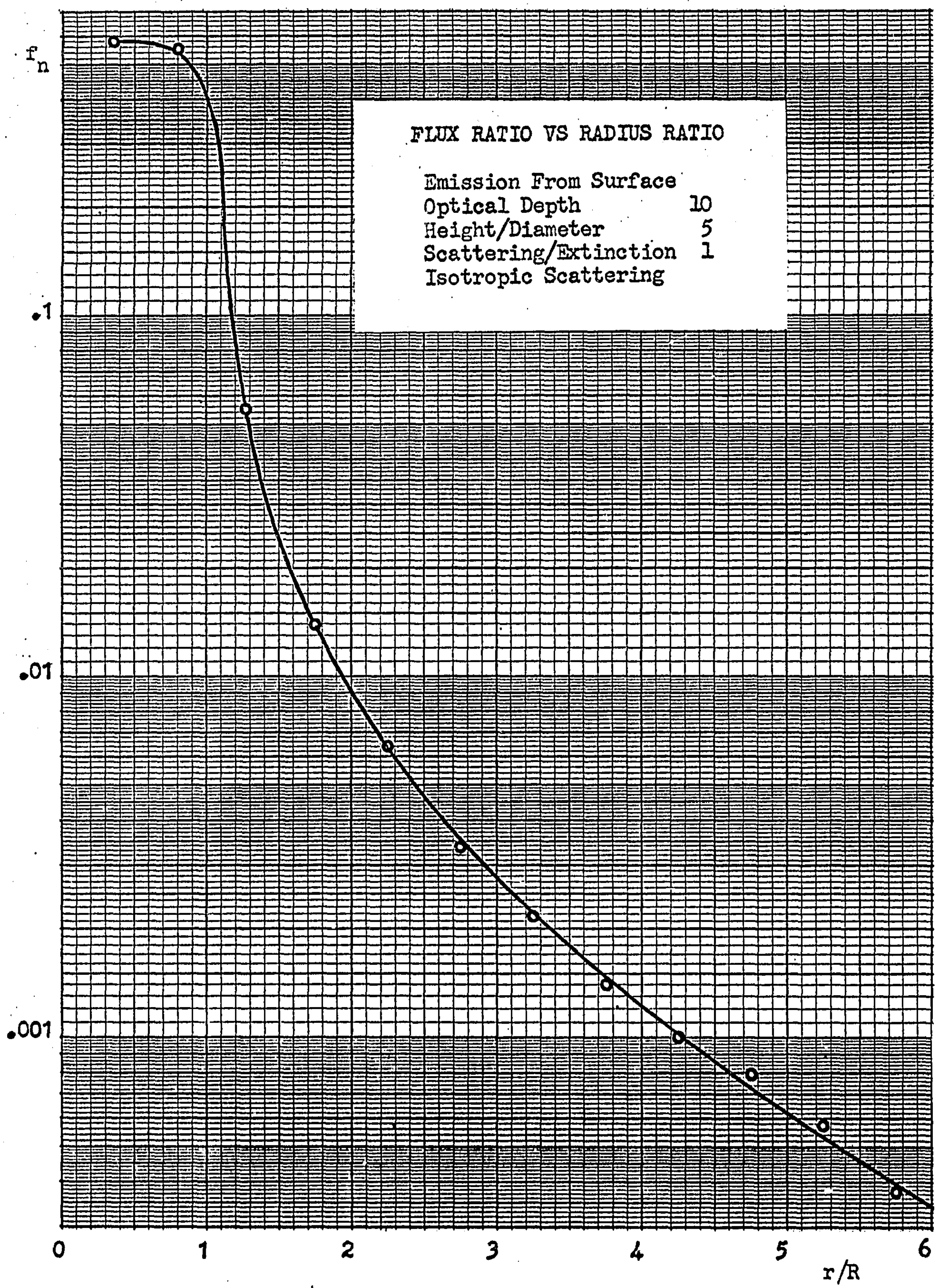

FLUX RATIO VS RADIUS RATIO
Emission From Surface
Optical Depth 10
Height/Diameter 5
Scattering/Extinction 1
Isotropic Scattering
f_n
.1
.01
.001
0
1
2
3
4
5
6
r/R

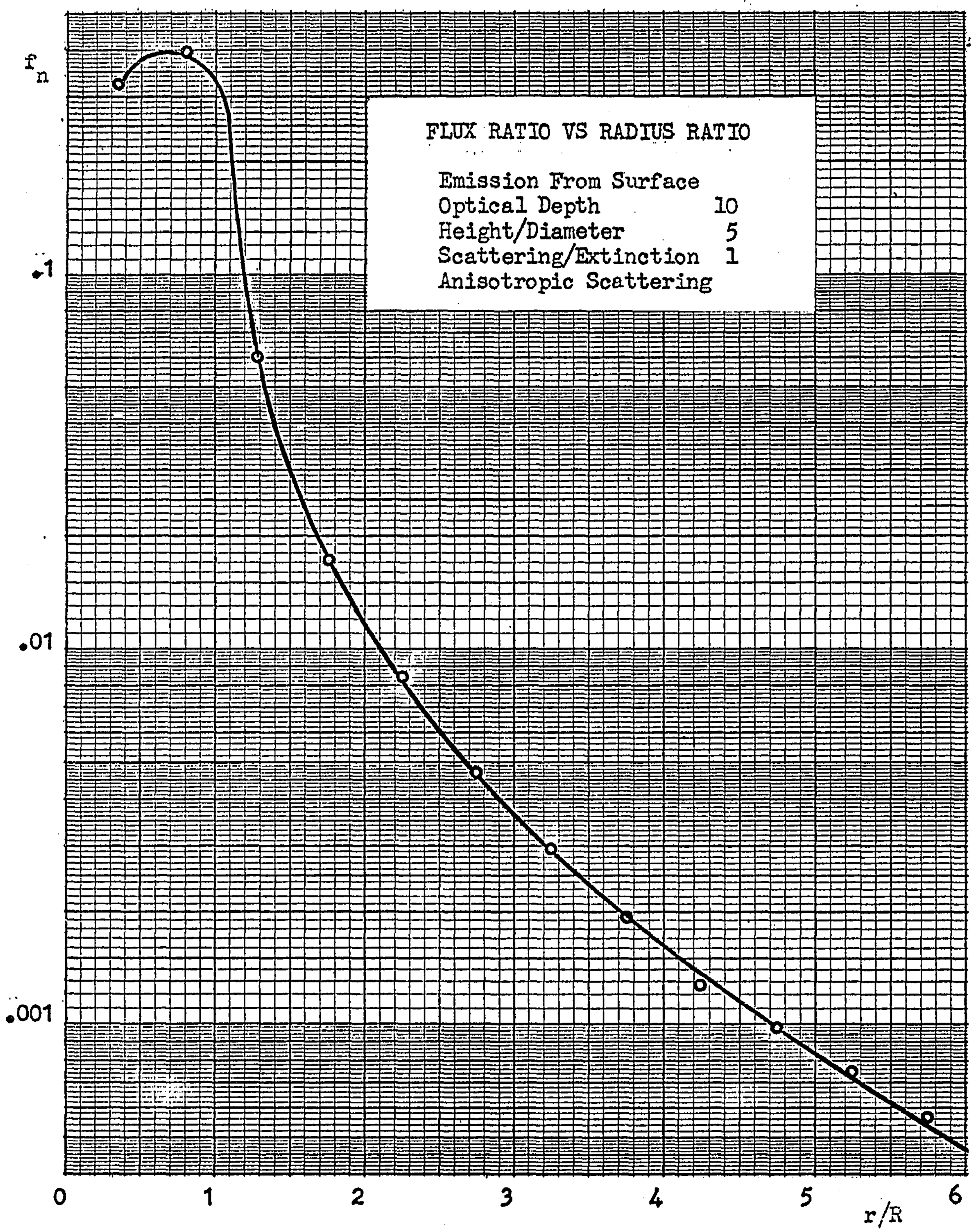

f_n
FLUX RATIO VS RADIUS RATIO
Emission From Surface
Optical Depth 10
Height/Diameter 5
Scattering/Extinction 1
Anisotropic Scattering
.1
.01
.001
0
1
2
3
4
5
6
r/R

CHAPTER VI

ERROR ANALYSIS

For a given ring (ring r) the Monte Carlo analysis can be viewed as a large number of independent trials with only two possible outcomes; a photon hits ring r or it does not. From physical aspects of the problem it is reasonable to assume that for a large sequence of emissions the relative frequency of hits in ring r will approach a limit. This limit

$$p_r = \text{(hits in ring r) / (n emissions)}_{n \to \infty}$$

is the probability that a photon will hit ring r or the probability of success in an independent Bernoulli trial.

A random experiment consisting of such trials with probability p for success and $1 - p = q$ for failure is governed by the binomial probability law which can be approximated by the normal probability law (34). The probability that a random experiment will have an observed value between given limits may be had by integration of the normal probability law over the appropriate interval. This can be translated into the probability that the observed value of a random experiment after n trials will differ by a small number ϵ from its true probability p. The result for m successes in n trials (see (36) and (25) equation 24) is that the probability of the inequality

$$\left| \frac{m}{n} - p \right| \leqq \epsilon \tag{6-1}$$

as n becomes large is given approximately by

$$P = \text{erf} \frac{t}{\sqrt{2}} \tag{6-2}$$

where

$$t = \epsilon \sqrt{\frac{n}{pq}} \tag{6-3}$$

It should be noted that the true probability for a hit in ring r is not known. However, a best estimate for p_r is available after n emissions from the ratio of hits to emissions. The use of this best estimate in the error analysis is the usual practice (25).

To obtain values of p_r from the numerical data given it is necessary to multiply by $(2r - 1)/4$ if emission is from the surface or by $(2r - 1)$ if emission is from the cloud.

Considering rings one through twelve, the values of p_r are of order .001 or greater in all cases calculated and the number of emissions is 10^5 or greater. Therefore equation (6-2) should enable one to obtain a good working estimate of the probable error associated with the Monte Carlo numerical results of this work.

Using (6-2) gives the following estimates.

p_r	Confidence	Error
.001	.954	20%
.001	.68	10%
.01	.998	10%
.01	.888	5%

These error limits hold for the individual points calculated. In the absence of a systematic error in the program it is expected that there is equal likelihood for the individual value to be high or low. Thus a smooth curve through the points should be close to the true values.

Figure 6-1 shows the variation of Monte Carlo numerical results as a function of the number of original emissions for a typical case. The relatively smooth behavior indicated lends further support to the belief that the final values do not differ greatly from the true values. At the least, one would anticipate that the values obtained suffice to indicate the important trends.

Figure 6-2 shows the result on a linear scale for ring eight starting with two different sets of initial random numbers. The answers are within ten per cent of each other after one hundred thousand emissions.

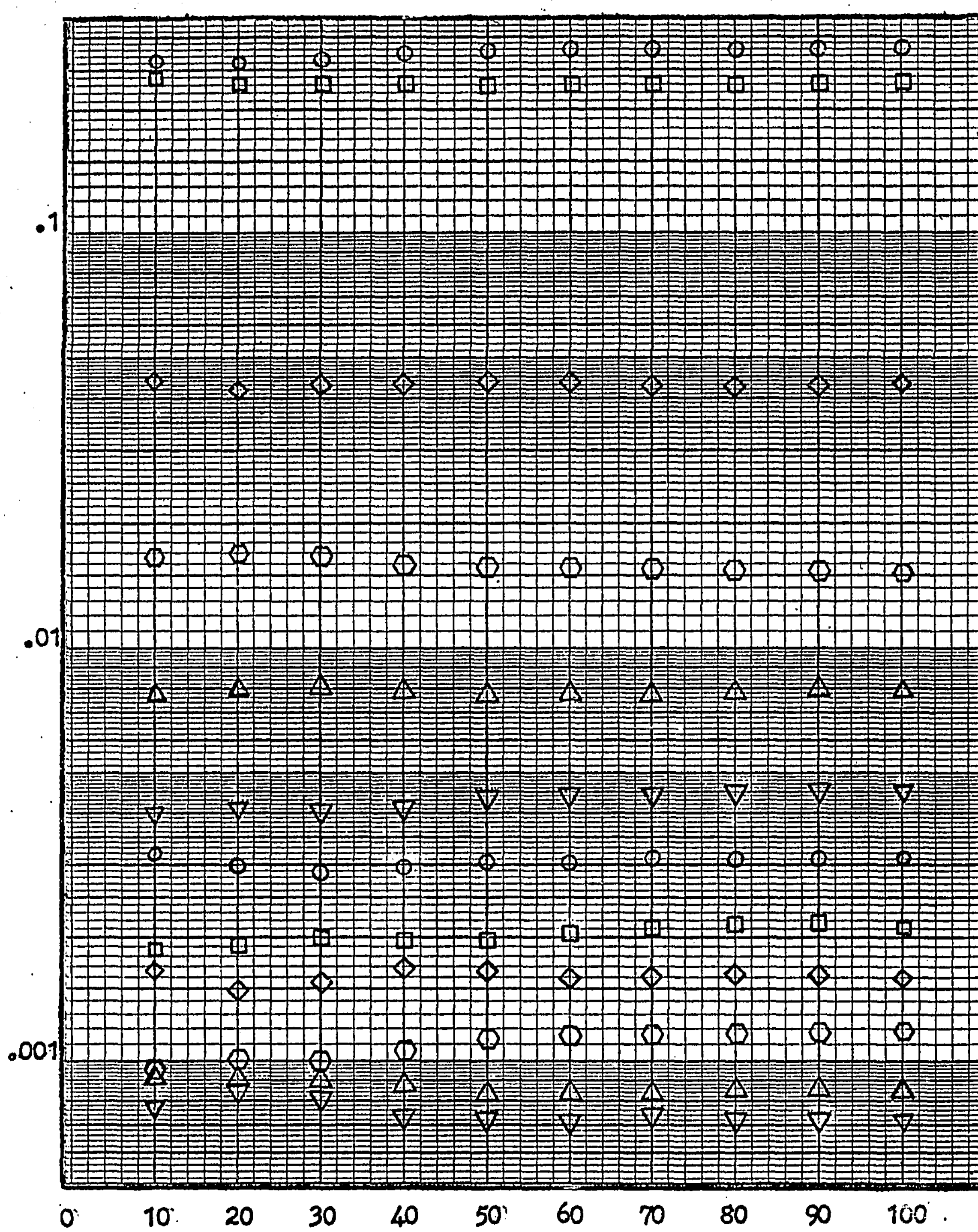

Figure 6-1. Flux Ratio versus Thousands of Original Emissions

Illustration of the variation of the Monte Carlo numerical result. Values are for rings 1 (top) through 12 (bottom). The optical diameter is two. Scattering is isotropic.

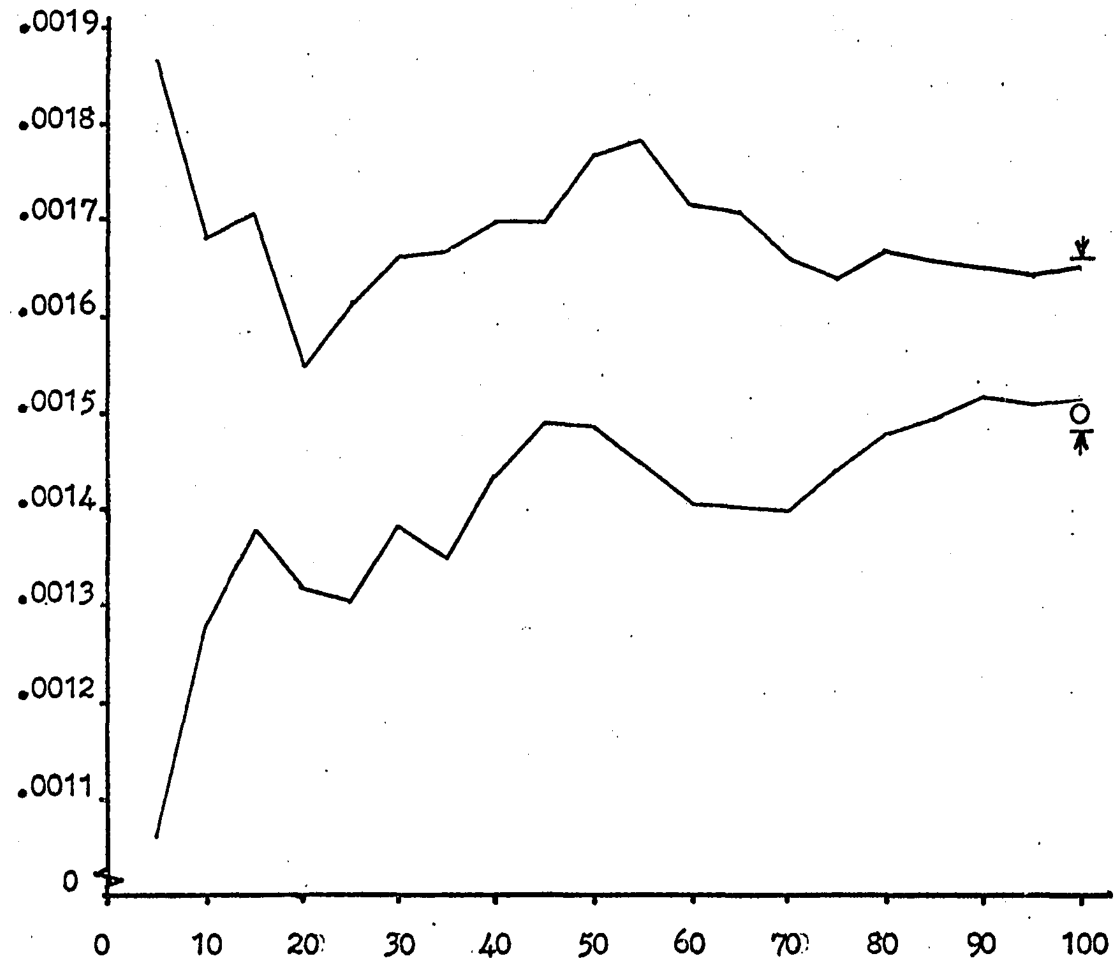

Figure 6-2. Flux Ratio versus Thousands of Original Emissions

Illustration of the variation of the Monte Carlo numerical result for two different sets of inital random numbers. The graph is formed by connecting the values of flux ratio for increments of five thousand emissions by straight lines. The values are for ring eight, the optical diameter is two, emission is from the base surface, and the scattering is anisotropic. The arrows indicate the area of overlap of ten per cent error for the two cases. There is a 98.26% probability that the correct value lies within these limits. The circle is the value obtained from a smooth curve through points for rings one through twelve.

CHAPTER VII

HEAT TRANSFER CALCULATIONS

Spectral Flux from a Black Surface

The intensity of radiation of a black body is given by

$$I_{bb}(T) = \int_0^\infty I_{b\nu}(T)d\nu$$

where

$$I_{b\nu}(T) = \frac{2h\nu^3 n^2}{c^2}\left[\frac{1}{e^{h\nu/kT} - 1}\right]$$

is Planck's expression for monochromatic intensity. To convert to spectral intensity one must define $I_{b\lambda}(T)$ such that

$$| I_{b\lambda}(T)d\lambda | = | I_{b\nu}(T)d\nu |$$

since the same energy is being represented (3). The relationship between frequency and wavelength is

$$\lambda = c/\nu$$

so that

$$d\lambda = -(c/\nu^2)d\nu$$

Therefore

$$I_{b\lambda}(T) = \frac{\nu^2}{c} I_{b\nu}(T) = \frac{2h\nu^5 n^2}{c^3}\left[\frac{1}{e^{h\nu/kT} - 1}\right]$$

or

$$I_{b\lambda}(T) = \frac{2hc^2 n^2}{\lambda^5}\left[\frac{1}{e^{hc/k\lambda T} - 1}\right]$$

Also

$$I_{bb}(T) = \int_{\infty}^{0} \frac{c}{\nu^2} I_{b\lambda}(T) \left(\frac{-\nu^2}{c}\right) d\lambda$$

or

$$I_{bb}(T) = \int_{0}^{\infty} I_{b\lambda}(T) d\lambda$$

The flux leaving the surface of a black body is

$$q_{bb}(T) = \int_{\omega} I_{bb}(T) \cos\theta \, d\omega$$

where θ is the polar angle between the outward surface normal and the central direction of the solid angle $d\omega$. Substituting for $I_{bb}(T)$ gives

$$q_{bb}(T) = \int_{\omega} \left[\int_{0}^{\infty} I_{b\lambda}(T) d\lambda \right] \cos\theta \, d\omega$$

Noting that $I_{b\lambda}(T)$ is not a function of θ and integrating over the hemispherical solid angle above the surface gives

$$q_{bb}(T) = \pi \int_{0}^{\infty} I_{b\lambda}(T) d\lambda$$

Define spectral flux $q_{b\lambda}(T)$ such that

$$q_{bb}(T) = \int_{0}^{\infty} q_{b\lambda}(T) d\lambda$$

Then by comparison

$$q_{b\lambda}(T) d\lambda = \pi \, I_{b\lambda}(T) d\lambda \tag{7-1}$$

is the energy per unit area per unit time contained in the wavelength interval λ to $\lambda + d\lambda$ which leaves the surface.

The spectral flux can also be thought of as the number of bundles of energy or photons corresponding to wavelengths between λ and $\lambda + d\lambda$

which leave surface s per unit time divided by the surface area and multiplied by the energy of each bundle

$$q_{b\lambda}(T)d\lambda = N(s,\lambda)\,\frac{e}{A_s}\,d\lambda \tag{7-2}$$

<u>Flux Incident on Ring n from a Black Surface at the Base of the Cloud</u>

The spectral flux incident on an area n per unit area and time can be defined similarly to equation (7-2). Thus

$$q_{n\lambda}(T)d\lambda = N(n,\lambda)\,\frac{e}{A_n}\,d\lambda$$

so that

$$q_{n\lambda}(T) = \frac{N(n,\lambda)}{N(s,\lambda)}\,\frac{A_s}{A_n}\,q_{b\lambda}(T)$$

Defining flux ratio

$$f(n,s,\lambda) = \frac{N(n,\lambda)}{N(s,\lambda)}\,\frac{A_s}{A_n} \tag{7-3}$$

gives

$$q_{n\lambda}(T) = f(n,s,\lambda)\;\pi\;I_{b\lambda}(T) \tag{7-4}$$

as the spectral flux at surface n as a result of emission from the black surface s.

If the spectral flux to a surface n from a black surface s is given by equation (7-4) then the total flux may be calculated from

$$q_n(T) = \int_0^\infty q_{n\lambda}(T)d\lambda = \pi \int_0^\infty f(n,s,\lambda)\quad I_{b\lambda}(T)d\lambda$$

Assuming the index of refraction of the media between surfaces to be unity

$$q_{n\lambda}(T) = 2\pi \int f(n,s,\lambda)\quad \frac{hc^2}{\lambda^5}\quad \frac{e^{-hc/k\lambda T}}{1 - e^{-hc/k\lambda T}}\,d\lambda$$

This can be evaluated following the lead of Love (3).

Let

$$x = hc/k\lambda T \qquad \lambda = hc/kxT \qquad d\lambda = (-hc/kx^2T)dx$$

Then

$$q_n(T) = 2\pi \int_0^\infty f(n,s,x) \quad \frac{x^3(kT)^4}{h^3\ c^2} \left[\frac{e^{-x}}{1 - e^{-x}}\right] dx$$

The Reiz quadrature can be used to evaluate

$$\int_0^\infty e^{-x}\Phi(x)dx = \sum_{p=1}^{M} a_p\Phi(x_p)$$

where a_p and x_p are weighting coefficients and quadrature points respectively.

Hence

$$q_n(T) = \pi T^4 \sum_{p=1}^{M} a_p f(n,s,x_p) \frac{2x_p^3k^4}{h^3c^2(1 - e^{-x_p})}$$

or

$$q_n(T) = \pi T^4 \sum_{p=1}^{M} A_p f(n,s,\lambda_p) \tag{7-5}$$

where

$$A_p = \frac{2a_px_p^3k^4}{h^3c^2(1 - e^{-x_p})} \tag{7-6}$$

and

$$\lambda_p = hc/kx_pT \tag{7-7}$$

The A_p's and λ_p's have been calculated by Love (3) for M = 5 and by Hickok (30) for M = 6, 7. Hickok showed that M = 7 gave improved values for heat transfer calculations. Therefore use M = 7.

Thus

$$q_n(T) = \pi T^4 \sum_{p=1}^{7} A_p f(n,s,\lambda_p) \tag{7-8}$$

where

$$A_1 = 0.14125 \times 10^{-11} \quad (\mathrm{BTU\ ft^{-2}hr^{-1}\ {}^oR^{-4}})$$

$$A_2 = 5.98749 \times 10^{-11}$$

$$A_3 = 22.65796 \times 10^{-11}$$

$$A_4 = 20.53423 \times 10^{-11}$$

$$A_5 = 4.93863 \times 10^{-11}$$

$$A_6 = .27503 \times 10^{-11}$$

$$A_7 = .00194 \times 10^{-11}$$

$$\sum_{n=1}^{7} A_n = 54.53653 \times 10^{-11}$$

$$\lambda_1 = 13.41488\ (10^4/T) \quad (T \text{ in } {}^oR,\ \lambda \text{ in microns})$$

$$\lambda_2 = 2.52236\ (10^4/T)$$

$$\lambda_3 = 1.00846\ (10^4/T)$$

$$\lambda_4 = .52845\ (10^4/T)$$

$$\lambda_5 = .31649\ (10^4/T)$$

$$\lambda_6 = .20336\ (10^4/T)$$

$$\lambda_7 = .13351\ (10^4/T)$$

Emission from a Volume Element

The following development parallels that of Love (3). Other derivations are available in the literature. (For example Jakob (31))

Experimental studies have shown that the intensity of radiant energy traversing a semi-transparent medium is decreased by absorption in proportion to the intensity and length of path. This experimental fact is commonly called Beer's Law and is mathematically expressed as

$$\frac{dI_\nu}{dx} = -\rho_c\ \kappa_\nu\ I_\nu \tag{7-9}$$

where I_ν is the monochromatic intensity in direction x, ρ_c is the density of the cloud or medium being traversed, and κ_ν is the monochromatic mass absorption coefficient.

Equation (7-9) was originally developed for the attenuation of beams of light and contains no term accounting for local emission of thermal radiation. Hence an additional term must be added to account for such emission when it exists.

$$\frac{dI_\nu}{dx} = -\rho_c \kappa_\nu I_\nu + J_\nu \tag{7-10}$$

For a medium in thermodynamic equilibrium the intensity of radiation will not change along a path so that dI_ν/dx is zero. Thus

$$J_\nu = \rho_c \kappa_\nu I_\nu$$

For a medium in which rapid chemical changes are not taking place a "local thermodynamic equilibrium" is approximated so that the emission from an elemental volume in any direction may be taken as $\rho_c \kappa_\nu I_\nu dV$, (3). Integration over all directions gives

$$4\pi \rho_c \kappa_\nu I_\nu dV$$

for the monochromatic emission of a volume element. In a medium in thermodynamic equilibrium, having a refractive index n, the intensity of radiation is n^2 times the intensity of radiation of a black body at the temperature of the medium. Hence the monochromatic emission (n = 1) becomes

$$4\pi \rho_c \kappa_\nu I_{b,\nu}(T) dV$$

This may also be expressed in spectral quantities as

$$4\pi \rho_c \kappa_\lambda I_{b,\lambda}(T) dV \tag{7-11}$$

where

$$I_{b\lambda}(T) = \frac{2hc^2n^2}{\lambda^5}\left[\frac{1}{e^{hc/k\lambda T} - 1}\right]$$

Integration over the complete wavelength band can be accomplished using the Reiz quadrature as in the preceding section

Thus

$$\begin{bmatrix}\text{energy per unit} \\ \text{time per unit volume}\end{bmatrix} dV = 4\pi\, \rho_c T^4 \left[\sum_{p=1}^{M} A_p\, \varkappa_{\lambda p}\right] dV \qquad (7\text{-}12)$$

where the A_p and λ_p are the weighting functions and quadrature points given in the preceding section.

The Apparent Emittance of the Particle Cloud, as Viewed in the Base Plane, Resulting from Emission within the Cloud

The data presented in Chapter V for emission from the particle cloud gives the number of original emissions (N_E), the number of scatterings (N_s) and a value for each ring n of $\Phi_{n\lambda}$ defined as[1]

$$\Phi_{n\lambda} = \frac{N_{Hn}}{N_E} \qquad (7\text{-}13)$$

where N_{Hn} is the number of hits in ring n. The values are for a given τ, $\frac{\sigma}{\beta}$, H/D, and scattering function. If the cloud is considered to be in radiative equilibrium then the data for $\frac{\sigma}{\beta} = 1$ can be used for any value of $\frac{\sigma}{\beta}$, with isotropic scattering, by calculating the number of photons absorbed and hence the number of photons reemitted (N_R) from

$$N_R = N_s\left(1 - \frac{\sigma}{\beta}\right) = N_s\,\frac{\varkappa}{\beta} \qquad (7\text{-}14)$$

For a uniform isothermal cloud of volume V the total energy emitted, which is equal to the sum of the original emissions and the reemissions

---

[1]The tabular data for cloud emission has an additional factor (2n - 1).

multiplied by the energy of each emission, can be obtained from equation (7-11) as

$$(N_E + N_s \frac{\varkappa_\lambda}{\beta_\lambda}) e d\lambda = 4\pi \rho_c V \varkappa_\lambda I_{b\lambda}(T)\, d\lambda \tag{7-15}$$

In (7-15) it has been assumed that the reemissions are uniformly distributed throughout the cloud (see appendix D).

The spectral energy hitting ring n is $N_{Hn} e d\lambda$ which can be obtained from equations (7-13) and (7-15) as

$$E_{n\lambda} d\lambda = N_{Hn} e d\lambda = \frac{4\pi \rho_c \varkappa_\lambda I_{b\lambda}(T) V N_E \Phi_n d\lambda}{(N_E + N_s \frac{\varkappa_\lambda}{\beta_\lambda})} \tag{7-16}$$

Now if the cloud is considered to be a diffuse cylindrical surface of the same size and temperature as the particle cloud the energy $E_{n\lambda} d\lambda$ could be expressed as

$$E_{n\lambda} d\lambda = \epsilon_\lambda \pi I_{b\lambda}(T)\, A\, F_{2n} d\lambda \tag{7-17}$$

where A is the surface area and F_{2n} is the configuration factor from the cylinder to ring n. Equating (7-16) and (7-17) and substituting $\pi R^2 H$ for the cylinder volume and $2\pi RH$ for the surface area gives

$$\epsilon_\lambda = \frac{2\rho_c \varkappa_\lambda R N_E \Phi_{n\lambda}}{F_{2n} (N_E + N_s \frac{\varkappa_\lambda}{\beta\lambda})}$$

or setting $\tau_\lambda = 2\rho_c \beta_\lambda R$

$$\epsilon_\lambda = \frac{\tau_\lambda \frac{\varkappa_\lambda}{\beta_\lambda} N_E \Phi_{n\lambda}}{F_{2n}(N_E + N_s \frac{\varkappa_\lambda}{\beta_\lambda})} \tag{7-18}$$

Using the Reiz quadrature and a similar development gives

$$\epsilon = \frac{2\pi\ \rho_c\ R\ N_E}{\sigma F_{2n}} \sum_{p=1}^{M} A_p \left[\frac{\kappa_\lambda\ \Phi_{n\lambda}}{N_E + N_s \frac{\kappa_\lambda}{\beta_\lambda}}\right]_{\lambda_p} \tag{7-19}$$

<u>The Apparent Emittance of the Particle Cloud, as Viewed in the Base Plane, Resulting from Energy Emitted by a Black Surface at the Base of the Cloud</u>

The scattering, by a rocket exhaust plume, of energy radiated to the plume from a high temperature combustion chamber motivates this derivation.

The spectral flux incident on ring n as a result of scattering of energy emitted by a black surface covering the base of the cloud is (equation 7-4)

$$q_{n\lambda} d\lambda = f(n,s,\lambda)\ \pi I_{b\lambda}(T_s)\ d\lambda \tag{7-20}$$

The value of $f(n,s,\lambda)$ is presented in the numerical data as flux ratio for given H/D, τ, $\frac{\sigma}{\beta}$, and scattering function.

Considering the cloud as a diffuse cylinder at temperature T_c, the spectral flux on ring n would be

$$q_{n\lambda} d\lambda = \epsilon_\lambda\ \pi I_{b\lambda}(T_c)\ F_{2n}(A_{cyl}/A_n)\ d\lambda \tag{7-21}$$

Now

$$A_{cyl} = 2\pi RH$$

$$A_n = \pi(.5R)^2\ (2n - 1)$$

so that from (7-20) and (7-21)

$$\epsilon_\lambda = \frac{f(n,s,\lambda)}{F_{2n}} \frac{I_{b\lambda}(T_s)}{I_{b\lambda}(T_c)} \frac{(2n - 1)}{16} \frac{D}{H} \tag{7-22}$$

If $f(n,s,\lambda)$ is not a function of wavelength

$$\epsilon = \frac{f_{ns}}{F_{2n}} \left(\frac{T_s}{T_c}\right)^4 \left(\frac{2n - 1}{16}\right) \frac{D}{H} \tag{7-23}$$

It should be remembered that f(n,s) is for a given optical diameter (τ), cylinder geometry (H/D), scattering to extinction ratio ($\frac{\sigma}{\beta}$) and scattering function. In addition it should be noted that some combinations of T_s/T_c could provide values for apparent emissivity which would be greater than 1.

<u>Flux Incident on Ring n from Emission within the Cloud</u>

The spectral energy incident on ring n is given by equation (7-16). The area of the nth ring for ring width of .5R is given by

$$A_n = (.5R)^2 \pi \, (2n - 1)$$

Substituting $\pi R^2 H$ for the volume of the cloud and dividing (7-16) by A_n gives

$$q_{n\lambda} d\lambda = \frac{16\pi \, \rho_c \, \varkappa_\lambda \, I_{b\lambda}(T) \, H \, N_E \, \Phi_{n\lambda} d\lambda}{(N_E + N_s \frac{\varkappa_\lambda}{\beta_\lambda})(2n - 1)}$$

$$= \frac{16\tau_\lambda \frac{\varkappa_\lambda}{\beta_\lambda} \frac{H}{D} \pi I_{b\lambda}(T) \, N_E \, \Phi_{n\lambda} d\lambda}{(N_E + N_s \frac{\varkappa_\lambda}{\beta_\lambda})(2n - 1)} \tag{7-24}$$

Using the Reiz quadrature to integrate over wavelength gives

$$q_n = \frac{16\pi \, H \, T^4 N_E}{D(2n - 1)} \sum_{p=1}^{M} A_p \left(\frac{\tau_\lambda \frac{\varkappa_\lambda}{\beta_\lambda} \Phi_{n\lambda}}{N_E + N_s \frac{\varkappa_\lambda}{\beta_\lambda}}\right)_{\lambda_p} \tag{7-25}$$

or for a gray cloud

$$q_n = \frac{16\tau \frac{\varkappa}{\beta} \Phi_n \frac{H}{D} N_E \, \sigma \, T^4}{(N_E + N_s \frac{\varkappa}{\beta})(2n - 1)} \tag{7-26}$$

The equations derived in this section are subject to the same limitations as equation (7-18). See Appendix D.

CHAPTER VIII

DISCUSSION OF RESULTS

Some qualitative results of this investigation are presented in Figures 8-1 through 8-12. The curves used in the comparisons are taken from Chapter V.

Figures 8-1 through 8-8 concern the case of emission from the surface at the base of the cloud. In Figures 8-1 through 8-5 the effect of isotropic and anisotropic scattering on the flux scattered back to the base plane by the particle cloud is compared. The comparison is made at five different values of optical diameter (τ). If one examines the curves at some given radius ratio ($r/R = 4$) and assumes that the flux emitted by the base surface is constant then the following effects can be noted. At an optical diameter of .5 the isotropic scattering result is 150 percent greater than the anisotropic result. This difference decreases to 100 percent at $\tau = 1$ and to 50 percent at $\tau = 2$. The Rayleigh scattering result, which was calculated at $\tau = 1$ and $\tau = 2$, coincides with the isotropic result. At $\tau = 5$ the result is essentially the same for isotropic and anisotropic scattering. At $\tau = 10$ the anisotropic result provides the greater flux, being some 30 percent higher than for isotropic scattering.

Figures 8-6 through 8-8 show the effect of other parameters on the

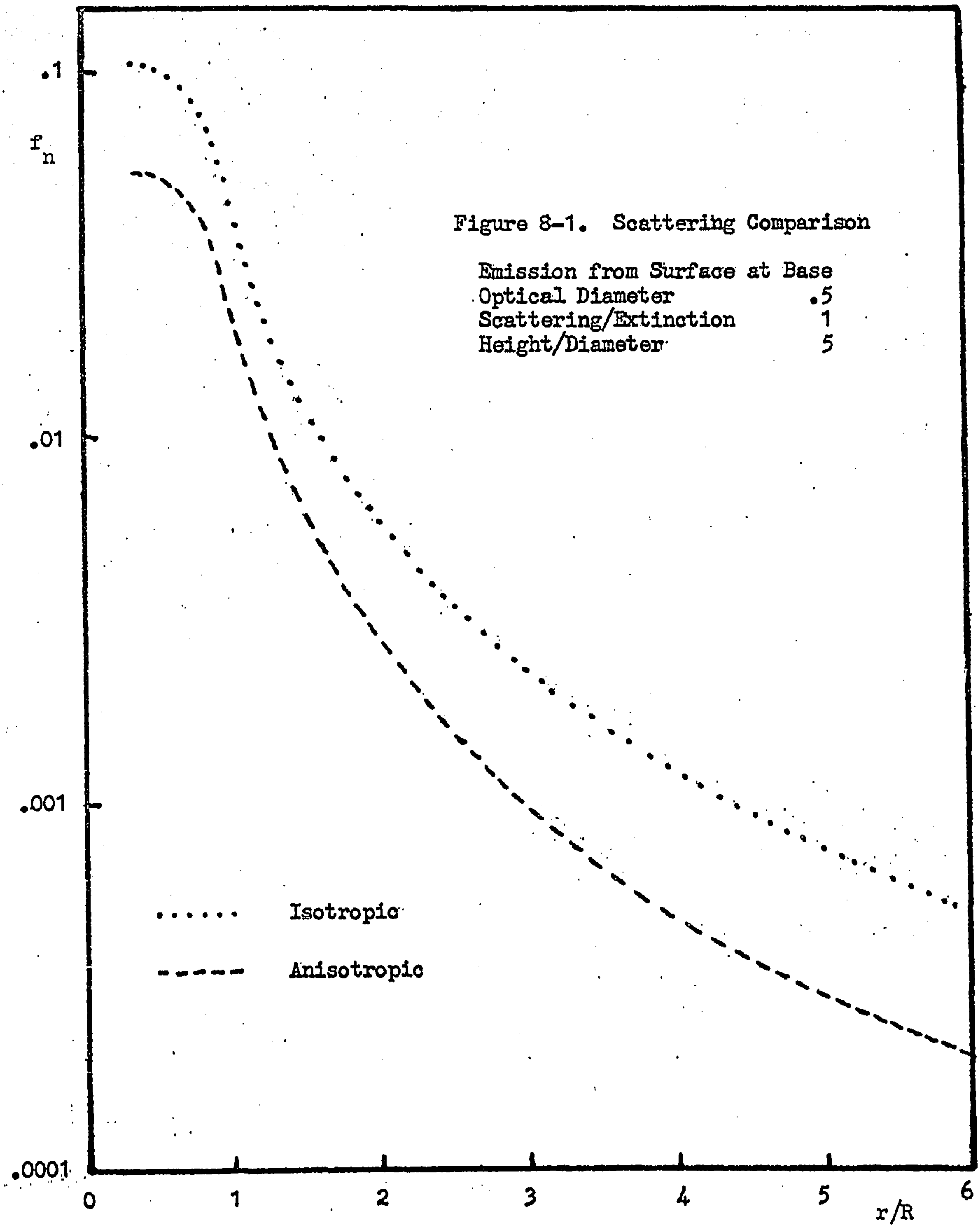
.1
f_n
.01
.001
.0001
0
1
2
3
4
5
6
r/R
Figure 8-1. Scattering Comparison
Emission from Surface at Base
Optical Diameter .5
Scattering/Extinction 1
Height/Diameter 5
Isotropic
Anisotropic

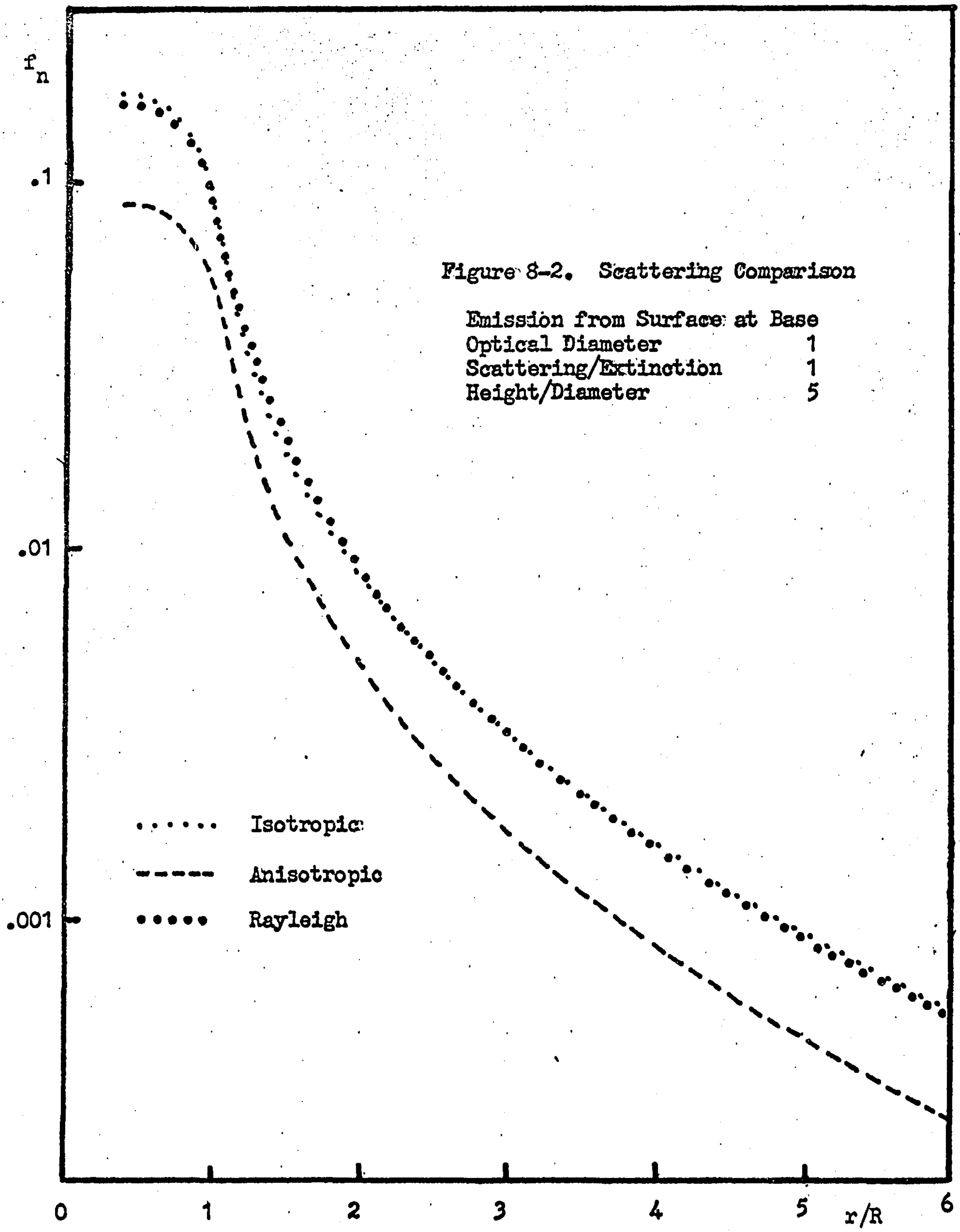
Figure 8-2. Scattering Comparison
Emission from Surface at Base
Optical Diameter 1
Scattering/Extinction 1
Height/Diameter 5
f_n
.1
.01
.001
Isotropic
Anisotropic
Rayleigh
0
1
2
3
4
5
6
r/R

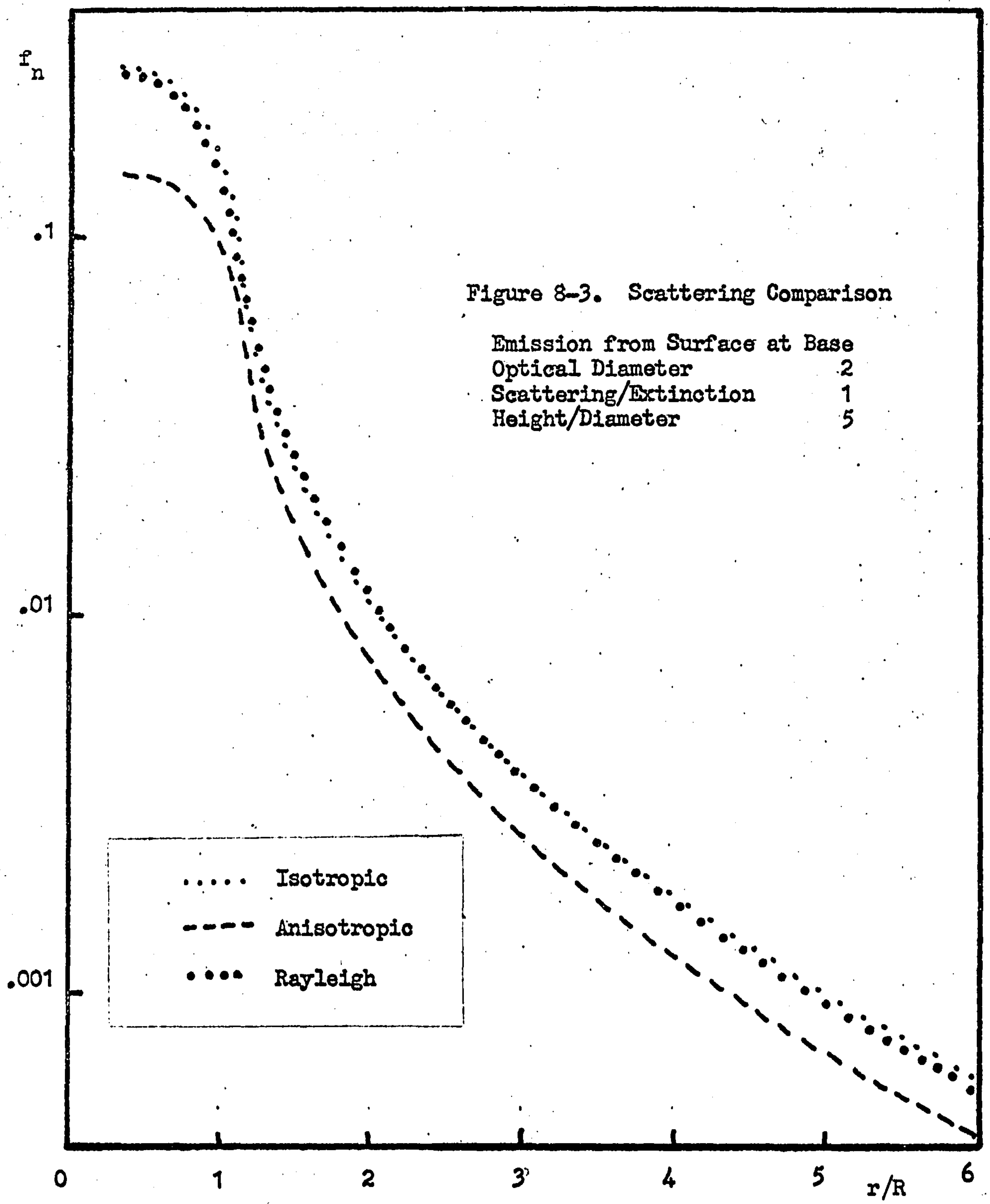

Figure 8-3. Scattering Comparison

Emission from Surface at Base
Optical Diameter 2
Scattering/Extinction 1
Height/Diameter 5

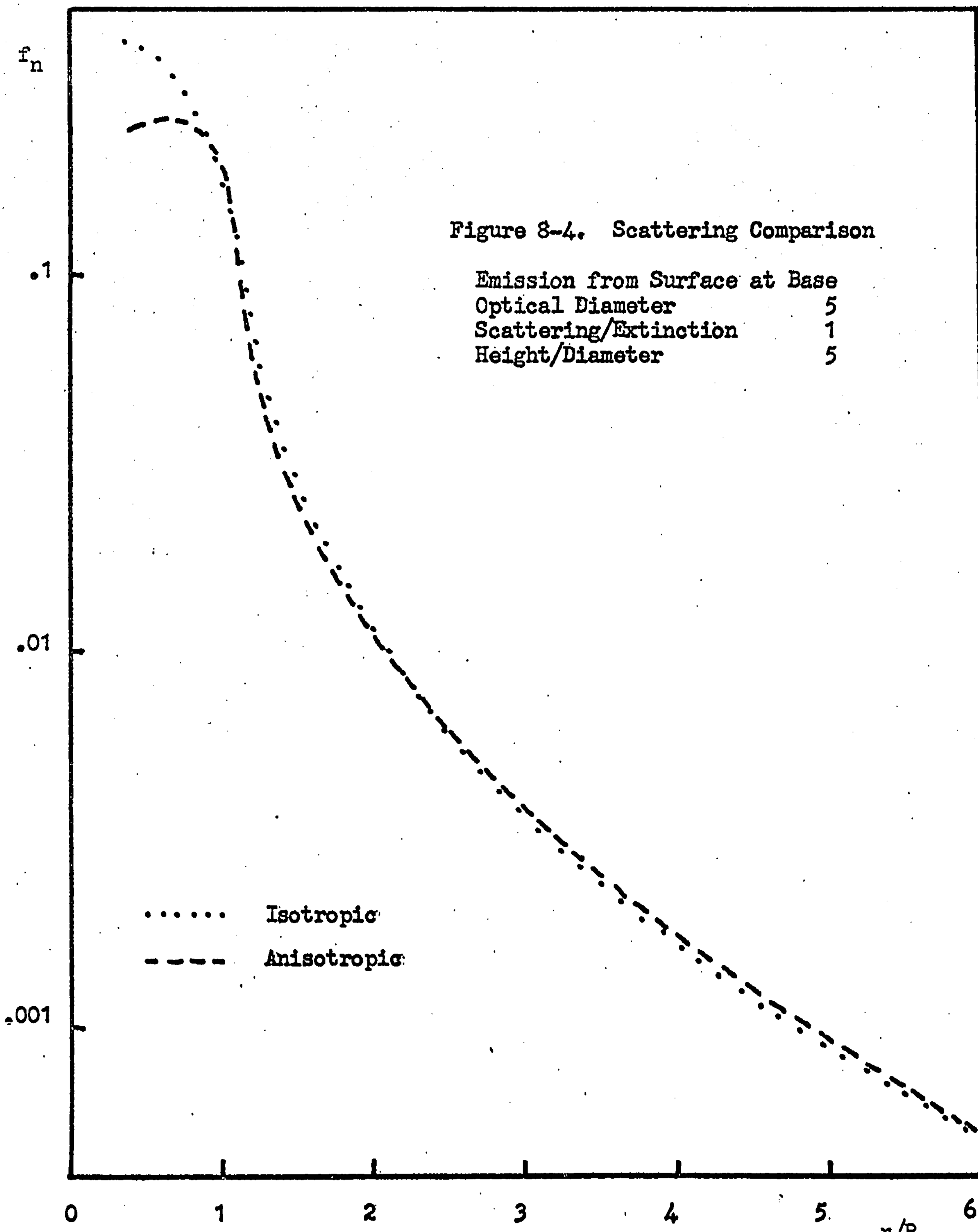

Figure 8-4. Scattering Comparison

Emission from Surface at Base	
Optical Diameter	5
Scattering/Extinction	1
Height/Diameter	5

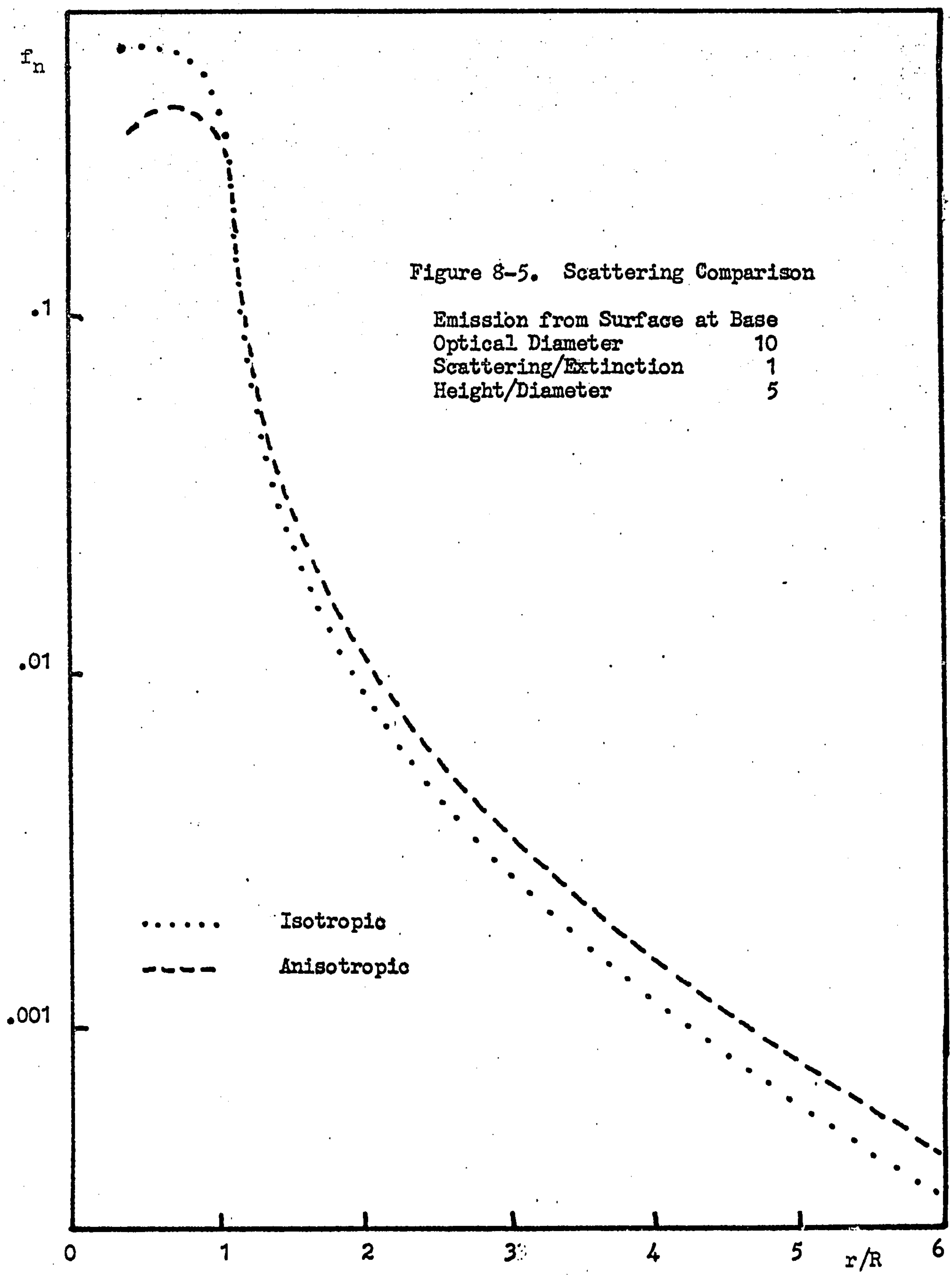

Figure 8-5. Scattering Comparison

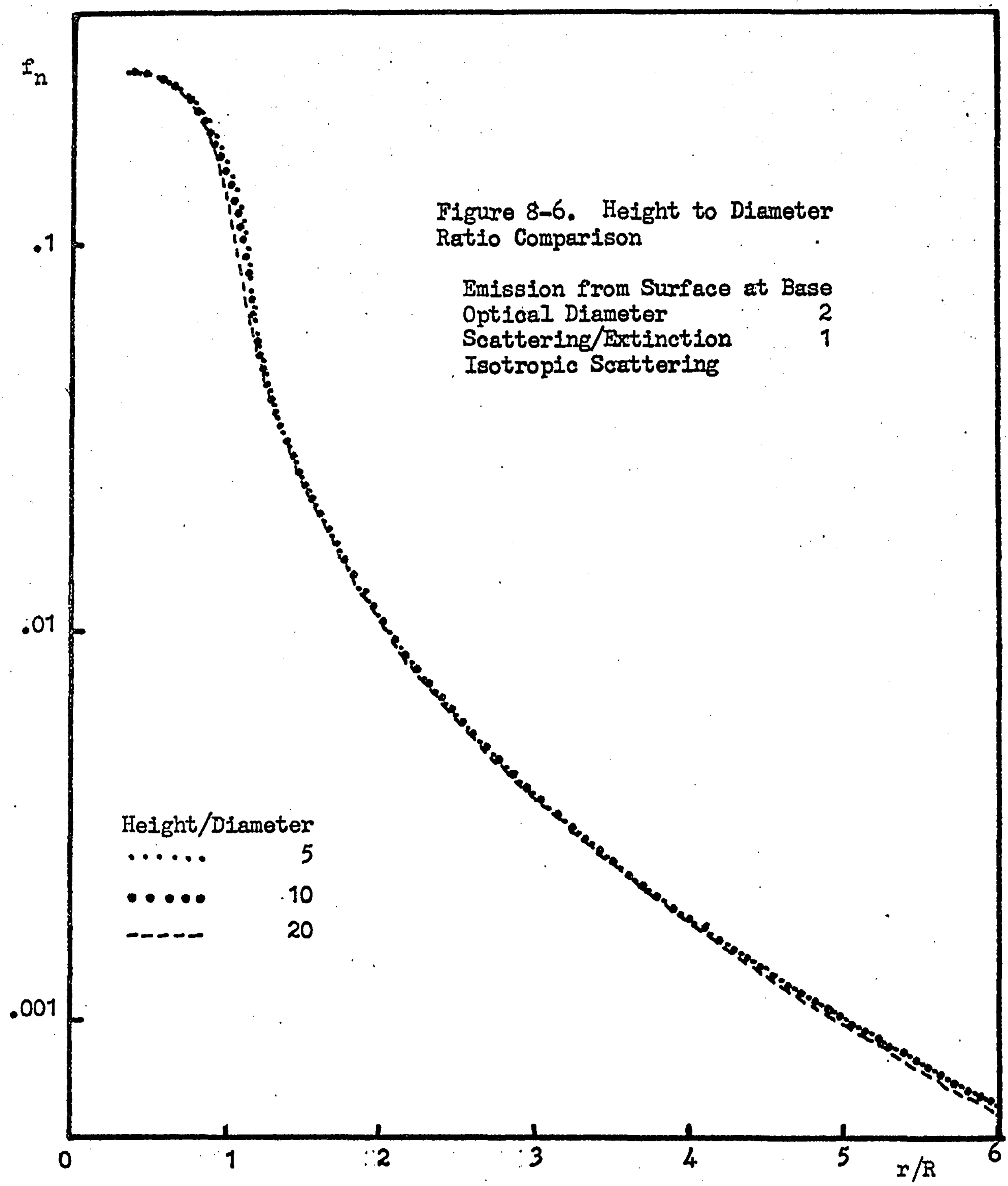

Figure 8-6. Height to Diameter Ratio Comparison

Emission from Surface at Base
Optical Diameter 2
Scattering/Extinction 1
Isotropic Scattering

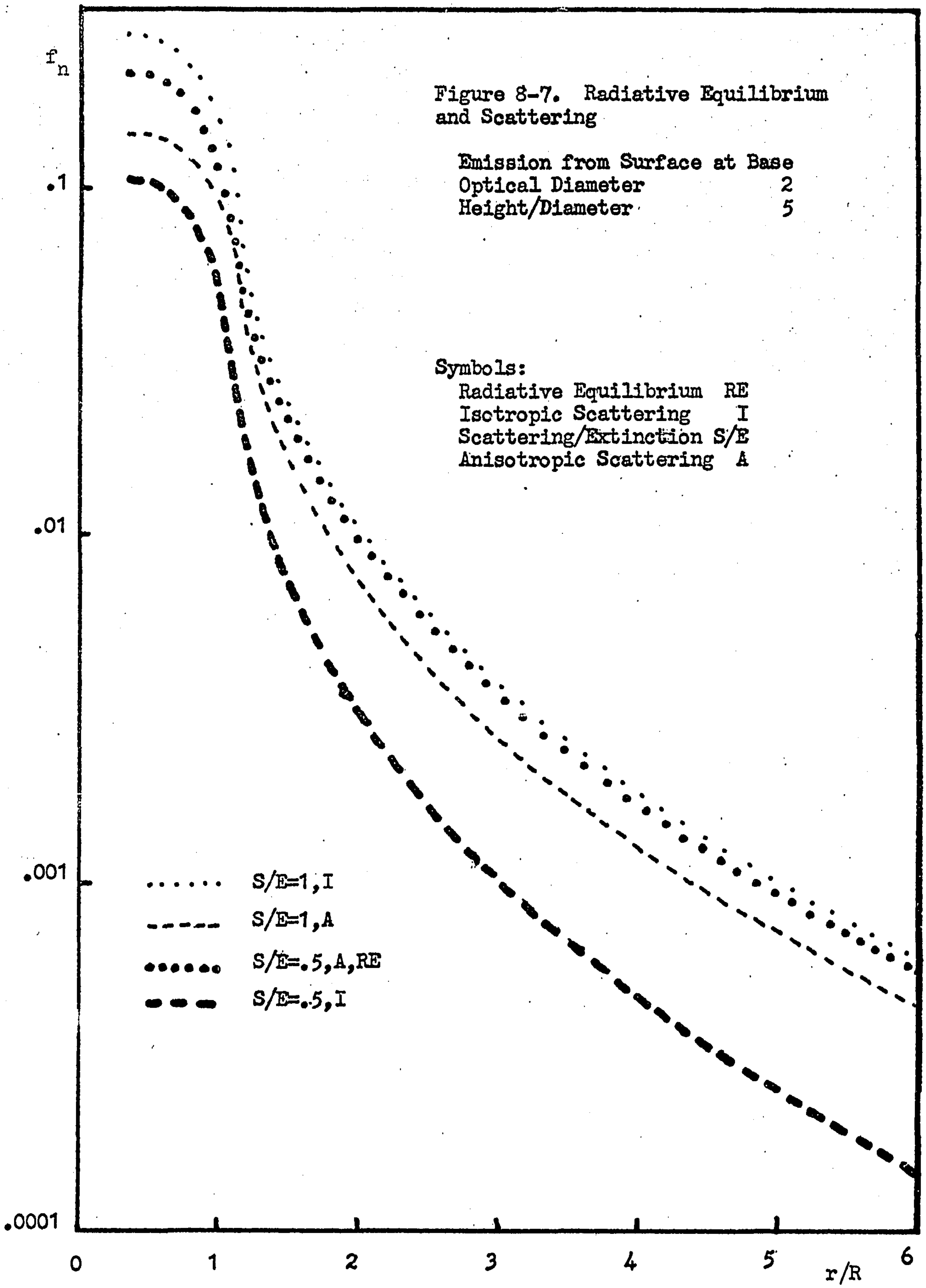

f_n
.1
.01
.001
.0001
0
1
2
3
4
5
6
r/R
Figure 8-7. Radiative Equilibrium and Scattering
Emission from Surface at Base
Optical Diameter 2
Height/Diameter 5
Symbols:
Radiative Equilibrium RE
Isotropic Scattering I
Scattering/Extinction S/E
Anisotropic Scattering A
S/E=1,I
S/E=1,A
S/E=.5,A,RE
S/E=.5,I

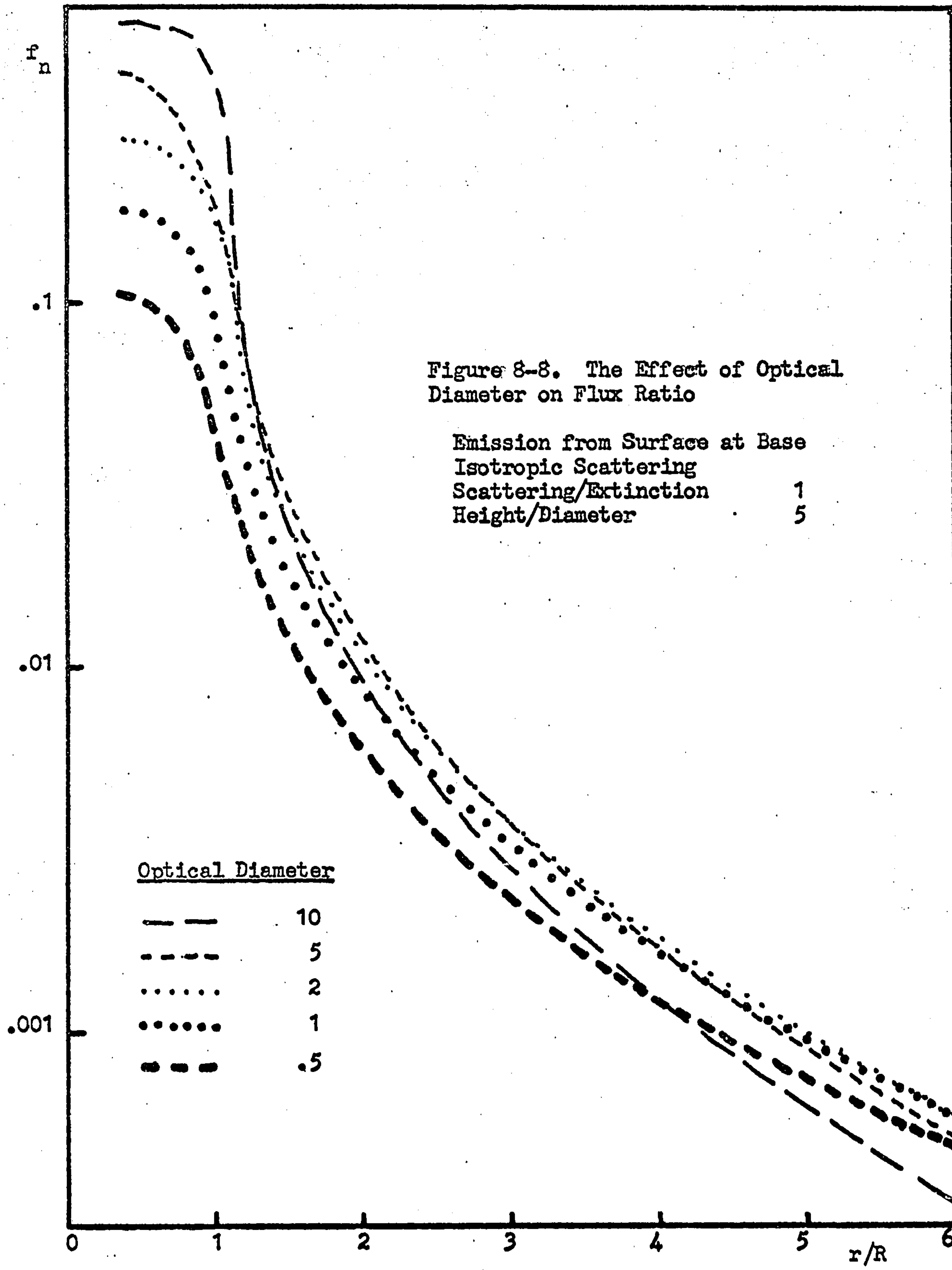
f n
.1
.01
.001
0
1
2
3
4
5
6
r/R
Figure 8-8. The Effect of Optical Diameter on Flux Ratio
Emission from Surface at Base
Isotropic Scattering
Scattering/Extinction 1
Height/Diameter 5
Optical Diameter
10
5
2
1
.5

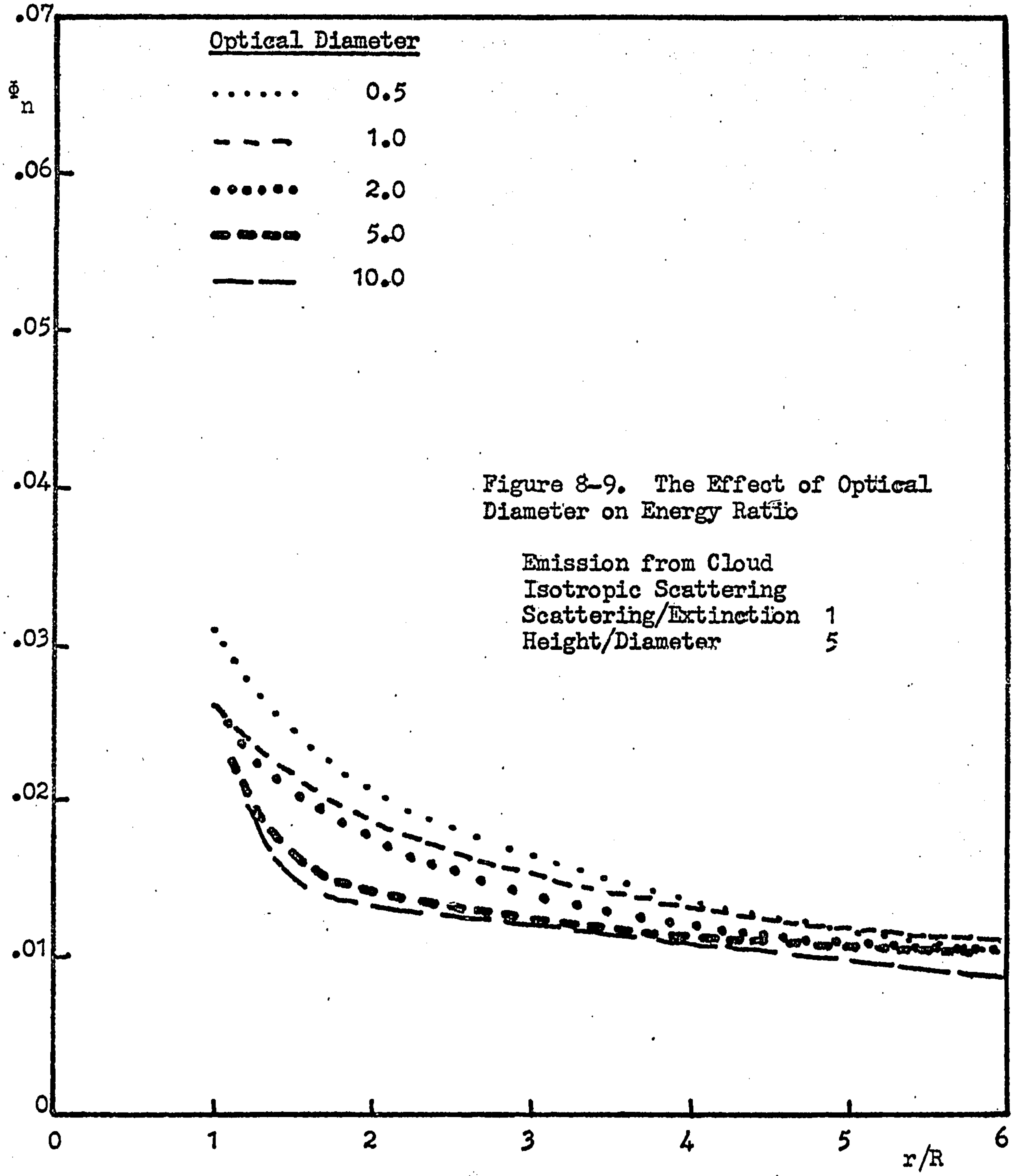

Figure 8-9. The Effect of Optical Diameter on Energy Ratio

Emission from Cloud
Isotropic Scattering
Scattering/Extinction 1
Height/Diameter 5

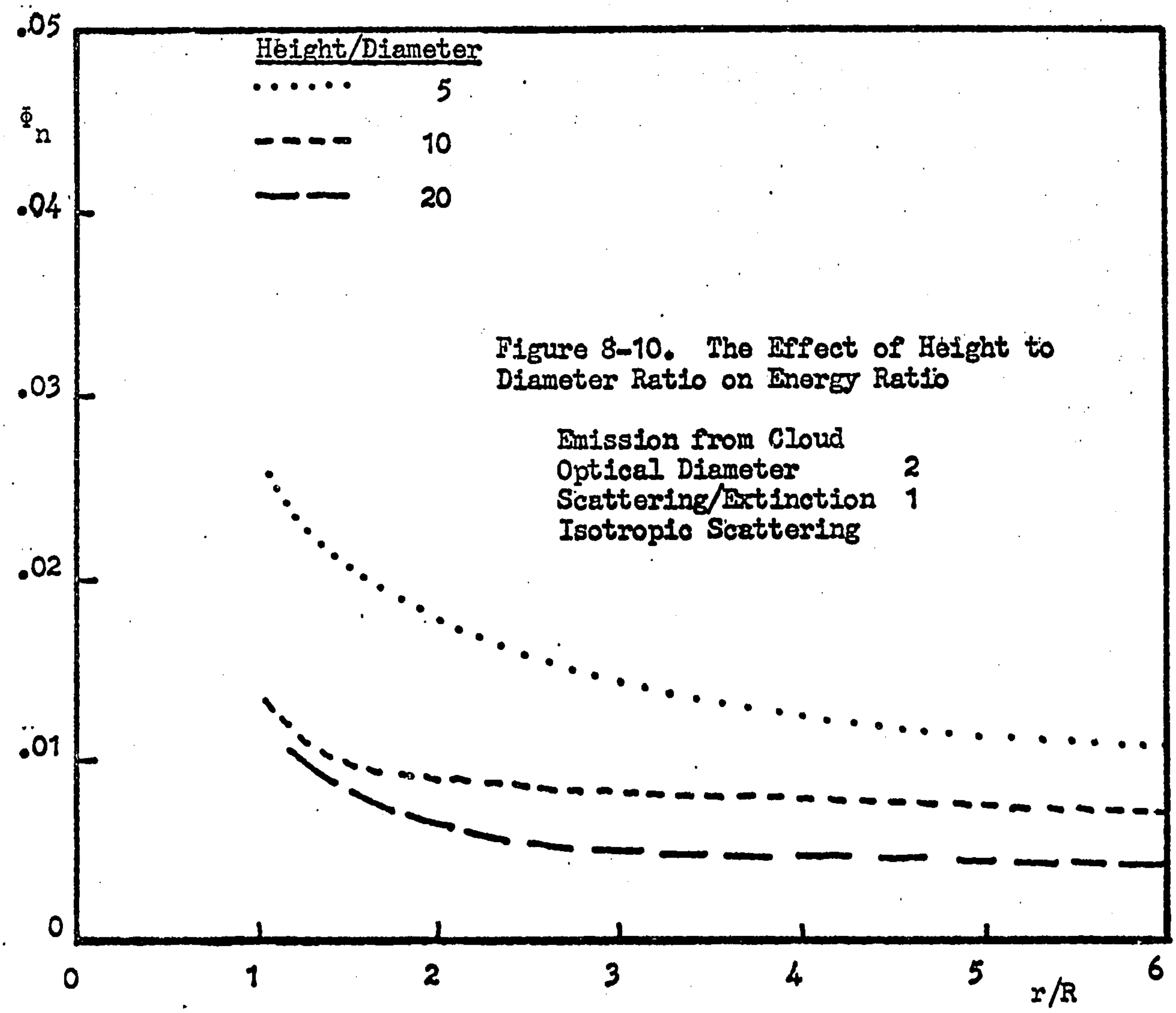

Figure 8-10. The Effect of Height to Diameter Ratio on Energy Ratio

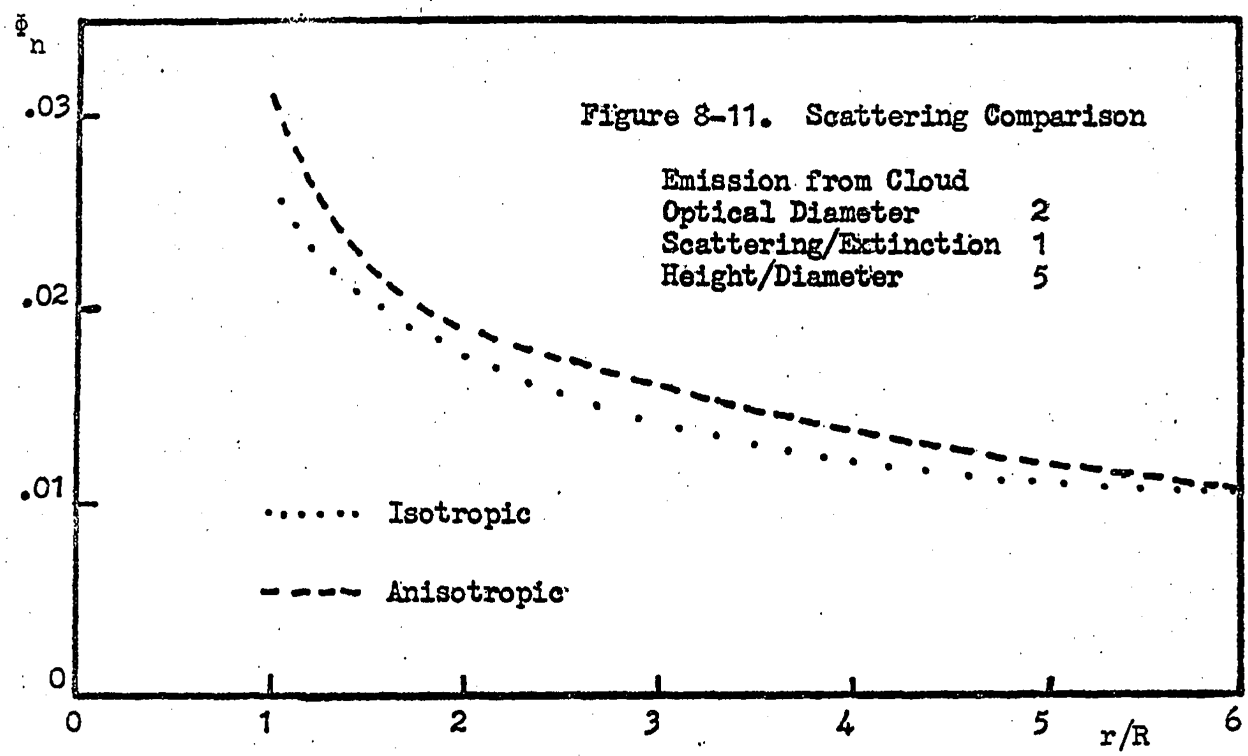

Φ_n
.03
.02
.01
0
Figure 8-11. Scattering Comparison
Emission from Cloud
Optical Diameter 2
Scattering/Extinction 1
Height/Diameter 5
Isotropic
Anisotropic
0
1
2
3
4
5
6
r/R

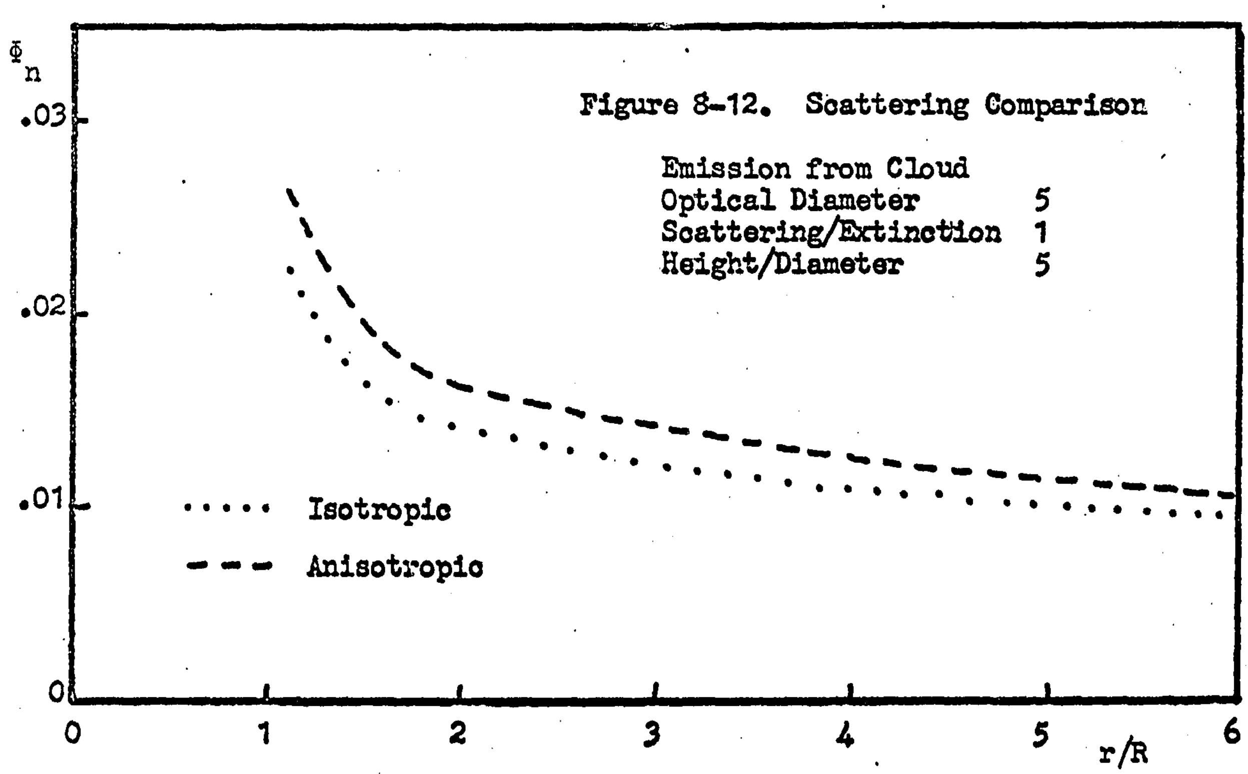

Φ_n
.03
.02
.01
0
Figure 8-12. Scattering Comparison
Emission from Cloud
Optical Diameter 5
Scattering/Extinction 1
Height/Diameter 5
Isotropic
Anisotropic
0
1
2
3
4
5
6
r/R

flux scattered back to the base plane.

Figure 8-6 shows the effect of the height to diameter ratio for isotropic scattering and $\tau = 2$. The effect is negligible.

Figure 8-7 shows the effect of scattering to extinction ratio for radiative equilibrium and non radiative equilibrium. It should be remembered that radiative equilibrium with isotropic scattering is independent of scattering to extinction ratio. The curves show that radiative equilibrium with anisotropic scattering moves the solution toward that of isotropic scattering as expected. Non radiative equilibrium gives a substantial reduction in flux. For example the flux is reduced by a factor of four at a radius ratio of four.

The effect of optical diameter is indicated in Figure 8-8.

Figures 8-9 through 8-12 concern the case of emission within the cloud. The original emissions are uniformly distributed throughout the cloud. The energy ratio is the ratio of the energy hitting at radius ratio r/R to the energy leaving the cloud and as such can be considered a quasi configuration factor.

Figure 8-9 shows the effect of optical diameter while Figure 8-10 shows the effect of height to diameter ratio at $\tau = 2$. Figures 8-11 and 8-12 compare the effects of anisotropic scattering and isotropic scattering. It is shown that for $\tau = 2$ and 5 anisotropic scattering gives higher values than isotropic scattering. This would correspond to a higher emittance for the anisotropic scattering cloud which agrees with the general observations of Rochelle (24).

In Figure 8-13 the apparent emittance of the particle cloud is compared with apparent emittance values of other particle clouds as present-

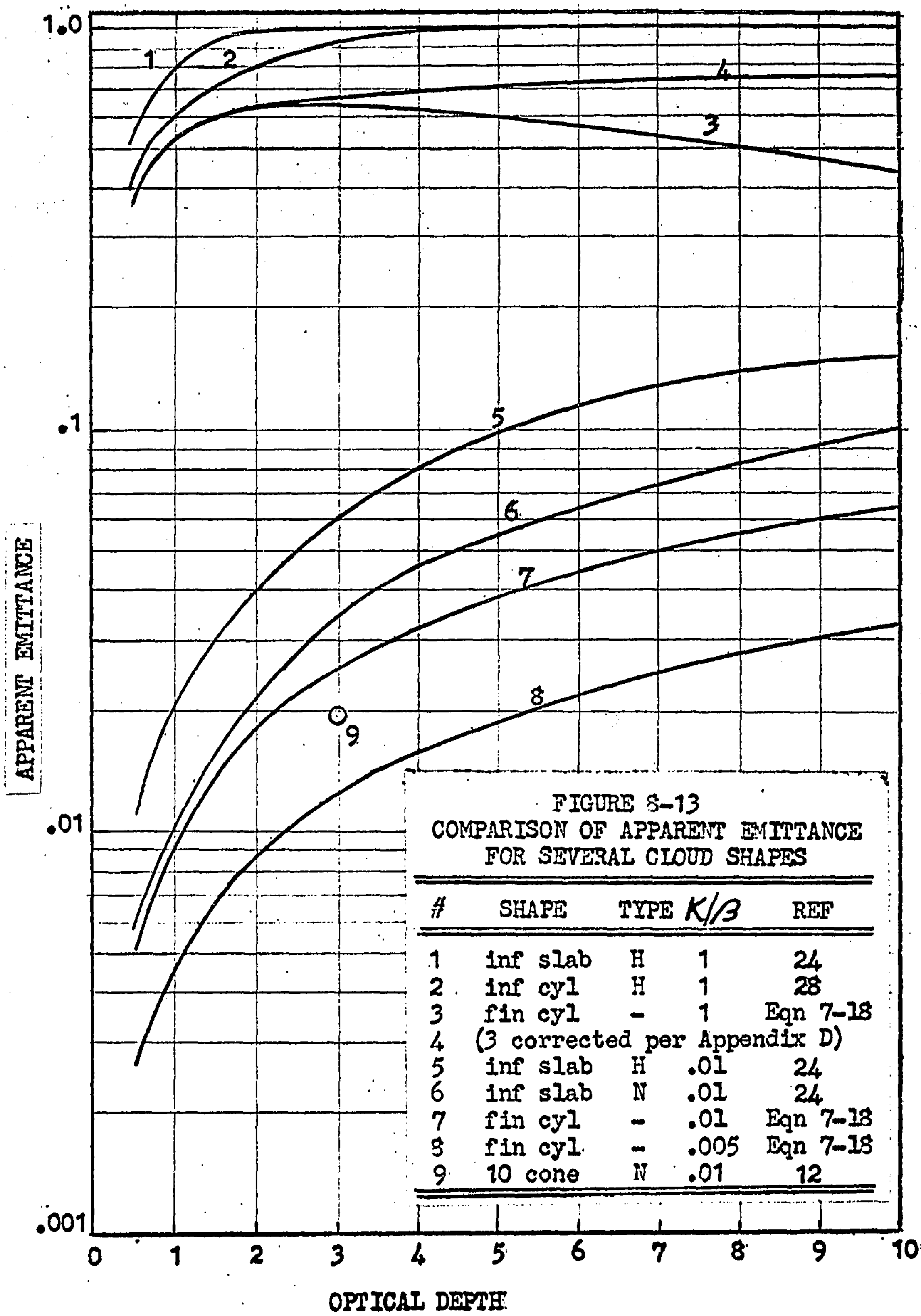

FIGURE 8-13
COMPARISON OF APPARENT EMITTANCE
FOR SEVERAL CLOUD SHAPES

#	SHAPE	TYPE	K/β	REF
1	inf slab	H	1	24
2	inf cyl	H	1	28
3	fin cyl	-	1	Eqn 7-18
4	(3 corrected per Appendix D)			
5	inf slab	H	.01	24
6	inf slab	N	.01	24
7	fin cyl	-	.01	Eqn 7-18
8	fin cyl	-	.005	Eqn 7-18
9	10 cone	N	.01	12

ed in the literature. Since the author knows of no other solution for finite cylindrical systems a strict comparison cannot be made. The approximate nature of equation 7-18 also makes a true comparison difficult. Nevertheless, some indication of the validity of the current solution may be afforded by a comparison with other related results. Hence, Figure 8-13.

The finite cylinder which is used in the comparison has a height to diameter ratio of five, isotropic scattering and is arbitrarily viewed from a radius ratio of four. The emittance is presented for three values of absorption to extinction ratio and is shown in curves 3, 7, and 8. Curve 4 reflects the correction applied to curve 3 as described in Appendix D.

Curves 1, 5, and 6 are taken from (24) and are for an infinite slab of finite thickness. Curve 2 is taken from (28) and is for an infinite cylinder of finite diameter. Point 9 is taken from (12) for a ten degree semi-infinite cone at a radius ratio of 2.

In (37, 38) Tien and Abu-Romia present curves for the "spectral apparent emissivity" in the base plane of a semi-infinite cylindrical gas body. The gas is assumed to be uniform and isothermal. As defined in (37), the "spectral apparent emissivity" is the ratio of the monochromatic radiative flux incident on a surface element to that which would leave the surface element if it were black and at the same temperature as the cloud. This definition of emissivity is somewhat unusual and is not an apparent emittance of the cylindrical cloud. Nevertheless it is instructive to compare the values of "spectral apparent emissivity" as calculated from this work with those of (37).

The appropriate values for the comparison are obtained by multiplying those from equation (7-18) by the factor $F_{2n}A_{cyl}/A_n$. The comparison is made for a radius ratio of 1.25. This corresponds to the midpoint of ring three which is close to the base of the cylinder and from which the finite cloud and the semi-infinite cloud should appear much the same. The results, shown connected by a smooth curve in Figure 8-14, seem to be in very good agreement.

As a quantitative illustration of the methods of this work it seems appropriate to consider an example problem. Suppose one desires to know the value of radiant flux at a point in the base plane of a finite cylindrical particle cloud and surface system with the following characteristics:

Cylinder Optical Diameter $\tau = 2$

Particle Cloud Temperature $T_c = 4500^{\circ}R$

Base Surface Temperature $T_s = 7200^{\circ}R$

Ratio of Absorption to Extinction $\kappa/\beta = .005$

Flux is desired at $r/R = 3.75$

Both isotropic and anisotropic scattering are to be considered.

The surface is black and the cloud gray.

Height to diameter ratio $H/D = 5$

Consider first the flux resulting from radiation emitted by the base surface and scattered by the particle cloud. Equation (7-8) applies and becomes

$$q_n(T_s) = T_s^{\,4}\, f_n\, \sigma$$

for a gray cloud. Since κ/β is very small it is reasonable to consider

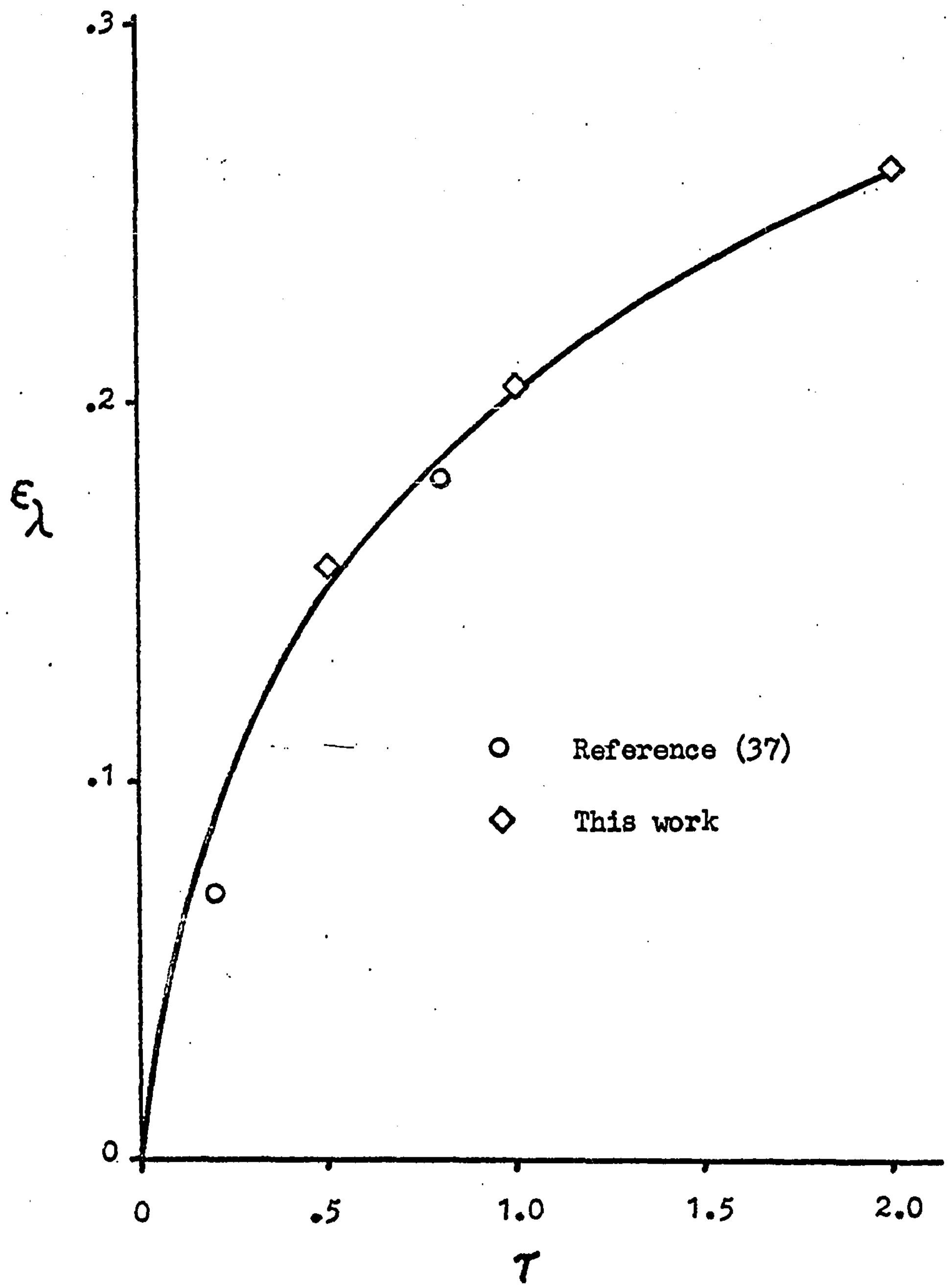

Figure 8-14. Spectral Apparent Emissivity versus Optical Diameter. Radius ratio is 1.25.

the scattering to extinction ratio as unity for this portion of the problem. Thus from page 78 f_n = .00215 for isotropic scattering and from page 79 f_n = .00145 for anisotropic scattering (assuming the anisotropic scattering function to be the one described in Chapter IV). The flux from the surface to the point is thus 9880 BTU Hr^{-1} Ft^{-2} for isotropic scattering and 6670 BTU Hr^{-1} Ft^{-2} for anisotropic scattering.

The flux resulting from emission within the cloud is found using equation (7-26). It should be noted that the radius ratio chosen for this problem corresponds to the midpoint of ring number eight[1]. Using n = 8 and data of pages 68, 69, 43 and 46 gives fluxes of 483 BTU Hr^{-1} Ft^{-2} for isotropic scattering and 525 BTU Hr^{-1} Ft^{-2} for anisotropic scattering.

The parameters of the above problem were chosen to be somewhat representative of those of a metalized propellant rocket with the base surface representing the high temperature combustion chamber radiating to the particle cloud. Of course allowance must be made for nozzle expansion ratio. This could be done in the program by reducing the radius of the emitting surface. In the absence of data for that condition, however, an approximation can be made by simply reducing the flux by a factor equal to the expansion ratio. If an expansion ratio of twenty is assumed then the flux components from the surface and from the cloud become of the same order of magnitude for the temperatures considered.

---

[1]It should be evident that the need for such a choice exists only because of the formulation of equation (7-26). It would be quite possible to combine Φ_n and (2n - 1) in a factor plotted as a function of radius ratio. This was not done in this work because of the need for Φ_n alone in equation (7-18) and the lack of physical significance of such a factor.

Thus both are important contributions to the total heat flux and attempts to determine the apparent emittance of rocket exhaust plumes from effective temperatures, configuration factors and heating rates (i.e., $\varepsilon_a = q_{ab}/\sigma T_a^4 F_{ba}$) as was done in (20) must include both considerations.

CHAPTER IX

CONCLUSIONS AND CLOSURE

The Monto Carlo method has been shown to be a feasible method for analyzing the radiative heat transfer to the base region of a cylindrical particle cloud. The effects of anisotropic scattering can be included through use of the approximation developed in Chapter IV.

The computer program presented in Appendix A is believed to be a useful tool for the investigation of certain aspects of radiant heating by metalized propellant rocket exhausts. Specifically, the importance of anisotropic scattering and searchlight effect on base heating could be fruitfully examined.

There does not seem to be any reason why the combined effects of gas-particle emission could not be examined in this way. It would appear to be a matter of simply specifying an appropriate emissive power distribution, rather than the uniform source used in this work, and summing over the applicable wavelength intervals. The same can be said for specified temperature distributions in the cloud as long as the extinction coefficient does not vary significantly with temperature.

A severe limitation exists in regard to other than uniform particle distributions. The author believes it is infeasible to consider distributions in which the extinction coefficient varies continuously along the photon path although it may be possible to section the cloud and permit different optical properties in each section. The difficulty arises in the need to determine the optical depth from any point in the cloud to the cloud surface along any direction. This limitation would not exist in plane parallel geometry so the method would seem to have even more promise for anisotropic scattering analyses in that geometry.

LIST OF REFERENCES

1. Rochelle, W. C. "Theory of Thermal Radiation from Liquid and Solid Propellant Rocket Exhausts," Preliminary draft of a Technical Memorandum, NASA/Marshall Space Flight Center, October 1966.

2. Carlson, D. J. "Metalized Solid Propellants Exhaust Plumes," AIAA Paper No. 66-652, Part II, June 1966.

3. Love, T. J. Radiative Heat Transfer. Columbus, Ohio: Charles Merrill Books Inc., 1968.

4. Sparrow, E. M. and R. D. Cess. Radiation Heat Transfer. Belmont, California: Brooks/Cole Publishing Company, 1966.

5. Van de Hulst, H. C. Light Scattering by Small Particles. New York: John Wiley and Sons, Inc., 1957.

6. Electromagnetic Scattering. M. Kerker, editor. The Macmillan Company, New York: 1963.

7. Love, T. J., Jr. "An Investigation of Radiant Heat Transfer in Absorbing, Emitting, and Scattering Media," USAF Aeronautical Research Laboratories Report ARL 63-3, Wright-Patterson AFB, Ohio: January 1963.

8. Love, T. J. and H. M. Hsia. "Radiative Heat Transfer Between Parallel Plates Seperated by a Non-Isothermal Medium with Anisotropic Scattering," Aerospace Research Laboratories Report ARL 65-211, October 1965.

9. Evans, L. B., C. M. Chu and S. W. Churchill. "The Effect of Anisotropic Scattering on Radiant Transport," ASME Journal of Heat Transfer, (August 1965), pp. 381-387.

10. Edwards, R. H. and R. P. Bobco. "Radiant Heat Transfer from Isothermal Dispersions with Isotropic Scattering," Aerospace Technology Research Report SSD 50134R, Los Angeles: Hughes Aircraft Company, 1965.

11. Bobco, R. P. "Directional Emissivities from a Two-Dimensional, Absorbing-Scattering Medium: The Semi-Infinite Slab,"

Aerospace Technology Research Report SSD 60072R, Los Angeles: Hughes Aircraft Company, 1966.

12. Bobco, R. P. and R. H. Edwards. "Radiation from an Absorbing Scattering Conical Dispersion with Non-Uniform Density," Aerospace Technology Research Report SSD 60571R, Los Angeles: Hughes Aircraft Company, 1966.

13. Howell, J. R. and M. Perlmutter. "Monte Carlo Solution of Thermal Transfer Through Radiant Media Between Gray Walls," ASME Journal of Heat Transfer, Vol. 86, No. 1 (February 1964), pp. 116-122.

14. Perlmutter, M. and J. R. Howell. "Radiant Transfer Through a Gray Gas Between Concentric Cylinders Using Monte Carlo," ASME Journal of Heat Transfer, Vol. 86, No. 2, (May 1964), pp. 169-179.

15. Howell, J. R. and M. Perlmutter. "Monte Carlo Solution of Radiant Heat Transfer in a Nongrey Nonisothermal Gas with Temperature Dependent Properties," AIChE Journal, Vol. 10, No. 4, (July 1964), pp. 562-567.

16. Corlett, R. C. "Direct Monte Carlo Calculation of Radiative Heat Transfer in Vacuum," ASME Journal of Heat Transfer, (November 1966), pp. 376-382.

17. Howell, J. R. "Calculation of Radiant Heat Exchange by the Monte Carlo Method," NASA TM X-52101, 1965.

18. Gryvnak, D. A. and D. E. Burch. "Optical and Infrared Properties of Al_2O_3 at Elevated Temperatures," Journal of the Optical Society of America, Vol. 55, No. 6 (June 1965), pp. 625-629.

19. Carlson, D. J. "Emittance of Condensed Oxides in Solid Propellant Combustion Products," Tenth Symposium (International) on Combustion. Pittsburg: The Combustion Institute, 1965.

20. Adams, J. M. "A Determination of the Emissive Properties of a Cloud of Molten Alumina Particles," Journal of Quantitative Spectroscopy and Radiative Transfer, Vol. 7, 1967, pp. 273-277.

21. Bauer, E. and D. J. Carlson. "Mie Scattering Calculations for Micron Size Alumina and Magnesia Spheres," Journal of Quantitative Spectroscopy and Radiative Transfer, Vol. 4 (1964), pp. 363-374.

22. Plass, G. N. "Mie Scattering and Absorption Cross Sections for Aluminum Oxide and Magnesium Oxide," Applied Optics, Vol. 3, No. 7 (July 1964), pp. 867-871.

23. Plass, G. N. "Temperature Dependence of the Mie Scattering and Absorption Cross Sections for Aluminum Oxide," Applied Optics, Vol. 4, No. 12 (December 1965), pp. 1616-1619.

24. Bartky, C. D. and E. Bauer. "Predicting the Emittance of a Homogeneous Plume Containing Alumina Particles, AIAA Journal of Spacecraft and Rockets, Vol. 3, No. 10 (October 1966), pp. 1523-1527.

25. Love, T. J. and R. A. Wheasler. "An Experimental Study of Infrared Scattering by Clouds of Particles," Aerospace Research Laboratories Report ARL 64-109, June 1964.

26. Love, T. J. and J. F. Beattie. "Experimental Determination of Thermal Radiation Scattering by Small Particles," Aerospace Research Laboratories Report ARL 65-110, June 1965.

27. Fontenot, J. E., Jr. "Thermal Radiation from Solid Rocket Plumes at High Altitude," AIAA Journal, Vol. 3, No. 5 (May 1965), pp. 970-972.

28. Morizumi, S. J. and H. J. Carpenter. "Thermal Radiation from the Exhaust Plume of an Aluminized Composite Propellant Rocket," AIAA Journal of Spacecraft and Rockets, Vol. 1, No. 5 (October 1964), pp. 501-507.

29. Carlson, D. J., C. H. Lewis, Jr., R. A. DuPuis and A. D. Bauer. "Solid Propellant Exhaust Radiation Studies Interim Technical Report No. 3, (AD 463290) Prepared for ARPA by Aeronutronic, Newport Beach, California: March 1965.

30. Hickok, R. L. "Radiation Heat Transfer in Evacuated, Non-Gray, Diffuse Enclosures," Unpublished M. S. Thesis, Norman, Oklahoma: The University of Oklahoma, 1963.

31. Jakob, M. "Heat Radiation," Proc. Phys. Soc. (London), Vol. 59, Pt. 5 (1947), p. 728.

32. Kahn, H. "Multiple Quadrature by Monte Carlo Methods," Mathematical Methods for Digital Computers. Edited by Ralston and Wilf. New York: John Wiley and Sons, Inc., 1960.

33. Hamilton, D. C. and W. R. Morgan. "Radiant-Interchange Configuration Factors," NACA Technical Note 2836, December 1952.

34. Parzen, E. Modern Probability Theory and Its Applications. New York: John Wiley and Sons, Inc., 1960.

35. Feller, W. An Introduction to Probability Theory and Its Applications, Vol. I, New York: John Wiley and Sons, Inc., 1950.

36. Uspensky, J. V. Introduction to Mathematical Probability. New York: McGraw-Hill Book Company, Inc., 1937.

37. Tien, C. L. and M. M. Abu-Romia. "Radiative Energy Transfer to Outer Base Regions of Cylindrical and Conical Gas Bodies," Institute of Engineering Research Report AS-63-4, University of California, Berkeley: 1963.

38. Tien, C. L. and M. M. Abu-Romia. "A Method of Calculating Rocket Plume Radiation to the Base Region," AIAA Journal of Spacecraft and Rockets, Vol. 1, No. 4 (August 1964), pp. 433-435.

APPENDIX A

THE COMPUTER PROGRAMS

The computer programs, and their imput formats, used in this work are listed in this appendix. The programs were originally written in FORTRAN II-D and converted to be compatible with the FORTRAN IV, IBM 7040 system at AFRPL. Subsequent modifications used FORTRAN IV. The random number generator was available and is presented for information only. It is listed in MAP.

The running times for these programs were almost a linear function of the optical diameter. Table A-1 gives an indication of the time required on the AFRPL 7040 per 10,000 photon histories.

TABLE A-1

COMPUTER EXECUTION TIME

Emission Source	Optical Diameter	Type Scattering	Time per 10,000 Histories
Cloud	2	I	5 (min.)
"	2	A	7
"	5	I	12
"	5	A	17
Surface	2	I	5

Surface	2	A	6
"	5	I	9
"	5	A	16

The Input Variables

Variable	Description
IPHIL	The number of printouts desired. The program prints results after completion of a fixed number (N) of photon histories. IPHIL determines the number of times the program will trace N photon histories. Thus IPHIL times N is the number of histories traced.
IREQ	Flag for non radiative equilibrium. If the value is other than zero or blank the cloud will not be in radiative equilibrium.
HTOD	The height to diameter ratio of the cloud.
TAU	The cylinder optical diameter.
SIGBET	The scattering to extinction ratio.
N	The number of histories traced between printouts.
ISO	Flag for scattering. If the value is other than blank or zero the cloud will use the anisotropic scattering approximation.
NR	The number of rings on which hits are to be recorded.
RW	The ratio of the width of a ring to the radius of the cloud.
BHD	The height of the base of the cloud above the plane on which hits are recorded divided by the cloud

diameter. It is used only when emission is from the cloud and is normally zero (blank).

SA, SB, ..., SJ Parameters of the anisotropic scattering approximation as described in Chapter IV.

Input Format

Card Number	Columns	Format	Variable
1	1-5	I 5	IPHIL
	5-10	I 5	IREQ
2	1-10	F10.2	HTOD
	11-20	F10.2	TAU
	21-30	F10.2	SIGBET
	31-35	I 5	N
	36-40	I 5	ISO
	41-45	I 5	NR
	46-60	F15.2	RW
	61-70	F10.2	BHD
3	1-50	5 F10.2	SA, ..., SE
4	1-50	5 F10.2	SD, ..., SJ

```
C     THEMAL RADIATION FROM A FINITE CYLINDRICAL CLOUD OF ABSORBING,
C     EMITTING AND SCATTERING PARTICLES
      DIMENSIONA(125)
      DIMENSION ARRING(125)
 4003 READ899,IPHIL,IREQ
  899 FORMAT(2I5)
      READ99,HTOD,TAU,SIGBET,N,ISO,NR,RW,BHD
   99 FORMAT(3F10.2,3I5,F15.2,F10.2)
      UA=.98765431
      UB=.91827363
      UC=.45678913
      UD=.64563847
      UE=.48407195
      UF=.47362935
      UG=.54397841
      UH=.67374981
      UI=.49178433
      UJ=.32721983
      UK=.79321459
      PI=.314159265E+01
      R=1.0
      H=2.0*HTOD
      DO 337 I=1,NR
      RIN=I
  337 ARRING(I)=2.*RIN-1.0
      IF(ISO)901,902,901
  901 READ 991,SA,SB,SC,SD,SE
      READ 991,SF,SG,SH,SI,SJ
  991 FORMAT(5F10.2)
      SA=SA/180.0*PI
      SB=SB/180.0*PI
      SC=SC/180.0*PI
      SD=SD/180.0*PI
      SE=SE/180.0*PI
      A1=.5*SA*SJ
```

```
      A2=.5*(SB-SA)*(SJ-SH)
      A3=(SB-SA)*SH
      A4=.5*(SC-SB)*(SH-SG)
      A5=(SC-SB)*SG
      A6=.5*(SD-SC)*(SG-SF)
      A7=(SD-SC)*SF
      A8=.5*(SE-SD)*(SI-SF)
      A9=(SE-SD)*SF
      A10=.5*(PI-SE)*SI
      C1=A1+A2+A3
      C2=C1+A4+A5
      C3=C2+A6+A7
      C4=C3+A8+A9
      AK=C4+A10
      S1=2.0*AK*SA/SJ
      S2=(SB-SA)/(SJ-SH)
      S3=S2*S2*SJ*SJ
      S4=(SC-SB)/(SH-SG)
      S5=S4*S4*SH*SH
      S6=(SD-SC)/(SG-SF)
      S7=S6*S6*SG*SG
      S8=(SE-SD)/(SI-SF)
      S9=S8*S8*SF*SF
      C1K=C1/AK
      C2K=C2/AK
      C3K=C3/AK
      C4K=C4/AK
      A1K=A1/AK
C     SET INITIAL VALUES
  902 ISCAT=0
      KABS=0
      IREM=0
      M=0
      IMISS=0
      IOUT=0
```

```
      DO 903 I=1,NR
  903 A(I)=0
      DO 5001 IPHM=1,IPHIL
      DO 100 I=1,N
C     PICK EMISSION POINT
    1 U=RAND1(UA)
      UA=U
      AZ1=U*.628318530E-01+PI/5.0
      U=RAND1(UB)
      UB=U
      Z1=U*H
      U=RAND1(UK)
      UK=U
      R1=R*SQRT(U)
C     PICK EMISSION DIRECTION
    2 U=RAND1(UC)
      UC=U
      THETA=2.0*PI*U
      U=RAND1(UD)
      UD=U
      COET=1.0-2.0*U
C     CALCULATE MAXIMUM INTERNAL PATH LENGTH
    3 COAL=-COS(AZ1-THETA)
      E=R1*COAL
      ELS=E+SQRT(E*E+R*R-R1*R1)
      SIET=1.0-COET*COET
      ELMAX=ELS/SIET
      IF(H-Z1-ELMAX*COET)5,6,6
    5 ELMAX=(H-Z1)/COET
      GOTO66
    6 IF(Z1+ELMAX*COET)65,66,66
   65 ELMAX=-Z1/COET
C     CALCULATE PROBABLE PATH LENGTH
   66 U=RAND1(UE)
      UE=U
```

```
      ELP=-ALOG(U)/TAU*2.0
C     DETERMINE IF PHOTON ESCAPES
      IF(ELMAX-ELP)60,60,7
C     DETERMINE SCATTERING OR ABSORBING POINT
    7 C=ELS*ELP/ELMAX
      R2=SQRT(C*C+R1*R1-2.0*E*C)
      Z2=Z1+COET*ELP
      SIBET=C/R2*SQRT(1.0-COAL*COAL)
      COBET=-(C*C-R1*R1-R2*R2)/(2.0*R1*R2)
      BETA=ATAN(SIBET/COBET)
      IF(BETA)15,16,16
   15 BETA=BETA+PI
   16 YAW=THETA-AZ1
      IF(YAW)21,22,22
   21 YAW=YAW+2.0*PI
   22 IF(YAW-PI)23,25,25
   23 AZ2=AZ1+BETA
      IF(AZ2-2.0*PI)55,55,24
   24 AZ2=AZ2-2.0*PI
      GOTO55
   25 AZ2=AZ1-BETA
      IF(AZ2)26,55,55
   26 AZ2=AZ2+2.0*PI
   55 AZ1=AZ2
      R1=R2
      Z1=Z2
C     DETERMINE IF SCATTERED OR ABSORBED
      U=RAND1(UF)
      UF=U
      IF(U-SIGBET)57,56,56
   56 KABS=KABS+1
      IF(IREQ)100,281,100
  281 IREM=IREM+1
      GOTO2
   57 ISCAT=ISCAT+1
```

```
C      PICK SCATTERING DIRECTION
       IF(ISO)904,28,904
C      ANISOTROPIC SCATTERING
  904  U=RAND1(UG)
       UG=U
       IF(U-A1K)700,701,702
  700  ETAD=SQRT(S1*U)
       GOTO905
  701  ETAD=SA
       GOTO905
  702  IF(U-C1K)703,704,705
  703  PM213=(S3-2.0*(U*AK-A1)*S2)
       IF(PM213.LT.0.0) PM213=0.0
       ETAD=SA+S2*SJ-SQRT(PM213)
       GOTO905
  704  ETAD=SB
       GOTO905
  705  IF(U-C2K)706,707,708
  706  PM213=(S5-2.0*(U*AK-C1)*S4)
       IF(PM213.LT.0.0) PM213=0.0
       ETAD=SB+S4*SH-SQRT(PM213)
       GOTO905
  707  ETAD=SC
       GOTO905
  708  IF(U-C3K)709,710,711
  709  PM213=(S7-2.0*(U*AK-C2)*S6)
       IF(PM213.LT.0.0) PM213=0.0
       ETAD=SC+S6*SG-SQRT(PM213)
       GOTO905
  710  ETAD=SD
       GOTO905
  711  IF(U-C4K)712,713,714
  712  PM213=(S9+2.0*(U*AK-C3)*S8)
       IF(PM213.LT.0.0) PM213=0.0
       ETAD=SD-S8*SF+SQRT(PM213)
```

```
      GOTO905
  713 ETAD=SE
      GOTO905
  714 ETAD=PI-SQRT(AK*(1.0-U)*2.0*(PI-SE)/SI)
  905 U=RAND1(UH)
      UH=U
      THETD=2.0*PI*U
      COETD=COS(ETAD)
      SIETD=SIN(ETAD)
      COTHD=COS(THETD)
      SITHD=SIN(THETD)
      SITH=SIN(THETA)
      COTH=COS(THETA)
      REX=SIETD*COTHD
      REY=SIETD*SITHD
      REZ=COETD
      RX=REX*SITH+REY*COET*COTH+REZ*SIET*COTH
      RY=-REX*COTH+REY*COET*SITH+REZ*SIET*SITH
      RZ=-REY*SIET+REZ*COET
      THETA=ATAN(RY/RX)
      IF(RX)112,113,113
  112 THETA=THETA+PI
      GOTO115
  113 IF(THETA)114,115,115
  114 THETA=THETA+2.0*PI
  115 COET=RZ
      GOTO3
C     ISOTROPIC SCATTERING
   28 U=RAND1(UI)
      UI=U
      THETA=2.0*PI*U
      U=RAND1(UJ)
      UJ=U
      COET=1.0-2.0*U
      GOTO3
```

```
C      DOES IT HIT THE PLANE
   60 IF(COET)62,61,61
   61 IMISS=IMISS+1
      GOTO100
C CALCULATE AND REGISTER RADIUS OF HITS ON REFERENCE PLANE
   62 ZZ1=Z1+2.0*BHD
      C=-ZZ1*SIET/COET
      R2=SQRT(C*C+R1*R1-2.0*E*C)
      RAT=R2/R/RW
      IRAT=RAT+1.0
      IF(IRAT- NR)715,715,69
   69 IOUT=IOUT+1
      GOTO100
  715 A(IRAT)=A(IRAT)+1.0
  100 M=M+1
      RM=M
      DO101 I=1,NR
  101 A(I)=A(I)/RM/ARRING(I)
C      OUTPUT
      PRINT98,TAU
   98 FORMAT(1H1,14X,22HCYLINDER OPTICAL DEPTH,F18.3)
      PRINT97,HTOD
   97 FORMAT(15X,24HHEIGHT TO DIAMETER RATIO,F16.3)
      PRINT977,BHD
  977 FORMAT(15X,29HBASE HEIGHT TO DIAMETER RATIO,F11.3)
      PRINT89,SIGBET
   89 FORMAT(15X,30HSCATTERING TO EXTINCTION RATIO,F10.3)
      IF(ISO)130,131,130
  130 PRINT92
   92 FORMAT(15X,22HANISOTROPIC SCATTERING//)
      SA=SA*180.0/PI
      SB=SB*180.0/PI
      SC=SC*180.0/PI
      SD=SD*180.0/PI
      SE=SE*180.0/PI
```

```
      PRINT91,SA,SB,SC,SD,SE
   91 FORMAT(20X,2HA=,F7.4,3X,2HB=,F7.3,3X,2HC=,F7.3,3X,2HD=,F7.3,3X,
     12HE=,F7.3//)
      PRINT911,SF,SG,SH,SI,SJ
  911 FORMAT(20X,2HF=,F7.4,3X,2HG=,F7.3,3X,2HH=,F7.3,3X,2HI=,F7.3,3X,
     12HJ=,F7.3///)
      GOTO132
  131 PRINT90
   90 FORMAT(15X,20HISOTROPIC SCATTERING//////)
  132 PRINT96
   96 FORMAT(15X,67HEMISSIONS  REEMISSIONS  ABSORPTIONS  SCATTERINGS   M
     1ISSES   OUTSIDE)
      PRINT95,M,IREM,KABS,ISCAT,IMISS,IOUT
   95 FORMAT(I20,3I13,I9,I10///)
      PRINT93,RW
   93 FORMAT(15X,21HHITS/EMISSIONS/(2N-1),13H RING WIDTH= ,F5.2,1HR//)
      PRINT94,(I,A(I),I=1,NR)
   94 FORMAT(15X,I3,F11.8,5X,I3,F11.8,5X,I3,F11.8,5X,I3,F11.8)
      DO 5000 I=1,NR
 5000 A(I)=A(I)*RM*ARRING(I)
      IF(ISO)5050,5001,5050
 5050 SA=SA/180.0*PI
      SB=SB/180.0*PI
      SC=SC/180.0*PI
      SD=SD/180.0*PI
      SE=SE/180.0*PI
 5001 CONTINUE
      GO TO 4003
      END
```

```
C     THERMAL RADIATION SCATTERED BY A FINITE CYLINDRICAL CLOUD OF
C     PARTICLES.  EMISSION IS FROM A BLACK SURFACE AT THE CLOUD BASE.
      DIMENSIONA(125)
      DIMENSION APAR(125)
 4003 READ899,IPHIL,IREQ
  899 FORMAT(2I5)
      READ99,HTOD,TAU,SIGBET,N,ISO,NR,RW
   99 FORMAT(3F10.2,3I5,F15.2,F10.2)
      UA=.98765431
      UB=.91827363
      UC=.45678913
      UD=.64563847
      UE=.48407195
      UF=.47362935
      UG=.54397841
      UH=.67374981
      UI=.49178433
      UJ=.32721983
      PI=.314159265E+01
      R=1.0
      H=2.0*HTOD
      DO 337 I=1,NR
      RIN=I
  337 APAR(I)=1./(RW*RW*(2.*RIN-1.))
      IF(ISO)901,902,901
  901 READ 991,SA,SB,SC,SD,SE
      READ 991,SF,SG,SH,SI,SJ
  991 FORMAT(5F10.2)
      SA=SA/180.0*PI
      SB=SB/180.0*PI
      SC=SC/180.0*PI
      SD=SD/180.0*PI
      SE=SE/180.0*PI
      A1=.5*SA*SJ
      A2=.5*(SB-SA)*(SJ-SH)
```

```
      A3=(SB-SA)*SH
      A4=.5*(SC-SB)*(SH-SG)
      A5=(SC-SB)*SG
      A6=.5*(SD-SC)*(SG-SF)
      A7=(SD-SC)*SF
      A8=.5*(SE-SD)*(SI-SF)
      A9=(SE-SD)*SF
      A10=.5*(PI-SE)*SI
      C1=A1+A2+A3
      C2=C1+A4+A5
      C3=C2+A6+A7
      C4=C3+A8+A9
      AK=C4+A10
      S1=2.0*AK*SA/SJ
      S2=(SB-SA)/(SJ-SH)
      S3=S2*S2*SJ*SJ
      S4=(SC-SB)/(SH-SG)
      S5=S4*S4*SH*SH
      S6=(SD-SC)/(SG-SF)
      S7=S6*S6*SG*SG
      S8=(SE-SD)/(SI-SF)
      S9=S8*S8*SF*SF
      C1K=C1/AK
      C2K=C2/AK
      C3K=C3/AK
      C4K=C4/AK
      A1K=A1/AK
C     SET INITIAL VALUES
  902 ISCAT=0
      KABS=0
      IREM=0
      M=0
      IMISS=0
      IOUT=0
      DO 903 I=1,NR
```

```
  903 A(I)=0
      DO 5001 IPHM=1,IPHIL
      DO 100 I=1,N
C     PICK EMISSION POINT
    1 U=RAND1(UA)
      UA=U
      AZ1=U*.628318530E-01+PI/5.0
      Z1=0
      U=RAND1(UB)
      UB=U
      R1=SQRT(U)
C     PICK EMISSION DIRECTION
    2 U=RAND1(UC)
      UC=U
      THETA=2.0*PI*U
      U=RAND1(UD)
      UD=U
      COET=SQRT(U)
C     CALCULATE MAXIMUM INTERNAL PATH LENGTH
    3 COAL=-COS(AZ1-THETA)
      E=R1*COAL
      ELS=E+SQRT(E*E+R*R-R1*R1)
      SIET=1.0-COET*COET
      ELMAX=ELS/SIET
      IF(H-Z1-ELMAX*COET)5,6,6
    5 ELMAX=(H-Z1)/COET
      GOTO66
    6 IF(Z1+ELMAX*COET)65,66,66
   65 ELMAX=-Z1/COET
C     CALCULATE PROBABLE PATH LENGTH
   66 U=RAND1(UE)
      UE=U
      ELP=-ALOG(U)/TAU*2.0
C     DETERMINE IF PHOTON ESCAPES
      IF(ELMAX-ELP)60,60,7
```

```
C     DETERMINE SCATTERING OR ABSORBING POINT
    7 C=ELS*ELP/ELMAX
      R2=SQRT(C*C+R1*R1-2.0*E*C)
      Z2=Z1+COET*ELP
      SIBET=C/R2*SQRT(1.0-COAL*COAL)
      COBET=-(C*C-R1*R1-R2*R2)/(2.0*R1*R2)
      BETA=ATAN(SIBET/COBET)
      IF(BETA)15,16,16
   15 BETA=BETA+PI
   16 YAW=THETA-AZ1
      IF(YAW)21,22,22
   21 YAW=YAW+2.0*PI
   22 IF(YAW-PI)23,25,25
   23 AZ2=AZ1+BETA
      IF(AZ2-2.0*PI)55,55,24
   24 AZ2=AZ2-2.0*PI
      GOTO55
   25 AZ2=AZ1-BETA
      IF(AZ2)26,55,55
   26 AZ2=AZ2+2.0*PI
   55 AZ1=AZ2
      R1=R2
      Z1=Z2
C     DETERMINE IF SCATTERED OR ABSORBED
      U=RAND1(UF)
      UF=U
      IF(U-SIGBET)57,56,56
   56 KABS=KABS+1
      IF(IREQ)100,281,100
  281 IREM=IREM+1
      GOTO28
   57 ISCAT=ISCAT+1
C     PICK SCATTERING DIRECTION
      IF(ISO)904,28,904
C     ANISOTROPIC SCATTERING
```

```
904 U=RAND1(UG)
    UG=U
    IF(U-A1K)700,701,702
700 ETAD=SQRT(S1*U)
    GOTO905
701 ETAD=SA
    GOTO905
702 IF(U-C1K)703,704,705
703 PM213=(S3-2.0*(U*AK-A1)*S2)
    IF(PM213.LT.0.0) PM213=0.0
    ETAD=SA+S2*SJ-SQRT(PM213)
    GOTO0905
704 ETAD=SB
    GOTO0905
705 IF(U-C2K)706,707,708
706 PM213=(S5-2.0*(U*AK-C1)*S4)
    IF(PM213.LT.0.0) PM213=0.0
    ETAD=SB+S4*SH-SQRT(PM213)
    GOTO0905
707 ETAD=SC
    GOTO0905
708 IF(U-C3K)709,710,711
709 PM213=(S7-2.0*(U*AK-C2)*S6)
    IF(PM213.LT.0.0) PM213=0.0
    ETAD=SC+S6*SG-SQRT(PM213)
    GOTO0905
710 ETAD=SD
    GOTO0905
711 IF(U-C4K)712,713,714
712 PM213=(S9+2.0*(U*AK-C3)*S8)
    IF(PM213.LT.0.0) PM213=0.0
    ETAD=SD-S8*SF+SQRT(PM213)
    GOTO0905
713 ETAD=SE
    GOTO0905
```

```
  714 ETAD=PI-SQRT(AK*(1.0-U)*2.0*(PI-SE)/SI)
  905 U=RAND1(UH)
      UH=U
      THETD=2.0*PI*U
      COETD=COS(ETAD)
      SIETD=SIN(ETAD)
      COTHD=COS(THETD)
      SITHD=SIN(THETD)
      SITH=SIN(THETA)
      COTH=COS(THETA)
      REX=SIETD*COTHD
      REY=SIETD*SITHD
      REZ=COETD
      RX=REX*SITH+REY*COET*COTH+REZ*SIET*COTH
      RY=-REX*COTH+REY*COET*SITH+REZ*SIET*SITH
      RZ=-REY*SIET+REZ*COET
      THETA=ATAN(RY/RX)
      IF(RX)112,113,113
  112 THETA=THETA+PI
      GOTO115
  113 IF(THETA)114,115,115
  114 THETA=THETA+2.0*PI
  115 COET=RZ
      GOTO3
C     ISOTROPIC SCATTERING
   28 U=RAND1(UI)
      UI=U
      THETA=2.0*PI*U
      U=RAND1(UJ)
      UJ=U
      COET=1.0-2.0*U
      GOTO3
C     DOES IT HIT THE PLANE
   60 IF(COET)62,61,61
   61 IMISS=IMISS+1
```

```
      GOTO100
C CALCULATE AND REGISTER RADIUS OF HITS ON REFERENCE PLANE
   62 C=-Z1*SIET/COET
      R2=SQRT(C*C+R1*R1-2.0*E*C)
      RAT=R2/R/RW
      IRAT=RAT+1.0
      IF(IRAT- NR)715,715,69
   69 IOUT=IOUT+1
      GOTO100
  715 A(IRAT)=A(IRAT)+1.0
  100 M=M+1
      RM=M
      DO101 I=1,NR
  101 A(I)=A(I)/RM*APAR(I)
C     OUTPUT
      PRINT976
  976 FORMAT(1H1,14X,47HEMISSION FROM BLACK SURFACE AT BASE OF CYLINDER
     1//)
      PRINT98,TAU
   98 FORMAT(15X,22HCYLINDER OPTICAL DEPTH,F18.3)
      PRINT97,HTOD
   97 FORMAT(15X,24HHEIGHT TO DIAMETER RATIO,F16.3)
      PRINT89,SIGBET
   89 FORMAT(15X,30HSCATTERING TO EXTINCTION RATIO,F10.3)
      IF(ISO)130,131,130
  130 PRINT92
   92 FORMAT(15X,22HANISOTROPIC SCATTERING//)
      SA=SA*180.0/PI
      SB=SB*180.0/PI
      SC=SC*180.0/PI
      SD=SD*180.0/PI
      SE=SE*180.0/PI
      PRINT91,SA,SB,SC,SD,SE
   91 FORMAT(20X,2HA=,F7.4,3X,2HB=,F7.3,3X,2HC=,F7.3,3X,2HD=,F7.3,3X,
     12HE=,F7.3//)
```

```
      PRINT911,SF,SG,SH,SI,SJ
  911 FORMAT(20X,2HF=,F7.4,3X,2HG=,F7.3,3X,2HH=,F7.3,3X,2HI=,F7.3,3X,
     12HJ=,F7.3///)
      GOTO132
  131 PRINT90
   90 FORMAT(15X,20HISOTROPIC SCATTERING//////)
  132 PRINT96
   96 FORMAT(15X,67HEMISSIONS  REEMISSIONS  ABSORPTIONS  SCATTERINGS   M
     1ISSES   OUTSIDE)
      PRINT95,M,IREM,KABS,ISCAT,IMISS,IOUT
   95 FORMAT(I20,3I13,I9,I10///)
      PRINT93,RW
   93 FORMAT(15X,10HFLUX RATIO,13H RING WIDTH= ,F5.2,1HR//)
      PRINT94,(I,A(I),I=1,NR)
   94 FORMAT(15X,I3,F11.8,5X,I3,F11.8,5X,I3,F11.8,5X,I3,F11.8)
      DO 5000 I=1,NR
 5000 A(I)=A(I)*RM/APAR(I)
      IF(ISO)5050,5001,5050
 5050 SA=SA/180.0*PI
      SB=SB/180.0*PI
      SC=SC/180.0*PI
      SD=SD/180.0*PI
      SE=SE/180.0*PI
 5001 CONTINUE
      GO TO 4003
      END
```

```
RANDOM NUMBER GENERATOR
RAND1   PZE       **
        SXA       AXT1,4
        LAC       RAND1,4
        CLA*      2,4
        TZE       LOAD
        STO       COMMON
        SSP
        LRS       27
        SUB       A1
        PAX       0,4
        TMI       A2
        TXH       A3,4,35
        STA       A4
        PXD       0,0
A4      LLS       **
        TRA       AB
A2      TXH       A3,4,34
        STA       A5
        PXD       0,0
A5      LRS       **
        TRA       AB
A3      TSX       S.XPRT,4
        PZE       ERM,,24
        TRA       S.JXIT
ERM     BCI       4,ARGUMENT OUT OF RANGE
LOAD    LDQ       RD
AB      MPY       5TO13
        STQ       DUM1
        CLA       DUM1
        LBT
        ADD       FX1
        STO       RD
        ARS       8
        ORA       200C
```

```
        FAD     200C
AXT1    AXT     **,4
        TRA*    RAND1
200C    OCT     200000000000
5TO13   DEC     1220703125
RD      DEC     5117
FX1     DEC     1
A1      OCT     200
COMMON  BSS     1
DUM1    PZE
        END
```

APPENDIX B

PROBABILITY CONSIDERATIONS

It is not the purpose of this section to develop the relations or prove the theorems of the theory of probability. It is, rather, to concisely state the relations and theorems which are used so that terminology will not be misunderstood, to indicate how these relations are applied, and to show the validity of the method of application. References 17, 34, 35, 36 were used in preparation of this appendix.

The term "random variable" is used to denote a real number whose value is determined by the outcome of a random experiment.

A "random experiment" is an emperical experiment characterized by the property that its outcome under a given set of circumstances is not always the same but rather differs in such a way that numbers exist between 0 and 1 which represent the relative frequency with which the different possible outcomes (events) occur in a long series of independent trials of the experiment.

A "random event" is one whose relative frequency of occurrence, in a very long sequence of trials of the random experiment in which the event may occur, approaches a stable limit value as the number of observations is increased toward infinity.

The "probability" of a random event is the limit value of its relative frequency of occurrence.

A "probability function" is a rule defined over the complete sample space S of a random experiment which assigns to every event A, a subset of the sample space S, a non negative real number denoted by P(A) and conforming to the following axioms

(1) $P(A) \geqq 0$

(2) $P(S) = 1$

(3) For a series of mutually exclusive events $A_1, A_2, \ldots, A_n$

$$P(A_1 \cup A_2 \cup \ldots \cup A_n) = P(A_1) + P(A_2) + \ldots + P(A_n)$$

A "numerical valued random experiment" is a random experiment whose sample description space is the set of all real numbers from $-\infty$ to $+\infty$.

The "distribution function", F(x), of a numerical valued random experiment is defined as having as its value at any real number x, the probability that an outcome of a trial of the experiment will be less than or equal to the number x. In addition

$$\lim_{x \to -\infty} F(x) = 0 \qquad \lim_{x \to +\infty} F(x) = 1$$

and for this work F(x) must be continuous monotone increasing between the values 0 and 1 for $0 \leqq x \leqq +\infty$

The "probability density function" is defined as

$$f(x) = \frac{d\ F(x)}{dx}$$

Since F(x) is continuous and monotone increasing

$$f(x) \geqq 0$$

and F(x) is continuous (except perhaps at a finite number of points). In addition

$$F(x) = \int_{-\infty}^{x} f(x)\ dx \qquad \int_{-\infty}^{+\infty} f(x)\ dx = 1$$

Jointly distributed random variables are independent if their joint distribution function can be written as the product of their individual distribution functions.

$$F(x,y,z) = F_1(x)\ F_2(y)\ F_3(z)$$

Jointly distributed random variables are independent if their joint probability density function can be written as the product of their individual probability density functions.

$$f(x,y,z) = f_1(x)\ f_2(y)\ f_3(z)$$

In general, given any joint probability density function $f(x_1,x_2,x_3)$ the individual density of any variate may be found by integrating the function with respect to all other variates between the limits $-\infty$ to $+\infty$. Thus

$$f(x_1) = \int_{-\infty}^{+\infty} f(x_1 x_2)\ dx_2$$

In this work values for the various variables must be chosen at decision points along the photon path. These values are to be chosen randomly but the distribution of values used for any one variable, after a large number of values have been chosen, must conform to the probability density function for that variable. Hence one must treat the selection of values for each variable as a numerical valued random experiment. The random event which occurs is that the value chosen will lie within some interval (i.e., between x and $x + \Delta x$). The probability function is defined in terms of the probability density functions. For example the probability that a value of x will lie between a and b is

$$P(a < x \leqq b) = \int_a^b f(x)dx = F(b) - F(a) \qquad \text{(B-1)}$$

Probability zero is assigned to those events defined on intervals of the sample description space which are not physically possible (i.e., probability of negative length is zero).

In selecting the values of the variables use is made of psuedo random numbers (32). For this work a psuedo random number, here after called random number, is defined to be a number between zero and one which is a member of a mathematically generated set of numbers uniformly distributed over the interval zero to one. That is to say, if a large number of random numbers are plotted as points on a line of length one, and the line is subsequently divided into equal subintervals, no matter how small, there will be about the same number of points in every interval. The random numbers can be reproduced as desired. It should be noted that "a large number" of random numbers is stressed. There is no implication that a small number will be evenly spaced on the interval zero to one.

Consider equation (B-1) and let $a = x$, $b = x + \Delta x$. Then

$$P(x < x_1 \leqq x + \Delta x) = \int_{x}^{x + \Delta x} f(x)dx \tag{B-2}$$

which, as a consequence of the continuity of $f(x)$ and the mean value theorem can be expressed as

$$P(x < x_1 \leq x + \Delta x) = f(\xi)\Delta x \tag{B-3}$$

where ξ lies between x and $x + \Delta x$. As Δx becomes very small then

$$\underset{\Delta x \to 0}{P(x < x_1 \leq x + \Delta x)} = f(x)\ \Delta x \tag{B-4}$$

Hence the limit value of the relative frequency of occurance of values of x_1 lying between x and $x + \Delta x$ is expressed by $f(x)\Delta x$. This can be interpreted as the fraction of the total number of values of x selected which lie between x and x + Δx. This is expressed as

$$\frac{N(x,\Delta x)}{N_T} = f(x)\Delta x \qquad \text{(B-5)}$$

Two convenient methods of insuring that values chosen correspond to (B-5) will be discussed. The first is illustrated using Figure B-1. The procedure would be to generate a large number of pairs of random numbers (R_x, R_y). The numbers would be considered points on the rectangular area of the figure, (Note x = 2Rx), and all of the points lying above the graph f(x) would be discarded. This would leave a uniform distribution of points covering the area under f(x). The x coordinates of these points would be the values selected for x. The shaded area is represented by the expression $f(x_1)\Delta x$ and, since the points are uniformly distributed, the fraction of the total number of points which lie in $f(x_1)\Delta x$, and hence the fraction of values of x between x_1 and $x_1 + \Delta x$ is

$$\frac{N(x_1,\Delta x)}{N_T} = \frac{f(x_1)\Delta x}{\text{Area Under } f(x)} = f(x_1)\Delta x$$

This is the distribution desired in order to satisfy equation (B-5).

The second method is to simply set the distribution function equal to a random number and solve for the variable.

$$F(x) = R$$

That this procedure satisfies equation (B-5) after a large number of values have been determined can be shown with the aid of Figure B-2. Suppose N_T values of R are used as F(x). The N_T values will be uniformly distributed along the ordinate between zero and one. To find the number of values of x chosen between x and x + Δx, consider the number of values of R which lie between F(x) and F(x + Δx). Since the values are uniformly distributed, the number between $F(x)$ and $F(x + \Delta x)$ is simply the total number multiplied by the length of the interval, $N_T\left[F(x + \Delta x) - F(x)\right]$. Since $F(x)$ is monotone increasing between zero and one, there is a unique value of x for every value of R. Therefore the number of values of x lying between x and $x + \Delta x$ is $N_T\left[F(x + \Delta x) - F(x)\right]$. Hence the fraction of values lying between x and $x + \Delta x$ is

$$\frac{N_T\left[F(x + \Delta x) - F(x)\right]}{N_T} = \frac{N(x,\Delta x)}{N_T}$$

or

$$\frac{N(x,\Delta x)}{N_T} = \left[\frac{F(x + \Delta x) - F(x)}{\Delta x}\right]\Delta x \tag{B-6}$$

As Δx goes to zero and N_T becomes large

$$\lim_{\Delta x \to 0} \frac{F(x + \Delta x) - F(x)}{\Delta x} = \frac{dF(x)}{dx} = f(x)$$

Thus as N_T becomes large (B-6) becomes a good approximation to (B-5). This latter method is employed throughout this work.

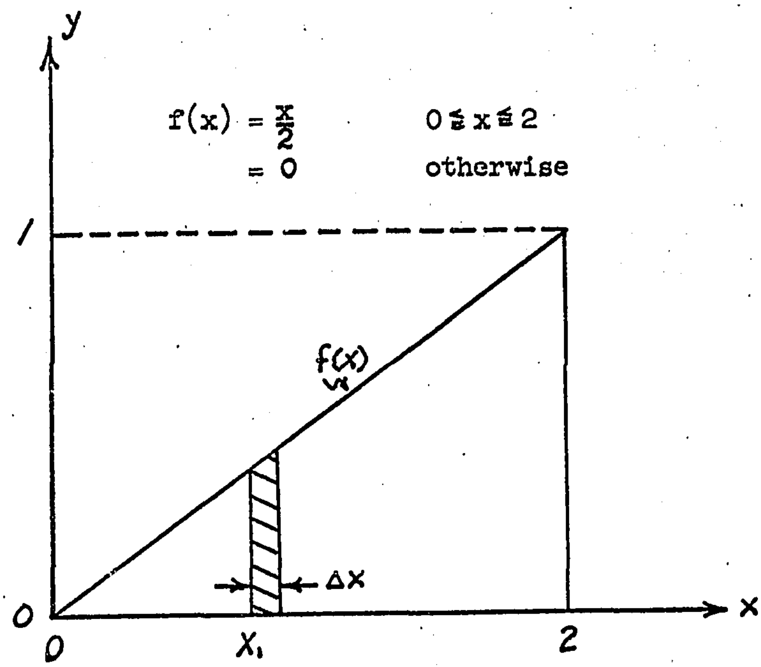

Figure B-1. Graph of f(x)

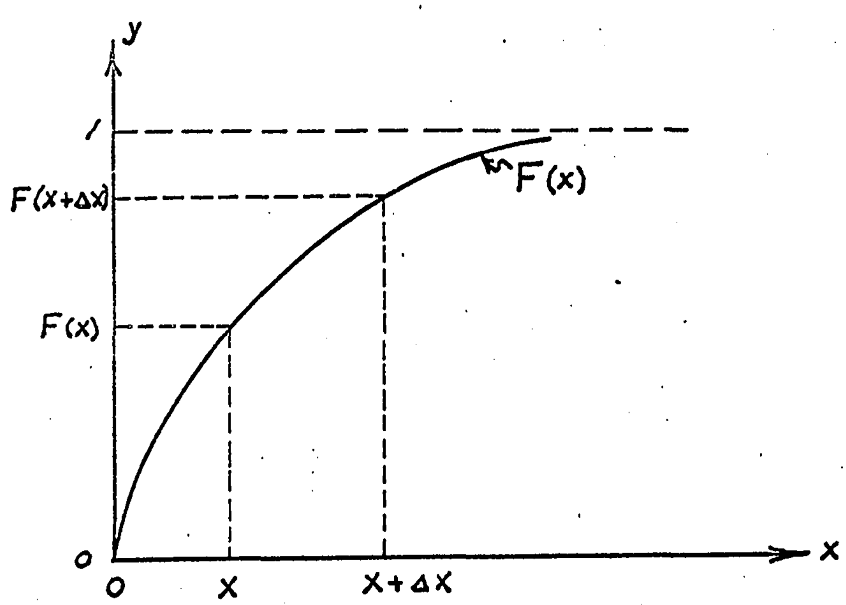

Figure B-2. Graph of F(x)

APPENDIX C

CONFIGURATION FACTORS FROM A FINITE RIGHT CIRCULAR CYLINDER TO SURROUNDING BASE RINGS

The configuration factors desired are indicated in Figure C-1. They are from the outside surface of the cylinder to the individual base rings (i.e., F_{25}).

Hamilton and Morgan (33) present values for the configuration factors in concentric finite cylinders (Figure C-2). In their work surface A_1 is the interior of the outer cylinder, surface A_2 is the exterior of the inner cylinder and surface A_3 is the base area between cylinders. They specifically present values for F_{12}.

Using configuration factor algebra one obtains

$$F_{23} = \frac{1}{2}(1 - \frac{A_1}{A_2} F_{12})$$

or

$$F_{23} = \frac{1}{2}(1 - \frac{d}{r} F_{12}) \qquad \text{(C-1)}$$

Continuing with the notation of Hamilton and Morgan let $D = d/r$ and $L = \ell/r$.

For use in this work $r = 1$ and $\ell = 10$. From Hamilton and Morgan and equation (C-1) the following values are obtained.

D	F_{12}	F_{23}
1.5	.641	.0193
2	.464	.0360
2.5	.358	.0525
3	.288	.0680
3.5	—	.0830*
4	.201	.0980
4.5	—	.1115*
5	.150	.1250
5.5	—	.1385*
6	.116	.1520

*Interpolated values

Using the summation rule of configuration factors one obtains the following configuration factors for the base rings.

$$F_{23} = .0193$$
$$F_{24} = .0167$$
$$F_{25} = .0165$$
$$F_{26} = .0155$$
$$F_{27} = .0150$$
$$F_{28} = .0150$$
$$F_{29} = .0135$$
$$F_{2-10} = .0135$$
$$F_{2-11} = .0135$$
$$F_{2-12} = .0135$$

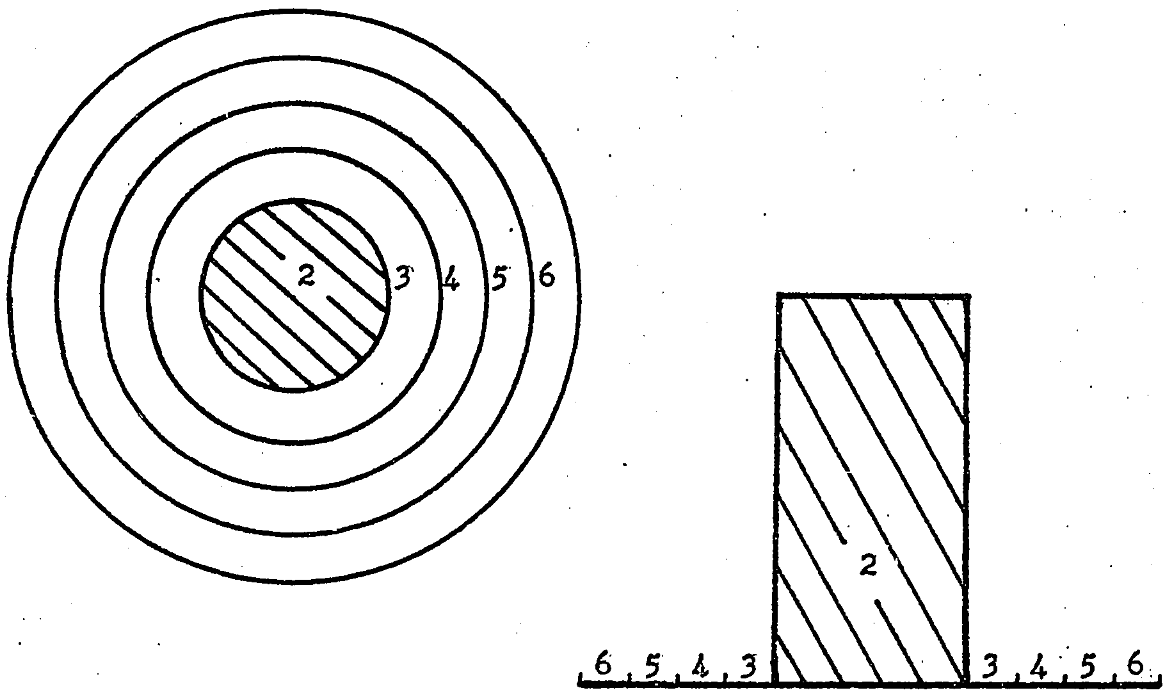

Figure C-1. Configuration Factor Geometry

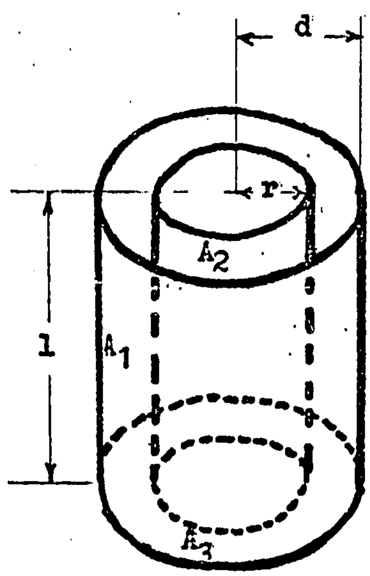

Figure C-2. Configuration Factor Geometry

APPENDIX D

ISOTHERMAL CLOUD APPROXIMATION

The assumption of an isothermal cloud implies that the emissive power of the cloud is the same throughout its volume. For the cases examined in this work, uniform source in a cloud in radiative equilibrium, the emissive power distribution depends on the optical diameter of the cloud. An indication of the effect of optical depth on emissive power can be had from the works of Howell and Perlmutter (13) and Perlmutter and Howell (14). In (13) the solution for the emissive power distribution of a gas between infinite non reflecting parallel plates is presented. It is shown that the distribution between the plates is flat (isothermal) for low optical depth but becomes markedly arched with its high point midway between the plates for optical depths above two. In (14) the distribution for concentric infinite cylinders is given. For the limiting case of no inner cylinder it is shown that the distribution of emissive power is symmetrical about the outer cylinder axis.

In Chapter VII an expression is derived for the apparent emissivity of the particle cloud resulting from emission within the cloud. The derivation assumes that emissions and reemissions are uniformly distributed throughout the cloud. Since the works cited above indicate that there is a marked departure from this condition for optical diameters above two, it seems appropriate to obtain a correction to the expression for the larger optical diameters. This is done as follows:

The distributions from (25) for optical depths of five and ten are assumed to apply along a cylinder diameter.

It is assumed that the radiation leaving the cloud is characteristic of radiation within one photon mean free path of the surface.

An average emissive power is determined for the portion of the cloud within one mean free path of the surface.

The ratio of the number of emissions and reemissions occuring if this average emissive power were uniformly distributed through the cloud to the number occuring for the uniform source case is determined.

The reciprocal of this ratio is a multiplicative correction factor to the emittance calculated by equation (7-18).

Approximate values for these correction factors are

τ	Correction
5	1.2
10	1.7